R. & M. No. 3503

R. & M. No. 3503

MINISTRY OF TECHNOLOGY

AERONAUTICAL RESEARCH COUNCIL
REPORTS AND MEMORANDA

Aerodynamic Loads on External Stores: A Review of Experimental Data and Method of Prediction

By P. Marsden, B.Sc. and A. B. Haines, B.Sc.

LONDON: HER MAJESTY'S STATIONERY OFFICE
1967
PRICE £2 5*s.* 6*d.* NET

Aerodynamic Loads on External Stores: A Review of Experimental Data and Method of Prediction

By P. Marsden, B.Sc. and A. B. Haines, B.Sc.

Reports and Memoranda No. 3503*
November, 1962

Summary.

A survey has been made of the available literature on the aerodynamic loads associated with the external carriage of pylon-mounted stores adjacent to wing-fuselage combinations.

The existing methods for estimating the store/pylon loads at both subsonic and supersonic speeds are reviewed with some indication of their accuracy, range of validity and the extent to which they have been verified experimentally. Illustrations are given showing how the loads vary with store position, wing geometry, Mach number and other factors. Particular stress is laid on the fact that the pylon-induced effects can make a very large contribution to the store loads. Details are also given of the complex flow fields adjacent to typical wing-fuselage combinations since these are vital to any real understanding of the problem.

None of the existing methods appears to be entirely satisfactory particularly for the transonic range where even the available experimental data are severely limited. In an attempt to meet one of the more important deficiencies, a new empirical method is presented (Section 7) for the estimation of store/pylon side force. This method is based on all the readily available evidence but needs further experimental verification.

LIST OF CONTENTS

*Replaces A.R.A. Report No. 5 — A.R.C. 24 509.

LIST OF CONTENTS—*continued*

LIST OF ILLUSTRATIONS

Figure

Figure

LIST OF ILLUSTRATIONS—*continued*

Figure

1. *Introduction.*

It is now generally accepted that any aircraft design with nacelles or stores mounted externally should be considered from the outset as a complete entity. It is not satisfactory first to design the clean configuration and then, at a later stage, to consider the effects of the various external additions. This is true, not merely when assessing the overall aircraft performance, stability and control, but also when designing the actual store-pylon configuration. Until recently, the aerodynamic loads acting on external store-pylon assemblies tended to be small as compared with the inertia loads that were present during some aircraft manoeuvres and as a result the structural design of the pylon, for example, was largely dictated by the inertia loads. Now, however, in many applications, the aerodynamic loads play a more vital part in the design and they should therefore be estimated more accurately than in the past. The most important load component is generally the store side force which can be very large for a store or nacelle mounted on a pylon beneath a sweptback wing. The side force acts in the direction of least structural strength of the pylon, and can produce large bending and twisting moments at the pylon/wing fixation. The choice of a suitable thickness for the pylon will always be a matter for compromise. On the one hand, it has to be thick enough to withstand the aerodynamic and inertia loads and to carry the various services required by the store (fuel pipes, electronic and electrical wiring, etc.). On the other hand, if it is too thick, there is a risk that the aerodynamic performance will be adversely affected or that buffeting will result. There is clearly, therefore, a strong urge to keep the pylons as thin as possible and to achieve this, the side force, yawing moment and rolling moment should be known accurately without any additional factors of safety to cover ignorance.

Many individual agencies have investigated methods for estimating the loads on underwing and underfuselage stores. Also, to help in the problem, several reports have described specific investigations into the flow fields adjacent to typical wing-fuselage combinations at both subsonic and supersonic speeds. In addition, there has been a large amount of wind-tunnel and flight testing to measure the loads on particular arrangements.

It was felt that the outstanding need was for a review of all the data that was available. This would show whether the data – often apparently contradictory at first sight – could be correlated, whether there were sufficient data to devise a new method for estimating the loads or whether one was still left with the necessity of testing all new proposed layouts.

Such a review has been undertaken by the Aircraft Research Association Limited, and this Report represents the substance of this work.

The search through the available literature produced a very large number of references, the contents of which were analysed. However, in an attempt to reduce the size of this report, only those references that are directly relevant have been included.

The overall conclusion from the review is that the existing methods of estimating the loads on external stores do not appear to be sufficiently reliable, particularly for the transonic speed range, where even the available experimental data are severely limited in scope. An attempt has been made, as described in Section 6 of the Report, to devise a new simple empirical method for estimating store/pylon side force. It is hoped that this will represent some advance on the methods previously available but it is realized that as more data are obtained, it may need constant revision.

2. *Flow Fields and Load Prediction Methods for Subsonic Speeds.*

The natural starting point for any discussion of the aerodynamic loads on external stores is to consider the flow fields in which they are placed. In the case of the normal underwing pylon-mounted arrangements and even more so for the case of overwing arrangements, these flow fields are likely to be very non-uniform with large variations of downwash, sidewash and local dynamic pressure with both chordwise and spanwise position relative to the wing. This is why the store loads can be completely different from what they would be on the stores in isolation.

Strictly, one should not just assume that the stores are in the flow field induced by the clean wing-fuselage. One should take account of the fact that this flow field itself will be modified by the presence of the store and its supporting pylon. As will be seen later in Section 4, this distinction can be very im-

portant at supersonic speeds, due to multi-reflection of the store and aircraft shock waves. Even at subsonic and transonic speeds, data are available (*see* Section 3.9.1.) showing that an underwing pylon mounted near the wing leading edge at a considerable angle of skew to the local airstream may considerably modify the flow field round the wing. In general however for subsonic speeds, it is safe just to consider the flow field due to the clean wing-fuselage combination and this is all that is attempted in the methods described in Section 2.1. below.

2.1. *Subsonic Flow Fields of wing-fuselage combinations.*

2.1.1. *NACA method.* One of the best available references for calculating the flow field beneath a wing is NACA Report No. 1327 (Ref. 11). As mentioned above, it merely considers the flow field beneath a wing in the absence of any store or pylon. It shows that the flow characteristics beneath a wing can be calculated if the lifting wing is assumed to be represented by a multiple arrangement (both chordwise and spanwise) of horseshoe vortices and if the effects of thickness are taken into account. The velocities induced by the aerofoil section-thickness distribution are modified by simple sweep theory for the case of a sweptback wing. The flow is considered to be potential and planar, and the effects of any boundary-layer separation together with the rolling up and displacement of the trailing vortex sheet have been neglected. The velocities induced by a unit horseshoe vortex in the vertical, lateral and longitudinal directions are computed using the equations given by Glauert in Ref. 2 and are presented in Ref. 1 for a large range of vertical distances below the wing. The computation has to be based on the spanwise load distribution of the wing in question and for the examples included in Ref. 1, this is calculated using the methods of Ref. 59. In this country, however, the spanwise load distribution would probably be computed either by lifting surface theory according to Multhopp (Ref. 4), or by Kuchemann's method (Ref. 5) or by the extremely simple rapid approximation to lifting-surface theory recently issued by the R.Ae.S. (Ref. 6). It should be noted that if the spanwise load distribution over the wing has been measured, this would enhance the accuracy of the subsequent calculations. The normal Prandtl-Glauert transformation can be used to allow for the possible effects of compressibility in the subcritical Mach-number range. It might be possible to extend the method slightly into the supercritical range by using the measured loadings at such Mach numbers rather than any predicted calculated values.

By way of illustration, Ref. 1 presents predicted and measured flow fields at low speeds beneath the 45 deg swept and the unswept wing-fuselage configurations shown in Fig. 2. Results are given for 0·5 and 0·75 times semispan since these are considered typical stations for mounting underwing stores.

Perhaps the first point to note about this method and the results is that the method as presented assumes that the effects induced by the fuselage can be ignored. To provide some justification for this assumption, the lateral variation of the upwash induced by the circular fuselage of the sweptback wing configuration of Fig. 2 was both calculated and measured with the result shown in Fig. 3. The ratio of fuselage diameter to wing span in this case was 0·13. It can be seen that at 0·5 and 0·75 times semispan, the fuselage-induced upwash was only 8 per cent and 3 per cent respectively of the wing incidence and it follows that it is reasonable to ignore the effects of the fuselage for these stations. This would not of course remain true further inboard, e.g. at 0·25 times semispan. One would then have to take account of the fuselage effects either using the curve of Fig. 3 as a guide, or by using the first method discussed in Section 2.1.2. below or by referring to the methods given in Refs. 7 and 8. Also, a highly theoretical treatment has been developed in Ref. 9 to determine the potential due to a fuselage considered as a distorted ellipse. The curve in Fig. 3 refers merely to the effects of the fuselage alone. There are also the effects of the fuselage on the exposed wing-span load distribution. Again, these will often be relatively small but methods are available, e.g. Ref. 10*, for estimating them if necessary. As a first step however in considering whether it is necessary to allow for the fuselage effects, Fig. 3 should be a useful guide; in using it, allowance should be made for changes in fuselage diameter, wing span and Mach number – for qualitative purposes, it will probably be fair to allow for Mach number by scaling y by the appropriate value of $\sqrt{1-M^2}$. In the remainder of this section, the results discussed are those for the wing alone.

*R.A.E. Report Aero. 2446 will also be helpful.

Fig. 4 compares theoretical values at mid semispan and 0·15c below the 45 deg swept wing configuration with those obtained experimentally. Except for certain detailed points mentioned below, the comparison can be taken as typical of those presented in Ref. 1. It will be seen that for this particular location, good qualitative agreement between measured and calculated values was obtained in all respects. In detail, however, certain differences are apparent. These include

(1) the downwash over the rear part of the chord at positive incidence tends to be overpredicted. This is possibly only as would be expected since viscous effects would reduce the loading over the rear, particularly out towards the tip. This trend should become more pronounced with increasing incidence and this is confirmed by the results which show that a significant discrepancy is present aft of about $0{\cdot}2c$ at $\alpha = 8$ deg as compared with merely aft of about $0{\cdot}75c$ at $\alpha = 4$ deg,

(2) ahead of the leading edge, the upwash at positive incidence is somewhat overpredicted. This is largely because the downwash in this region at zero incidence, i.e. the downwash contribution from the wing thickness, is not estimated correctly. This is not as significant as (1) above but is rather more surprising – it may indicate a failing in the application of the simple sweep concept. The discrepancy became larger as z decreased and as one approached the tip,

(3) at negative incidences, it is quite likely that in the tests, a leading-edge separation was present over the lower surface and this could help to account for the discrepancies between the calculated and measured values of downwash,

(4) the sidewash angles tend to be underpredicted ahead of the leading edge and overpredicted further aft. For the unswept wing of Fig. 2, the underprediction of the sidewash ahead of the leading edge was more pronounced,

(5) the increase in local dynamic pressure below the swept wing at negative incidence is underpredicted. On the other hand, the loss in dynamic pressure below the wing at positive incidence is predicted quite reasonably.

Despite these detailed discrepancies, it is clear that the method is capable of providing a very good idea of the flow characteristics beneath a sweptback (or unswept) wing and that therefore there is some point in studying the trends predicted by calculations by this method. Figs. 5 to 8 have been reproduced to illustrate some of these main trends. Fig. 5 shows the effect of vertical position on the flow characteristics at mid semispan and $\alpha = 8$ deg. Figs. 6 to 8 show the effects of incidence on the sidewash, downwash and dynamic pressure ratio at $z = 0{\cdot}15c$ for both 0·5 and 0·75 times semispan. All these figures illustrate the very large changes that occur with position and in particular, the very rapid changes in downwash and sidewash with chordwise position near the wing leading edge. These effects become much more pronounced with increasing C_L and as the wing is approached in the vertical sense. All the curves illustrate at a glance the basic reason why it is so difficult to extrapolate the loads measured on one particular store configuration to other applications which are similar but not exactly the same. To help in the later discussion, it will be useful to list some of the major effects, *viz*,

(a) the changes in downwash are largest close to the wing leading edge. For example, for the most extreme case, $z/c = 0{\cdot}1$, included in Fig. 5 for $\alpha = 8$ deg, the value changes from an upwash of about 5 deg at a position $0{\cdot}1c$ ahead of the leading edge to a downwash of about 5 deg, $0{\cdot}1c$ aft of the leading edge. $(\partial\varepsilon/\partial x)$ near the leading edge increases rapidly with decreasing z and the maximum upwash and downwash tend to occur closer to the leading edge at small z,

(b) the maximum values of sidewash at $\alpha = 8$ deg for this 45 deg sweptback wing example are higher than the maximum values of downwash. For example, for $z = 0{\cdot}1c$, a maximum value of about 7 deg occurs close to the leading edge as compared with 5 deg of downwash. This sidewash is in the sense of the flow being directed outwards, i.e. positive σ,

(c) even at $\alpha = 0$ deg, significant sidewash is still present, varying from about $+2$ deg well ahead of the wing leading edge to about -2 deg below the wing mid-chord. The sidewash at zero incidence is of course induced by the wing sweep. It is probable that this effect is significant for angles of sweep greater than about 25 deg,

(d) also, it should be noted that the downwash is not trivial at zero incidence due to the effects of wing thickness. Even for this 6 per cent thick, 45 deg sweptback wing, there is about 2·5 deg of downwash

near the wing leading edge at zero incidence with correspondingly about 2·5 deg of upwash near the trailing edge. Very crudely the downwash at zero incidence would vary as (t/c x cosΛ). The numerical values of downwash are therefore smallest at a small positive incidence rather than at zero incidence,

(e) relatively large changes in local dynamic pressure can occur at appreciable positive or negative incidence, e.g. at $\alpha = 8$ deg, the local dynamic pressure ratio falls to near 0·8 near the wing leading edge while at $\alpha = -8$ deg a maximum value of 1·5 is predicted near 0·2c for the present example. It follows that it is quite conceivable that the most severe stressing case for an underwing store configuration could occur at negative g conditions in a manoeuvre when the local dynamic pressure ratio could be relatively high. Also, with inappropriate choice of store position, the sidewash and downwash could be high, e.g. at $\alpha = -8$ deg peak values of σ and ε of -12 deg and -15 deg are predicted (Figs. 6, 7),

(f) the values of both sidewash and downwash at $\alpha = 8$ deg are higher at 0·75 than at 0·5 times semispan. For example, the peak upwash ahead of the wing leading edge is increased from about 4 deg to about 6 deg. One should be careful about identifying these trends as an effect of 'approaching the wing tip'. A more relevant factor is probably that the peak of the spanwise C_L – distribution probably occurs nearer 0·75 than 0·5 times semispan. Distortions of the chordwise loading would occur towards the tip which would tend to accentuate the values of upwash and sidewash close to the wing leading edge but these effects would at least to some extent be offset by the fact that the local values of C_L would decrease outboard of say, 0·75 times semispan. The flow region near the tip over a sweptback wing is obviously complex in character and one should be wary of extrapolating the trends evident in Figs. 6 to 8 to stations outboard of 0·75 times semispan. This restriction is not likely to be too important in practice in the present context.

It is obvious that the mean values of ε, σ and dynamic pressure ratio applicable to any store immersed in these flow fields will vary not merely with the position of the store but very radically with the size of the store. Some general remarks about the effects of flow fields such as those shown in Figs. 5 to 8 on the different store loads will be given later both in Section 2.2.1. and at the start of Section 3 which deals with the effects of the various geometrical parameters. A reminder is perhaps worthwhile that the induced angles ε and σ must be combined with the geometric angles of incidence and sideslip respectively, to be applicable for use in the load estimation procedures given in Ref. 11.

Ref. 1 does not contain any experimental evidence on the effects of Mach number in the subsonic range. Some calculated results using the analogous wing concept are however included and a comparison between the calculated values for $M = 0$ and $M = 0{\cdot}8$ is shown in Fig. 9. Comparisons are presented for $C_L = 0$, and for both a constant incidence (8·1 deg and a constant C_L ($C_L = 0{\cdot}49$). It will be seen that the qualitative trends remain the same at $M = 0{\cdot}8$ as at M = 0. Quantitatively, as might be expected, making the comparison at a constant C_L rather than at a constant incidence tends to eliminate the effects of Mach number but it still remains true that even on this basis, the peak values of ε and σ and the minimum values of q/q_∞ near the wing leading edge are more pronounced at the higher Mach number. The chordwise gradients in ε and σ therefore increase with Mach number. It is by no means certain that these trends would occur in practice. Indeed, it is quite possible that the chordwise gradients in ε and σ near the leading edge could decrease with Mach number even in the sub-critical range. The predictions shown in Fig. 9 are based on a first-order theory and it is known that this would not be entirely satisfactory for estimating the effect of Mach number on the surface pressure distribution close to the leading edge. For example, for a symmetrical aerofoil at zero incidence, the suctions close to the leading edge would tend not to vary much with Mach number whereas further aft near the section maximum thickness, they would increase at least as rapidly as any prediction by the Glauert first-order theory. In the absence of any direct experimental verification therefore, one should perhaps treat the prediction of the Mach-number effects close to the leading edge by the present method (as shown in Fig. 9) with some reserve. If one avoids this region however, the conclusion from Fig. 9 that Mach-number effects at a constant C_L are relatively small elsewhere should be perfectly valid.

2.1.2. *Other American methods.* Several other methods have been in use in USA for predicting the flow field beneath a wing. Fig. 10 presents a comparison of the flow characteristics predicted by one of these methods with some experimental results for the 0·33 times semispan station below a 35 deg sweptback

wing-fuselage configuration at $M = 0{\cdot}70$ and low incidence. Reasonable agreement between the measured and calculated values is shown. This method, which is applicable up to the critical Mach number of the wing, is based on an iterative procedure and linearised potential flow theory. The effects on the flow field over all aircraft components other than the wing and the fuselage are neglected as is the effect of the presence of the store in modifying this flow field. The total potential at a point below the aircraft wing is taken to be the sum of the potentials due to the fuselage alone, the wing alone and the interference potential due to fuselage effects on the wing flow. The effect of the wing on the fuselage flow field is neglected. The total potential at a point is then differentiated to derive the perturbation velocities and hence the sidewash and downwash angularities.

No direct comparison of these results in Fig. 10 with those given earlier is possible because of the difference in aircraft geometry. Qualitatively, however, they are clearly similar despite the fact that these are results for $M = 0{\cdot}7$ whereas the flow fields in Figs. 5 to 8 were for incompressible flow. One point that should be noted is that the downwash close to the leading edge at effectively zero incidence is as much as 5 deg whereas for the 45 deg sweptback wing discussed earlier it was only about 2·5 deg. The larger value in the present case is because the wing is thicker and less swept (about 11 per cent as compared with 6 per cent and 35 deg rather than 45 deg).

In another available method, an attempt is made to allow for the effect of the pylon in modifying the flow field round the wing. On the other hand, this method does not make any allowance for fuselage effects arguing that applications of interest usually involve stores mounted a large distance from the wing root. Further, the method does not include any allowance for wing sweep and this effectively restricts the useful application of the method to cases where the wing sweep is less than say, 25 deg because as seen earlier, higher angles of sweep can appreciably modify the sidewash characteristics and hence the side load on the store and its pylon.

On the other hand, this last method is an improvement on those discussed earlier in that it allows for three-dimensional effects and for the spanwise load distribution over the wing. The flow field due to incidence is assumed to be due to a lifting line with elliptical span loading. For consideration of the wing flow field, distances in the spanwise and vertical directions are multiplied by $\sqrt{1-M^2}$ to allow for Mach-number effects. Thus the wing flow field is a function of x, $\sqrt{(1-M^2)}y$ and $\sqrt{(1-M^2)}z$ rather than of x and y. The flow field due to the pylon is shown to be a function of x and $\sqrt{1-M^2}$. The flow field due to wing thickness is determined by obtaining the potential flow about a Joukowski aerofoil similar to the wing section at the pylon centreline, having modified this section to allow for compressibility effects. The method of small perturbations is then used to obtain the incremental flow fields due to the thickness and camber differences between this modified section and the comparable Joukowski section. If the pylon is swept, an approximation is introduced by considering a comparable straight pylon with a constant section equivalent to the actual section at the store-pylon junction.

2.1.3. *Comparison of methods.* The three methods which have been discussed above differ primarily in the importance attached to the contribution of the various components to the flow field in the vicinity of the store. If results are required for stations between say, 0·5 and 0·8 of the wing semispan (where the effects of the fuselage and the complicated flow patterns near the wing tip can be neglected) and if the wing is unswept, all three methods should be applicable up to the aircraft critical Mach number, and all three appear to give reasonable agreement with experiment. If the wing has significant sweepback, the third method cannot be used. For locations closer to the fuselage, the inclusion of fuselage effects, as in the second method, is clearly required. The region near the wing tip requires analysis which does not appear in the literature in a simplified usable form. The NACA method might be capable of being used beyond the aircraft critical Mach number if experimental load distributions over the wing are known and if these are used rather than predicted subcritical loadings.

It may be invidious to draw comparisons as to the relative accuracy of the three methods for applications where the assumptions of all three remain valid but it seems fair to emphasise that the NACA method is sound in principle and certainly, Ref. 1 is the most illuminating report from which to obtain

a good idea of the major features of the underwing flow fields. It must be admitted that the NACA method however requires considerable computation work as a result of the large number of spanwise and chordwise horseshoe vortices required for the adequate representation of the aircraft wing. This three-dimensional approach is probably not justified for straight and swept wings of high aspect ratio and small taper ratio at locations close to the mid semispan station, since two-dimensional considerations have been shown to give reasonable correlation with experiment in this region.

2.2. *Methods of Predicting Store Loads at Subsonic Speeds.*

Broadly speaking, the methods for predicting the store loads can be divided into two classes, *viz*, those that use predicted or measured flow fields as their basis and those which are derived from an analysis of actual measurements of the loads* on different store arrangements. Most of the American methods to be discussed below fall into the first category while the British methods are of the second type.

At first sight, methods based on a knowledge of the actual flow field in the vicinity of the store appear attractive. It will be realised however from consideration of Figs. 5 to 8 that application of such methods cannot be entirely plain sailing. The difficulty lies in knowing what are the mean values of ε, σ and q/q_∞ to use in estimating the loads over the store. For many applications, the store length will be comparable with the local wing chord and it is quite clear therefore that large variations in ε, σ and q/q_∞ may occur over the length of the store. To some extent, this difficulty can be met by noting which parts of the store are likely to give the main aerodynamic forces and moments, e.g. the forebody or any tail fins if present but even so, there is obvious room for uncertainty particularly if the store extends forward to near or ahead of the wing leading edge. For stores that are relatively small compared with the local wing chord, the analysis should be more certain.

Another drawback of methods that involve a calculation of the flow field in which the store is immersed is that these methods are necessarily somewhat lengthy. There is therefore also a place for the shorter semi-empirical methods based on an analysis of measurements of store loads. If reliable methods of both sorts are available, the shorter empirical-type method could be used for a broad survey of the loads for a wide range of different possible store arrangements on a given aircraft and then the more accurate method based on an estimate of the flow fields could be used in an attempt to obtain a better quantitative result for any favoured arrangements. In the succeeding sections, the available methods of both types are reviewed with the flow-field type methods being taken first since these form a logical sequel to the discussion of the flow fields themselves in the previous Section (2.1.). The NACA methods will be considered first since for these, more comparisons with experiments are available to judge their reliability. Also, as will be seen in Section 2.2.1. below, the NACA literature includes not only methods for estimating the loads on the stores themselves under the influence of the wing flow field but include one possible method for estimating the pylon-induced effects on the store loads, again related to the flow field in which the pylon-store arrangement is immersed.

2.2.1. *NACA methods.* The two main NACA references giving methods for predicting the store loads, once the flow field characteristics are known, are NACA RM L54 J20 (Ref. 11) and NACA RM L55 E10a (Ref. 12). In both these reports, the pylon-induced effects are ignored and the experimental measurements used for comparison with the predicted values are for stores sting-supported from the rear in the presence of the wing flow field but with no pylon present. This point cannot be emphasised too strongly.

The method detailed in Ref. 13 presupposes a knowledge of the local flow angularity and dynamic pressure into which the store is submerged, and of the variation with incidence of the force and moment coefficients on the store when mounted in isolation with no wing present. The flow field characteristics can either be predicted theoretically by the methods discussed earlier in Section 2.1. or and perhaps preferably measured values obtained by angularity and pressure surveys can be used if available. The comparisons included in Ref. 13 are based on measured flow surveys. It should be noted that the angularity contours given in the report in this case are resultant flow angularities, α_1 and β_1, where $\alpha_1 = \alpha - \varepsilon$ and $\beta_1 = \beta + \sigma$.(*see* Fig. 1b).

*or detailed pressure plotting data.

The method clearly depends upon the accuracy with which the flow properties have been determined and on whether appropriate average values of these quantities are taken when estimating the loads. The practice followed here was to derive the appropriate values of mean downwash, sidewash and dynamic pressure by averaging the local values of these quantities at the approximate centroids of the store nose, wing, and tail. The cylindrical part of the store (if any) is assumed to carry no force or moment, following potential flow theory for bodies of revolution.

Results were obtained for a store model mounted in various locations beneath a 45 deg sweptback wing with the store having a length of 1·12 times the wing mean chord, a fineness ratio of 18·41 and having both fins and wings. No pylon was present in the tests so that the results do not include the pylon-induced effects on the store loads. This point is referred to again later.

Figs. 11 and 12 shown some of the results of this investigation obtained at $\alpha = 8{\cdot}2$ deg, $\beta = 0$ deg; and give experimental downwash and sidewash contours together with experimental and theoretical load estimates at the mid semispan location and two alternative vertical locations. The coefficients presented here are based on the exposed area of two store wings and on the mean chord of the store wing, and hence do not conform to the usual references of the store frontal area and the length of the store. The store force and moment characteristics are presented as functions of the chordwise position of the store centre of gravity relative to the leading edge of the wing chord. Also presented in Figs. 11 and 12 are the isolated store force and moment levels to show the degree of induced deviation.

The report concludes that by the use of the isolated store data and the measured flow-field characteristics, the longitudinal forces and moments acting on the store while in the presence of the wing-fuselage combination could be estimated with fair accuracy. Although the lateral forces and moments predicted were qualitatively correct, there were some large discrepancies in absolute magnitude (*see* Fig. 12). The conclusion regarding the longitudinal forces and moments certainly seems justified by the comparison in Fig. 11. The lateral comparison in Fig. 12 is however undoubtedly disappointing, bearing in mind that measured flow field data were being used. It will be seen that although the predictions are reasonably accurate in suggesting where the side force and yawing moment on the store are likely to be at their maximum, these maximum values are greatly underestimated – by a factor of 2 or more. The report suggests that one possible reason for these differences may be the fact that the estimation procedure used does not account for any mutual interference effects between the flow fields of the store and the wing-fuselage combination.

The same sort of approach with broadly similar results was followed in a later NACA Report, RM L55 E10a (Ref. 12). This report includes some of the theoretical and experimental flow field data that are compared in more detail in Ref. 1 which was discussed earlier in Section 2.1.1., but its relevance here lies in the fact that it includes comparisons between measured and predicted longitudinal and lateral forces and moments for a store mounted at a wide range of chordwise positions, $0{\cdot}15c$ below the wing chord plane at the mid semispan station of the sweptback wing-fuselage configuration shown in Fig. 2. This comparison is reproduced here as Fig. 13 and is of particular interest because two sets of predicted loads are included, *viz.* those based on the measured flow fields and those based on the predicted flow fields. Once again, it should be stressed that these loads are those induced by the wing-fuselage; no pylons were present in these tests. Another important point to remember about the results is that the store length is about 1·3 times the local wing chord, i.e. it is a particularly large store in relation to the wing and that is why the changes in C_N and C_Y with chordwise position are relatively gentle. With a smaller store, C_N and C_Y would tend to be much more sensitive to small changes in chordwise position.

It will be seen that, except possibly for the normal force on the store in the further aft positions, the differences between the predictions based on the measured or alternatively the estimated flow fields are much less significant than any discrepancies between either set of predictions and the measured store loads. For positions of the store centre ahead of the wing leading edge, both the normal force and side force are appreciably underestimated by either method; for positions further aft, the normal force estimate is reasonable but the side force is still underestimated. The longitudinal load centre is given reasonably; the estimate of the lateral centre begins to diverge from the measured values ahead of the leading edge. In practical terms, the most serious discrepancy is once again the underestimate of the side force particu-

larly for the positions ahead of the leading edge. This is the same conclusion as that arrived at previously in Ref. 11 discussed above. Experimental data on store loads for other store configurations mounted beneath the same wing-fuselage configuration are given in Refs. 13 and 14 and a few of these are reproduced again in Ref. 12. It seems clear that comparison of these with predicted values would lead to similar conclusions.

To sum up, it seems that fair qualitative success has been achieved in predicting store loads by these methods, using either measured or theoretical flow-field data. Quantitatively, however, the results are somewhat disappointing, particularly when estimating the side force and yawing moment on stores lying in a region of large sidewash. For such applications, it is usual to find that the measured side-force values are at least twice those predicted. Further detailed analysis would be needed to decide whether these discrepancies are due to the inadequate nature of the first-order theory which ignores the interaction of the store on the flow field round the wing or whether the fault lies more in the procedure proposed for obtaining the mean angles of sidewash over the store.

For many practical applications, the discrepancies between predicted and measured values noted above may be less important than the pylon-induced effects on the store loads which have not so far been considered. An extreme example illustrating this point is shown in Fig. 14 which compares the side loads with and without a pylon for a store mounted 1·0d below the leading edge at 0·6 times semispan for a 45 deg sweptback wing aircraft at $M = 0{\cdot}9$. For this example, it will be seen that the pylon-induced effects increase C_Y at say, $\alpha = 10$ deg from about $-0{\cdot}15$ to about $-0{\cdot}66$. For this condition, therefore, the pylon-induced effects contribute about 0·5 to C_Y and this should be compared with the error due to the methods of estimating the side loads in the absence of a pylon which would probably have amounted to about 0·1 in C_Y. It is true that this may be a rather extreme example (*see* Section 3.8 below); with longer pylons and the store further from the wing, the pylon-induced effects would make a smaller contribution to the total store loads. Nevertheless, the example is fairly typical of current practice and may be sufficient to prove the point that in the long term, it may be much more important to derive a satisfactory method for estimating the pylon-induced effects than to refine the methods discussed above for estimating the store loads in the absence of a pylon.

Only one NACA reference (Ref. 15) appears to give a method for estimating the pylon-induced effects and even in this case, the method appears to be strictly derived from an analysis of results at supersonic speeds. Even so, there seems to be some chance that the method could be used as a first guide at subsonic speeds if the calculations are based on the local values of sidewash computed or measured at subsonic speeds, i.e. the distinction between subsonic and supersonic speeds would be expected to lie primarily in the different values of sidewash than in the succeeding calculation. Perhaps hopefully therefore, the method can be included at this point. It consists merely of the two curves given in Fig. 15. One of these gives the side force on the pylon and the other the side force on the store, induced by the pylon. The figure is extracted directly from Ref. 15 and there is some ambiguity in the use of the symbol β. The report quotes β as being as usual, the angle of sideslip but in almost all the comparisons discussed in Ref. 15, $\beta = 0$ and the side force on the store is due to the sidewash, σ. It appears therefore that it is quite legitimate to interpret the curves in Fig. 15 as indicating the variation of $(\partial C_Y/\partial\sigma)$ where σ is the local sidewash assumed to be acting on the store. It will be noticed that when the store diameter is about 1·6 times the pylon span, the pylon-induced store side force is almost as large as the side force on the pylon. These pylon-induced effects will be discussed in more detail in the more appropriate later Sections of the Report (4.3., 3.8., 5.7., and 6.).

2.2.2. *Other American methods.* Various other American methods are available for estimating the store loads in terms of the geometric properties of the store and the flow field characteristics at selected representative points. Broadly speaking, however, these methods do not show any advantage over the NACA method discussed above although in one case, there is an attempt to take into account the effect of the pylon in modifying the flow field in which the stores are immersed. Comparisons between measured store loads and estimates by one of the methods indicated that the variation of C_N, C_Y, C_m and C_n with incidence can be predicted fairly accurately but the absolute values of any of these quantities at a given incidence showed poor correlation with experiment. Two of the other methods examined were concerned

only with the normal force and pitching moment on the store and did not include any reference to store sideforce or yawing moment. In one report, the suggestion is made that the store can be adequately represented by three concentrated lift-producing components: nose, wing in presence of body, and tail in presence of body with wing interference. The assumption that the body lift acts at the nose ignores the effects of viscosity in distributing the body lift along the axis of the body, but this effect should be small except at high incidence. The local velocity and incidence at each of the three component parts can be expressed as a function of the known flow field.

2.2.3. *R.A.E. methods.* The R.A.E. methods for estimating the loads on external stores at subsonic speeds are based on an analysis of actual measurements of store loads as obtained from both balance and pressure plotting tests. The methods fall therefore into the second category as defined at the start of Section 2.2. in that there is no specific attempt to relate the loads to the flow fields in which the stores were immersed. This second type of approach leads of course to methods that are much simpler to apply than the American methods discussed above but it is probably more dangerous to extrapolate beyond the range of the experimental data forming the basis of the analysis.

The R.A.E. methods were progressively developed and their range of application widened as recorded in a series of R.A.E. Technical Notes Nos. Aero 1715, 2205 and 2394 (Refs. 16, 17 and 18). These all relate to an analysis of low-speed test data; in addition, R. & M. 2951 (Ref. 19) gives a little evidence as to the effects of Mach number at subsonic speeds.

The first note, Ref. 16, is a very short early note, dated 1946, giving the results of an analysis of tests made in the R.A.E. 5 ft wind tunnel during 1944 on streamlined bodies of revolution with and without fins, and on bluff and faired bodies mounted at various positions beneath wings of thickness/chord ratios varying from 12 per cent to 18 per cent. The tests were made before wings had any appreciable sweepback and so this is one obvious major restriction to the formulae presented. Also, the note is mainly concerned with store lift, drag and pitching moment with only passing reference to side force and yawing moment. There is no mention of pylon-induced effects or of pylon loads and it is stated that the method should not be applied to stores with a length/wing chord ratio outside the range 0·5 to 0·9.

The second and third notes (Refs. 17 and 18) are much more comprehensive. In Ref. 17, empirical expressions are derived for the calculation of the forces and moments acting on streamlined bodies of revolution (without fins or wings) mounted on pylons beneath a 40 deg sweptback wing. The expressions are based on the results of extensive pressure measurements reported in Refs. 20, 21, 22 and 23 and theoretical treatments given in Refs. 24 and 25. The method determines the loads on the isolated store, the interference effects caused by the wing, and the interference effects caused by the supporting pylon. The methods are strictly applicable only to wings of 40 deg sweepback and a thickness/chord ratio of 8·5 per cent but plausible suggestions are made as to how the expressions should be modified to allow for small differences in wing sweepback or thickness. In the second note (Ref. 18), the methods are further revised with particular reference to the store pitching moments and yawing moments on the basis of additional data obtained both for stores mounted at 57 per cent of the semispan on a 40 deg sweptback wing and for stores mounted at 0 per cent and 66·7 per cent of the semispan for an unswept wing. The range of different store installation geometries covered in the tests analysed in these two notes is indicated in the following Table:

Reference	17	18
Wing sweep	45 deg	45 deg, 0 deg
Pylon chord	$< 0{\cdot}3c$	$0{\cdot}25c - 0{\cdot}57c$
Pylon length	$0{\cdot}96t - 1{\cdot}90t$	$0{\cdot}35t - 1{\cdot}60t$
Position of store nose	$0{\cdot}5c - 0{\cdot}8c$ ahead of L.E.	$0{\cdot}26c - 0{\cdot}46c$ ahead of L.E.
Store length	$0{\cdot}96c - 1{\cdot}28c$	$1{\cdot}10c$
Store fineness ratio	6 :1, 8 :1	6·5 :1

where t = local wing thickness
c = local wing chord

The revised formulae in Ref. 18 were prompted partly by the wider range of configurations covered in the later tests and partly by the fact that additional measurements were made – for example, the tests included detailed pressure plotting in the store-pylon junction. These pressure-plotting measurements showed for instance that the pylon side force was greater than thought earlier when the pressure measured on the tank surface had been extrapolated into the junction.

The formulae for estimating the wing interference were completely revised between the two notes. In the final version, the parameters for estimating the pitching moment were related to the square root of the pylon length rather than simply to the pylon length while the yawing moments due to sideslip were taken as functions of the pylon length rather than as functions of fore and aft position. From the earlier discussion of the characteristics of the flow field beneath a sweptback wing, one might have expected that the yawing moment due to sideslip would under appropriate conditions be a function of either or both of these variables and hence, to be able to draw a conclusion that one variable is much more important that the other suggests that the analysis is being strongly influenced by the specific configurations being analysed. This reinforces the view that the validity of any method of this type must rest largely on whether the configurations that have been tested experimentally are judged to be representative of current practice or not.

In all three notes just discussed, it is emphasised that the methods would probably cease to apply once any shock waves are present in the flow. Even before then, in the subcritical Mach-number range, there is some confusion as to whether one would expect the results to be independent of Mach number or whether they should vary according to the Glauert factor. Even a phrase like 'varying as the Glauert factor' can be ambiguous because when considering wing-induced effects, it is presumably $(1-M^2)^{-\frac{1}{2}}$ but when considering isolated store forces, it is $(1-M^2)^{-\frac{1}{4}}$. On the assumption that the wing-induced effects are usually the more important $(1-M^2)^{-\frac{1}{2}}$ seems the more appropriate. R. & M. 2951 (Ref. 19) dated 1952, includes some measurements of store normal force and pitching moment for a range of Mach number for an 8:1 strut-supported tank beneath a 40 deg sweptback wing. This report concludes that the Mach-number effects in the subcritical range can be summed up as follows:

(a) the low speed value of the store normal-force coefficient should be used for stressing purposes at high Mach number – i.e. no compressibility correction,

(b) for store pitching-moment coefficients, the value at $\alpha = 0$ deg should be scaled up by the Glauert factor while the rate of change of store pitching-moment coefficient with incidence should be left independent of Mach number.

It is emphasised that these conclusions are based on just a single test for a store supported beneath a 10 per cent thick, 40 deg sweptback wing at 0·52 times semispan and may not be applicable to other store positions or to wings of different sweep and thickness. As already noted in Section 2.1.1., Mach-number effects even in the subcritical range could depend very much on the position of the store relative to the wing leading edge. Once shock waves are present, larger variations in the store forces and moments could be expected as will be discussed later in Section 3.10.

To sum up, these R.A.E. methods, particularly the formulae for estimating store pitching moments and yawing moments as given in Ref. 18, are clearly useful for estimating store loads at subcritical speeds. They are relatively simple and easy to apply and they have the great merit of including the pylon-induced effects. On the other hand, it should be noted that the more reliable second and third notes do not offer formulae for the estimation of the pylon loads and so one cannot use the methods to obtain estimates for the total store plus pylon loads. The main drawback of the methods however is undoubtedly the fact that they should not be used for store-pylon geometries lying well outside the range quoted in the Table above or for applications where the wing sweep is notably greater than about 40 deg or where the stores have wings or fins.

Fig. 17 gives an illustration of what can happen if the methods are applied outside their proper working range. This Figure gives a comparison between estimated and measured loads for the store configuration shown in Fig. 26: as can be seen, this is a finned store of length somewhat greater than the local wing chord and with the nose extending a little way ahead of the wing leading edge. It was mounted at about mid-semispan of the gross wing. Fig. 17 shows that while certain features, e.g. C_n and $(dC_m/d\alpha)$, are estimated reasonably correctly, there are significant differences between estimate and measurement as regards C_N, C_{m_0} and $(dC_Y/d\alpha)$. In particular, the side force at high incidence is considerably underestimated, e.g. at $\alpha = 12$ deg, the estimated C_Y is only $-0{\cdot}15$ as compared with a measured value of $-0{\cdot}43$. Various factors could contribute to this poor estimate of side force but probably the most important is the chordwise position of the store. As noted above, the nose of the store is a little way ahead of the wing leading edge and is therefore in a region of large sidewash (*see* for example Fig. 6). The store configurations which formed the basis of the R.A.E. methods of estimation, usually have the mid point of the store somewhere near the wing leading edge with the nose being about $0{\cdot}5c$ ahead. While this admittedly results in a high mean sidewash over the store, the fact that the sidewash is high over the middle part of the store is probably relatively unimportant; what matters more is the value of sidewash over the nose of the store (and over the tail fins at the rear). It follows therefore that because the sidewash over the nose of the store for the configuration in Figs. 17 and 26 is higher than for the standard arrangement forming the basis of the method of estimation, one would expect to find that $(dC_Y/d\alpha)$ would be underestimated. This is in fact the case (Fig. 17). This also suggests that the relatively good agreement in C_n in Fig. 17 may be coincidental. There could be two compensating factors as regards C_n. On the one hand, there is the extra side load as compared with the estimate over the nose of the store while on the other hand, there is the side load on the fins which is not allowed for in the method of estimation which assumes a simple body of revolution with no fins or wings.

Store loads have also been estimated by the R.A.E. method for the configuration shown in Fig. 20 and for an incidence of 6 deg. Once again it was found that the estimate of side force is poor, the estimated value being about $-0{\cdot}43$ as compared with a measured value (at $M = 0{\cdot}80$) of about $+0{\cdot}05$. In this case, therefore, the method gives an overestimate of $(-C_Y)$ whereas in the previous example, it gave an underestimate. There are three main reasons why the store side force for the example of Fig. 20 could be smaller than that estimated by the R.A.E. method. First, the store is mounted relatively far inboard at 0·25 times semispan; second, the tip of the nose of the store is roughly in the plane of the wing leading edge and so the store forebody is in this case downstream of the wing leading edge and third, the wing-fuselage junction shape is severely waisted. On the first point, the variation of sidewash with spanwise position beneath a sweptback wing has already been noted in section 2.1.1. while the chordwise position of the store implies that not only would the mean sidewash be less than for the arrangements forming the basis of the R.A.E. method but also the nose of the store may not be in a region of much greater sidewash than if it was say, 0·4 to $0{\cdot}5c$ ahead of the wing leading edge. It is possible that if the store had been mounted at about 0·5 times semispan and if there had been no special shaping on the fuselage, the store side force would again have been underestimated as in the first example.

These two examples should suffice to illustrate that application of the R.A.E. methods should certainly be restricted to the range of geometries as specified in the Table earlier in this Section. If not, considerable errors in the estimation of store side force may result and these errors can be in the sense of an over-

estimate or of an underestimate. Similarly, one feels that any agreement on yawing moments or pitching moments between estimate and measurement could be coincidental.

Another point incidentally brought out by these comparisons is that any method of estimation when allowing for the chordwise position of the store should preferably take note of the position of the store nose and of any tail fins rather than just being related to the mid point of the store. It is true that this could be a somewhat academic point in practice because it is usually found that the length of typical stores is fairly comparable with the local wing chord. This is why for simplicity in the new A.R.A. method for estimating side force as described in Sections 2.2.4. and 6 below, the chordwise position of the centre of the store has been retained as a parameter. This practice makes it more likely however that the reliability of the method of estimation may depend critically on the size of the store and may fail for example if very small stores are being considered.

2.2.4. *New empirical method* (see *also Section* 6). From the discussion above of the R.A.E. methods, it will be clear that such methods are attractive from the point of view of being relatively simple and easy to apply but nevertheless are basically restricted to the range of store-pylon geometries covered in the tests which are analysed to form the basis of the methods. In relation to current requirements, the main limitations of the R.A.E. methods can be summarised as follows:

(1) they appear to be particularly weak in estimating store side force which as noted several times already, may be the critical component when designing an efficient store-pylon arrangement,

(2) except for the very early and outdated note (Ref. 16) they do not give a method for estimating the loads on the pylon itself,

(3) they are at their most reliable when the store nose is about 0·3 to 0·8c ahead of the wing leading edge but this is too restrictive for current practice where, as seen above, the store nose may often be nearer the leading edge,

(4) they include no allowance for the effects of store spanwise position. It would be very difficult to devise a semi-empirical method to cope with all spanwise positions but at least it should be possible to devise factors to cover say the range from 0·25 to 0·8 times semispan,

(5) they are basically methods for incompressible flow with just some suggestions for how the loads could vary in the subcritical Mach-number range whereas the need is for a method for the prediction of the loads over the full speed range from low speeds to supersonic speeds.

To meet these deficiencies, a new empirical method has been devised for the estimation of store (and pylon) side force. This will be described in detail in Section 6 but it is worth stating here what is the range of applications for which it is hoped the method should prove reasonably reliable. The aim has been to cope with the wing-store-pylon configurations likely to be of most interest in the immediate future. This implies that the method should be suitable for

(a) wing designs ranging from say, 30 deg to 40 deg sweptback wings of moderate taper to say, 60 deg delta planforms,

(b) pylons with a thickness/chord ratio of say, 5 or 6 per cent, a maximum thickness of 3 to 4 in, a depth below the wing of 10 to 12 in and a chord of the order of half the local wing chord,

(c) stores of streamline shape with a diameter of say, 14 to 20 in, a length of from 115 to 160 in, a fineness ratio of order 7·5 to 8·5 and with or without small fins with a span of about 1·4 times the store maximum diameter with a fin gross aspect ratio in the region of 1·4 and a fin leading-edge sweepback of about 45 deg.

With the above geometry, the ratio of store length to the local wing chord would be in the region of 0·8 to 1·1 for the sweptback wings or 0·5 to 0·8 for the delta wings; the ratio of store maximum diameter to local wing chord would be in the region of 0·10 to 0·15 or 0·06 to 0·09 respectively and the store centreline would be about one store diameter below the wing.

The method is designed to cope with a range of spanwise positions from say, 0·25 to 0·8 times wing semispan, for a range of chordwise positions from well ahead to well behind the wing leading edge and for a range of depth from 0·5 to 3·0 times store diameter below the wing. The method provides estimates for the speed range from low speeds up to $M = 2{\cdot}0$. It gives expressions for the store loads in the presence

of the wing without any pylon, for the pylon-induced effects on the store and for the loads on the pylon itself so that one can obtain the total store-pylon loads.

The method has been based on an analysis of all the available relevant data. There is a significant amount of data at subsonic speeds up to about $M = 0{\cdot}9$ and for supersonic Mach numbers such as $M = 1{\cdot}6$ to $2{\cdot}0$ but there is very little in the transonic range. It is hoped that further tests may be made in this range to substantiate the interpolated trends that have been suggested. This is very important since it is quite conceivable that the maximum loads may occur in this range. If further testing shows that the maximum loads may occur in this range. If further testing shows that the method as presented is basically sound, the hope is that it could be extended to include other factors, e.g. at the moment, there is no direct allowance for wing sweep on the assumption that the sweepback is not going to vary dramatically from one aircraft to another in the immediate future. Also, the method could be extended to cover other components; at the moment, it is limited merely to store side force.

3. *Experimental Data on Store Loads at Subsonic Speeds.*

A large amount of experimental evidence is available giving store loads at speeds up to about $M = 0{\cdot}94$ for a variety of store-pylon configurations mounted at a wide range of positions on a variety of wing-body combinations.

The major trends in the variation of the store loads with the different parameters will already have become apparent from the discussion in Section 2 dealing with the flow fields in which the stores are placed and the various methods for estimating the store loads at subsonic speeds. Nevertheless, it may be useful now to discuss each of the parameters in turn and to show how they influence the store loads with illustrations from appropriate experimental data. It will be realised from what has been said already that this is more difficult than may appear at first sight since the influence of all the parameters is very interrelated, e.g. the effect of store chordwise position will depend very much on the size of the store relative to the local wing chord. Hence in all that follows in this Section, one must always remember the basic features of the flow fields as described in Section 2.1.

The major parameters can be thought of in seven groups, *viz*,

(1) store shape, size and position;

in this group, the major variables are store chordwise position, spanwise position, depth and the store shape including the effects of fins or wings,

(2) aircraft geometrical characteristics;

in this group, we can include wing sweep, wing thickness/chord ratio, fuselage contouring, etc,

(3) aircraft attitude;

this includes aircraft incidence and aircraft sideslip,

(4) effects of pylon;

the pylon-induced effects will clearly depend on the pylon length, thickness and its position relative to both the store and the wing,

(5) store-aircraft angle;

this includes store tilt and store skew relative to the aircraft,

(6) Mach number,

(7) interaction effects between two or more stores on the same wing panel.

These variables will now be discussed in turn.

3.1. *Effect of Store Chordwise Position.*

Chordwise location is the most significant position parameter because of the large variations in sidewash and downwash with chordwise position in the flow field beneath a sweptback wing (*see* Figs. 4 to 7). For example, as already noted, at an incidence of 8 deg and at a depth of $0{\cdot}1c$ below the 45 deg sweptback wing considered earlier, Fig. 5 shows that in the pitch plane, the flow angle changes from an upwash of about 5 deg at a position $0{\cdot}1c$ ahead of the leading edge to a downwash of about 5 deg, $0{\cdot}1c$ aft of the leading edge. Under the same conditions, the sidewash is about 7 deg close to the wing leading edge but decreases appreciably both ahead and behind this position. The effects of these changes in the local

flow direction (and of the changes in local dynamic pressure) on the loads on a typical store with wing-type lifting surfaces can be seen in Figs. 11 and 12. Summarising briefly the main trends at positive incidence,

(a) the store normal force is at its maximum when the store is some way ahead of the wing leading edge and is relatively small (or even negative) when the store is situated well aft,

(b) the store pitching moment varies from being nose-down for very far forward positions to being strongly nose-up when the centre of the store lies a little way ahead of the wing leading edge to being small and nose-down when the store is further aft,

(c) the store side force is at its maximum for this case when the front of the store lies a little way ahead of the wing leading edge. This conclusion could be very much related to the particular store being tested with its cruciform wings and fins. The examples discussed at the end of Section 2.2.3., for a store having merely fins at the rear, or no fins at all suggested that the store side force could then be at a maximum when the store centre was aft of the wing leading edge with the store nose lying just ahead of the leading edge. Obviously this is a conclusion that depends critically on the actual shape of the store and one must also be careful about the use of loose phrases like 'close to the wing leading edge',

(d) as for the store pitching moments, the yawing moments exhibit what could be called a 'quasi-harmonic' variation with store position, being at their maximum (nose-inward) when the centre of the store lay some distance ahead of the leading edge – about 0·4 to 0·5c in this particular instance. This is because for such a store position, the fins at the rear are in the region of very high sidewash close to the wing leading edge and there is no compensating effect from the forward part of the store.

The conclusions listed above were based on the results for $\alpha = 8$ deg as shown in Figs. 11 and 12. Results for a range of incidence from $\alpha = -8$ deg to $+12$ deg for the same store-aircraft combination are given in Figs. 18a and b. It should be noted that the sketches on the figures that illustrate the store being tested are merely intended to be illustrative; in fact, the store was the same for Figs. 11, 12 and 18. The vertical location of the store relative to the wing in Fig. 18 is the same as the nearer of the two positions in Figs. 11 and 12 but it is likely that similar qualitative trends would have been obtained at other vertical positions.

The effects of chordwise position on normal force are not greatly affected by incidence but this is not true of the pitching and yawing moments or to a lesser extent, of the side force. Fig. 18a shows that whereas the pitching moments at high positive incidence are at their greatest (in a nose-up sense) for positions of the store centre a little way ahead of the wing leading edge, the maximum values at negative incidence are recorded with the store centre much further forward, i.e. at about 0·75c ahead of the leading edge while with the store centre roughly below the wing leading edge large nose-down moments are recorded at negative incidence. These changes with incidence can be related to the downwash characteristics shown in Fig. 7. For a negative incidence such as $\alpha = -8$ deg, Fig. 7 shows that there is relatively large downwash below the wing leading edge and very large upwash over the rear of the section, both maxima occurring further aft than at positive incidence and both maxima being larger in magnitude than at the corresponding positive incidence. These differences between the downwash characteristics at positive and negative incidence relate largely to the contribution from the thickness effects which can be seen in the results for zero incidence. The downwash results explain therefore why the nature of the variation of the store pitching moments with chordwise position at small incidences is more akin to that obtained at negative incidence than to that at large positive incidences.

Although one can thus establish good qualitative correlation between the store pitching moments and the downwash characteristics, it is clear that the precise variation of store pitching moments with chordwise position must depend critically on the presence and position of the wings and fins on the store. This is also true of the store normal-force characteristics as will be discussed below in Section 3.4. Briefly, for a store that is a simple body of revolution or which merely has relatively small tail fins, the effects of chordwise position on the store normal force and pitching moment would have been less pronounced but probably still the same in character, e.g. a reduction in $(dC_N/d\alpha)$ as the store is moved rearward and a 'quasi-harmonic' variation in C_m. It should be noted however that for such a store, the values of $(dC_N/d\alpha)$

would probably be negative (*see* Figs. 20 and 27 for example) and so 'a reduction in $(dC_N/d\alpha)$ as the store is moved rearward' could imply that the absolute values of $|C_N|$ at high α were greater for the more rearward positions.

Incidence also has an effect on the variation of the store yawing moments with chordwise position as shown in Fig. 18b. For all incidences there is a tendency for the largest store yawing moments to be recorded when the store centre is at about $0{\cdot}5c$ ahead of the wing leading edge, the yawing moments being nose-inward at positive incidence and outward at negative incidence. When the store centre is near the wing leading edge, the yawing moments tend to be small whatever the incidence but this result is again obviously dependent on the particular store being investigated and would not necessarily be true for a store without tail fins. With the store centre aft of the leading edge, e.g. near $0{\cdot}5c$, the yawing moments are still fairly small at positive incidence but can rise to large values, nose inward, at negative incidences. This is because the store nose is then in the region of the large negative sidewash which develops somewhere aft of the leading edge, e.g. near $0{\cdot}3c$ at $\alpha = -8$ deg in Fig. 6. The yawing moments under these conditions might have been even more pronounced if there had been no tail fins on the store. Finally, Fig. 18b shows that the store position giving maximum side force also tends to depend on incidence being for this application, somewhat aft of the leading edge at positive incidence and somewhat ahead of the leading edge at negative incidence. Once again, this last result could be dominated by the fact that with the store centre slightly ahead of the wing leading edge, the tail fins are in the region where the largest sidewash develops at negative incidence.

In addition to Figs. 11, 12 and 18, which have been analysed in detail, Fig. 13 presents another example of the variation of store loads with chordwise position; qualitatively, the trends are similar to those discussed above.

It is hoped that this discussion will have shown that even though the effects of store chordwise position may appear large and perhaps random in nature at first sight, they can be explained at least qualitatively in terms of the characteristics of the local flow field beneath the wing. Quantitatively, however, they clearly depend on many other variables and in particular on the length and shape of the store nose and on the presence and position of any wings or fins on the store. Also, all the examples discussed have been for stores in the absence of any pylon and clearly in some cases, the picture could be modified significantly by the pylon-induced effects.* Nevertheless, it is perhaps possible to draw just one or two general conclusions as follows:

(1) the store loads and moments will not in general approach their freestream values until the store c.g. is about 1 to 1·5 wing chords ahead of the wing leading edge,

(2) the store side force and normal force will tend to be at their maximum when the store c.g. or in some cases the store nose is somewhere near the wing leading edge (enough has been said to show that this is a very general statement but with the examples discussed, it may be possible to be more precise when considering a specific store arrangement),

(3) at low or negative incidences, the store pitching moments will tend to be strongly nose-up when the store c.g. is well ahead of the wing leading edge (e.g. $0{\cdot}75c$ ahead) and strongly nose-down when the store c.g. is near the leading edge; at positive incidences, i.e. when applying 'g' during manoeuvres, the pitching moments could be nose-up if the store c.g. is near or slightly ahead of the wing leading edge,

(4) the yawing moments for a store with fins could be at their largest (nose-inward for positive incidences or nose-outward for negative incidences) when the store c.g. is say $0{\cdot}5c$ ahead of the leading edge or more strictly, when the tail fins are in the region of large sidewash near the leading edge; at negative incidences, they could also be large, nose-inward, when the store centre was well aft of the leading edge. For an unfinned store, the store yawing moments for positions ahead of the leading edge would be much smaller but the values for far aft positions could be greater.

As might have been expected the positions giving maximum forces do not necessarily give the largest moments and *vice versa*.

---

*Experimentally, this was not found to be the case with the configuration in Fig. 18, but this is because the pylon is relatively long and the store relatively far below the wing.

3.2. *Effect of Spanwise Position.*

The nature of the variation of store loads with spanwise location is primarily a function of the chordwise position of the store. There is not a great deal of evidence at subsonic speeds but it seems that if one leaves out of consideration the region very close to the side of the fuselage and also the region close to the wing tip, there will be a tendency for the loads to increase as the store is moved outward under a sweptback wing. For example, Figs. 6 and 7 show that the values of both sidewash and downwash at $\alpha = 8$ deg below a 45 deg sweptback wing were higher at 0·75 times semispan than at 0·5 times semispan, e.g. the maximum upwash ahead of the wing leading edge increased from about 4 deg to about 6 deg. To some extent, these trends would be a function of the spanwise lift distribution on the aircraft wing. However, certainly as regards side force, this trend for the loads to increase with distance out along the span have been found fairly generally from an analysis of the results and the variation has been built into one of the empirical factors in the new suggested method for estimating store side force. This can be seen in Fig. 45 which shows the variation of $(dC_Y/d\alpha)$ with spanwise position; what this variation means in terms of the side load on the store depends also both in practice and in the formulae of the empirical method, on the store chordwise position. It will be seen that the changes in the store-alone values are relatively small, but much larger changes are apparent with the store plus pylon – induced values and in the total store plus pylon values. Analysis of the available data suggests that the side force at zero incidence is fairly independent of spanwise position and also, Fig. 52 shows that the variation of $(dC_Y/d\beta)$ with spanwise position is less pronounced: inboard of about 0·5 times semispan, $(dC_Y/d\beta)$ tends to decrease as one moves in but outboard of 0·5 times semispan, there is little change. Comments in the literature suggest that store yawing and rolling moments may vary most with spanwise position.

It is important to note that the regions close to the fuselage and to the wing tips have been excluded from the above discussion. One cannot be precise about what is meant by 'a region close to the fuselage' although graphs such as Fig. 3 may help in defining this for a particular application. Broadly, except at high subsonic speeds and in the transonic range, one might hope that the trends discussed should apply over most of the wing from 0·25 to 0·8 times semispan. In practice, these restrictions about the remarks not applying to the root and tip regions may not matter very much since both structural and performance considerations may often dictate a store position near mid semispan.

3.3. *Effect of Vertical Location.*

Alteration of the spacing between a streamlined store and a swept wing from about 1 to 3 store diameters does not significantly change the character of the variation of the store forces and moments with chordwise position. This is indicated by the comparison in Figs. 11 and 12 where results are given for store depth of 0·15 and 0·37c. It will be seen that reducing the depth from 0·37c to 0·15c increases the maximum forces and moments by a factor of between 2 and 2·5. For store side force, Fig. 50 indicates the variation with store vertical position that has been back-figured from an analysis of the available data; the variation is particularly rapid for depths less than one store diameter.

It should be remembered that the comparison in Figs. 11 and 12 are for store loads in the absence of a pylon. Even allowing for the pylon loads and the pylon-induced effects, however, it is still likely that the total forces and moments will increase as the store is moved towards the wing. This can be seen from Fig. 15. Suppose one considers a reduction in height of pylon from say, 1·6 to 0·8 times store diameter, one finds that after allowing for the reduction in pylon area, the pylon loads are virtually the same while the pylon-induced effects are actually more than doubled. In other words, the reduction in pylon area has failed to compensate for the increase in $\frac{1}{A_p}(dC_Y/d\beta)$ or $\frac{1}{A_p}(dC_Y/d\sigma)$ with d/b_p as shown in Fig. 15.

Once again one should add the reservation that the variation of the store loads with depth of store is a function of the chordwise position of the store. When the store is very close to the wing, the wing-induced store loads can assume very large values (particularly the store side force). Fig. 19 extracted from Ref. 26 shows the effect of decreasing the store depth from 1 to $\frac{1}{2}$ store diameter below at 45 deg sweptback wing at $M = 0{\cdot}90$, for a store of fineness ratio 8·58 located at 0·60 semispan with the store mid point close to the local wing leading edge. The results are again measured in the absence of a pylon. It will be seen

that the normal force, pitching moment and yawing moment show only small changes as the spacing decreases, but the side force values are increased threefold at an incidence of 10 deg. The reason why side force is more affected than the other components is of course that the sidewash is of the same sign over the whole length of the store and therefore the changes in sidewash with vertical position at different chordwise stations all have an additive effect as regards side force; with regard to the yawing moments, the effects over the forward part of the store and the effects towards the rear tend to compensate for one another. Similarly, as regards normal force and pitching moment, the changes in the upwash ahead of the wing leading edge with vertical position tend to compensate for the changes in downwash aft of the leading edge.

3.4. *Effect of Store Shape (Including Fins).*

No general statements can be made regarding the variations of store loads with store shape without a detailed knowledge of the flow field into which the store is submerged and the relationship of the flow to the major force-producing components of the store. In the examples already discussed, there has been reference to the possible effects of the store nose shape and to the presence and position of any wings or fins on the store. Also, it is clear from the earlier discussion that the size of the store relative to the local wing chord could be an important parameter both in determining how the store loads vary with position and in determining the actual magnitudes of the loads. For example, a relatively small store placed in a region of high upwash just ahead of the wing leading edge could experience a very large normal force and a small store placed close to the leading edge in a region of large sidewash could experience a very large side force; on the other hand, the possibility of large pitching or yawing moments would probably not be so great for a small store.

It is worth giving one illustration of what can result from the addition of fins and wings to a streamlined body of revolution. Fig. 20 extracted from Ref. 27 shows the effect of adding fins to a streamlined store located at 0·25 times semispan beneath a 45 deg sweptback wing with the store mid-point at about the local wing mid-chord position. The store fins are thus located aft of the wing trailing edge, but also probably close enough to the fuselage to be influenced by fuselage effects. Pylon-induced effects are included in these measurements.

Without the fins, the store normal force decreases with incidence (*see* Section 3.6. below) but with the fins added, the lift on the fins is sufficient to give a positive value for $(dC_N/d\alpha)$ as for the examples of Figs. 11 and 18; the extra lift at the rear naturally gives a nose-down pitching moment. These effects are much more pronounced at $M = 0{\cdot}96$ than at $M = 0{\cdot}80$. The absolute values of C_Y and C_n are also changed by addition of the fins but there is less effect on $(dC_Y/d\alpha)$ and $(dC_n/d\alpha)$.

The results in Fig. 20 should merely be viewed as an illustration of the possible effects from adding tail fins to a store. The precise magnitude of these effects will clearly depend significantly on the position of the tail fins in relation to the wing flow field. For example, in Fig. 20, the tail fins are aft of the wing trailing edge and thus in a region where there is relatively little variation of sidewash with incidence but where $(d\varepsilon/d\alpha)$ is relatively large. If the store had been mounted further forward with its mid-point ahead of the wing leading edge, the fins at the rear would have been in a region where both the sidewash σ and the resultant local flow direction in pitch $(\alpha - \varepsilon)$ varied more rapidly with incidence (Figs. 6 and 7). This means that with the store in a further forward position, the fins could have a larger effect on the rate of change with incidence of all the components, *viz.* C_N, C_m, C_Y and C_n. Hence to take just one of these points, it would be quite wrong to conclude from Fig. 20 that the addition of tail fins is unlikely to have much effect on $(dC_Y/d\alpha)$ or on $(dC_n/d\alpha)$.

3.5. *Effect of Aircraft Geometry.*

Even at subcritical speeds before shock waves are present, many features of the fuselage and wing geometry could have an influence on the flow fields beneath the wing and hence on the external store loads. Perhaps the most important variables are the wing thickness/chord ratio, the wing sweepback, the spanwise lift distribution across the wing as determined by its planform and warp, the ratio of fuselage

diameter to wing span and whether the wing-fuselage junction is specially shaped, e.g. to suit area-rule considerations. All these factors will affect the critical Mach number and in this respect, their effect on the store load characteristics can possibly be judged if one knows their effect on the clean aircraft stability and performance. Some of the principal effects at sub-critical speeds are noted below:

(1) to a first order, the downwash near zero lift will depend on the product $(t/c \cos \Lambda)$. This is illustrated by a comparison of the downwash results in Fig. 10 with those in Fig. 7. For the 11 per cent thick, 35 deg swept wing in Fig. 10, the downwash close to the leading edge at effectively zero incidence is about 5 deg whereas for the 6 per cent thick, 45 deg sweptback wing in Fig. 7, it is only about 2·5 deg. This would have a major effect on the store pitching moments and in general, the thicker the wing, the greater will be the pitching tendency of the released store. In addition, the downwash field could depend to a lesser extent on wing camber; small amounts of camber tended to reduce the initial angular acceleration of the store upon release,

(2) most of the data presented as illustrations in this report are for wings having a quarter-chord sweepback of about 45 deg. For moderate changes in sweepback around this value, one can probably assume that the lateral load components at zero sideslip vary roughly as $\sin \Lambda$. This would of course be correct in the limit for an unswept wing but there should not be too much reliance on this simple rule because changes in sweep particularly above 45 deg could also change the *shape* of the sidewash contours and thus have an effect for example on the variation of store loads with chordwise position. This would be particularly true for store positions well out along the span and could be expressed another way by saying that the region where tip effects may modify the usual trends with spanwise position could depend on wing sweep,

(3) the effects of wing planform (other than sweep) and wing warp can probably be allowed for crudely by calculating the spanwise lift distribution over the wing. For example, the fairly minor differences that might be found between store loads mounted under sweptback wings of moderate taper and on the other hand, delta wings of about the same sweepback could probably be allowed for if one knew the local C_L at the store position and then assumed that the values of such factors as $dC_Y/d\alpha$ were related on the basis of the same dC_Y/dC_L where C_L is the local lift coefficient,

(4) the ratio of fuselage diameter/wing span is important in determining the extent of the span over which the fuselage-induced effects should be taken into account. Previously when considering the effects of store spanwise position, it was emphasised that the trends being discussed were for the region of the wing where the fuselage effects could be ignored and loosely it was said that for many applications, this would be true outwards from about 0·25 times semispan. Clearly, this must depend on the relative size of fuselage and must be assessed with the help of curves such as that in Fig. 3. An example of where the store loads are evidently influenced by fuselage-induced effects even when the store is at 0·28 times semispan is provided by Fig. 21. It will be seen that the variation of C_Y with incidence with the basic fuselage is rather greater when the store is at 0·28 semispan than when it is at mid semispan: this is at variance with the general trend as discussed in Section 3.2. and hence the fuselage-induced effects must be influencing the results for the store at the inner station,

(5) Fig. 21 also shows that changes in fuselage shape to meet area-rule considerations or to improve the isobar pattern over the wing also have an appreciable effect on the lateral-flow field and hence on the loads induced on stores particularly at positions close to the fuselage. The major effect shown in this figure which is taken from Ref. 15 is for the indented fuselage to reduce the magnitude of C_Y and C_n at zero incidence. In general, this decrease is maintained throughout the incidence range. The results in Fig. 21 refer to the store alone in the absence of a pylon; if the store were connected to the wing by a pylon, much larger differences would be apparent. It should also be noted that the results are for $M = 1{\cdot}2$; no similar comparison at subsonic Mach numbers has been found.

3.6. *Effect of Aircraft Incidence.*

The effects of aircraft incidence have already been discussed in some detail in Section 3.1. when considering the effects of store chordwise position. The effects of these two variables are very interrelated. In general, increasing incidence either positively or negatively tends to increase the absolute values of the

store loads but as can be seen for example from Fig. 18, the rate of variation with incidence depends both on the store chordwise position and on which component is being considered. With the centre of the store some distance ahead of the wing leading edge, the variation of store pitching moment with incidence could be trivial and similarly, with the store centre somewhere near the wing leading edge, the variation of yawing moment with incidence would be small.

An analysis of a large number of different experimental results has shown that in many cases, the store normal force can be taken as varying linearly with incidence over quite a wide range, e.g. from about $\alpha = -4$ to $\alpha = 12$ deg for the standard 45 deg sweptback wing layout shown in many of the figures of this report. For stores with wings or fairly large fins, $(dC_N/d\alpha)$ should be positive with the value depending primarily on the downwash characteristics in the region of the wings or fins. As noted earlier, $(\alpha - \varepsilon)$ will increase more rapidly with α in the region ahead of the wing leading edge than further aft and this explains why for this type of store, $(dC_N/d\alpha)$ tends to be largest when the store centre is somewhere near or slightly ahead of the wing leading edge (Fig. 18). For stores that are simple bodies of revolution or which merely have small tail fins, however, $(dC_N/d\alpha)$ is likely to be negative as shown in Figs. 20 and 27. This trend is indeed predicted in Ref. 17, the R.A.E. method for estimating store normal force. The R.A.E. analysis shows that the negative values of $(dC_N/d\alpha)$ do not depend on whether a pylon is present or not and are therefore due to wing-induced effects rather than pylon-induced effects. In this context, the wing-induced effect that matters is not the downwash but the difference between the local velocities along the top and the bottom of the store. This difference would become more pronounced with increasing incidence in the sense of there being higher velocities along the bottom of the store and hence a down load on the store. For a simple body with no fins, Ref. 17 shows that the negative values of $(dC_N/d\alpha)$ become larger as the store nose moves from a far forward position back towards the wing leading edge and this is what might have been expected from the dynamic pressure surveys shown in Figs. 4 and 8. It follows that for stores mounted further forward than those illustrated in Figs. 20 and 27, the negative $(dC_N/d\alpha)$ trend would be less pronounced.

Store pitching moment coefficients are also generally linear over a small incidence range near $\alpha = 0$ deg but rolling-moment coefficients (for stores with wings and fins) tend to be non-linear. There are quite a number of cases in which the store side force and yawing moment vary in a non-linear manner; for example, both Figs. 20 and 22 give results where $(dC_Y/d\alpha)$ is much smaller near $\alpha = 0$ deg than at high positive incidence. These results draw attention to the dangers involved in extrapolating low-incidence trends.

Section 3.1. contains a more detailed account of the effects of incidence as shown by the fairly comprehensive results of Fig. 18 and there is no need to repeat this description here. One point that is worth making however is to stress that for some applications, the negative g conditions at negative incidence may provide the most severe stressing case. This is not merely because for some positions, the sidewash and downwash can be larger at negative incidence than at the corresponding positive incidence but because of the effects of incidence on the local dynamic pressure below the wing as illustrated in Fig. 8. Near $0{\cdot}2c$, for example, the predicted local dynamic pressure ratio for $\alpha = -8$ deg was about 1·5 as compared with only 0·8 at the corresponding positive incidence; further, Fig. 4 shows that predictions of the increase in the dynamic pressure below the wing at negative incidence can be very conservative. It follows that in addition to the possibility of large angles of flow over the store at negative incidence, the local dynamic pressure could be quite large. The effects of this would be most apparent for stores having a major load-carrying component situated somewhere near $0{\cdot}2$ to $0{\cdot}4c$ aft of the wing leading edge.

3.7. *Effect of Aircraft Sideslip.*

Ref. 28 presents the results of an investigation at high subsonic speeds ($M = 0{\cdot}50$ to 0·94) of the effects of sideslip on the aerodynamic loads on finned and unfinned stores mounted from the wing of a swept wing-fuselage model. A tip-mounted store and an underwing pylon-mounted store at 0·33 times semispan were investigated over a sideslip range from -12 deg to $+12$ deg at various values of incidence. The results for the pylon-mounted finned store were only presented at $M = 0{\cdot}5$ and 0·7 at an incidence of

about 6·5 deg owing to experimental difficulties in the tests. Approximately linear variations of yawing moment, side force and rolling moment with sideslip are evident, whilst normal force and pitching moment show a 'quasi-harmonic' variation.

Ref. 27 contains similar results over the Mach-number range $M = 0{\cdot}8$ to $M = 1{\cdot}43$ for finned and unfinned stores at 0·25 times semispan and also for an under-fuselage location. Some results from these tests are given in Figs. 23 and 24.

Fig. 23 shows the effect of sideslip on the store longitudinal components. In particular, increases in β (of either sign) give a considerable reduction in the store normal force. For example, at $\alpha = 5{\cdot}6$ deg, for the finned store, C_{N_S} at $\beta = 0$ deg is about 0·30 but this normal force can be entirely eliminated by the effects of 8 deg of sideslip. It can also be noted that the effects of sideslip are not quantitatively the same at $\alpha = 0$ deg and at $\alpha = 5{\cdot}6$ deg and therefore it is not just sufficient to determine the effects of α at zero sideslip and the effects of β at a single incidence and then add them together; there is some cross-coupling between the two effects.

Fig. 24 shows the effect of sideslip on the store side force and yawing moments at $\alpha = 5{\cdot}7$ deg and $M = 0{\cdot}80$ while the effect of Mach number on the variation of store side force with sideslip at $\alpha = 0$ deg from the same tests is given in the lower carpet of Fig. 22. (The upper carpet in Fig. 22 gives the corresponding picture for the effects of incidence at zero sideslip; the data in Fig. 20 are also from the same series of tests).

Various features of the results in Figs. 24 and 22 call for comment. First, for the unfinned store at 0·25 times semispan, the variation of the store side force and yawing moment with sideslip is at least twice as large as the variation with incidence. This is particularly true at the higher transonic Mach numbers, i.e. there is a greater increase with Mach number in $(dC_Y/d\beta)$ than in $(dC_Y/d\alpha)$. This characteristic has been incorporated in the charts of the new empirical method for estimating store side force as can be seen by comparing Figs. 47 and 53. It is important to realise that the relative values of $(dC_Y/d\beta)$ and $(dC_Y/d\alpha)$ at any given Mach number are a function of other variables such as the store spanwise and chordwise position. The data being considered here were obtained for a store mounted relatively far inboard and relatively far back on the local chord (*see* Fig. 20). Both these factors would tend to reduce the values of $(dC_Y/d\alpha)$ quite markedly but would have less effect on $(dC_Y/d\beta)$. For example, the comparative effects of spanwise position on $(dC_Y/d\alpha)$ and $(dC_Y/d\beta)$ are shown in Figs. 45 and 52. Hence, the fact that for the present configuration, the variation of the lateral loads with sideslip is more than twice the variation with incidence is a conclusion that should *not* be generalised too far. For a store mounted at say, 0·7 times semispan with its centre somewhere near the wing leading edge, one might easily find that the variation with incidence was greater than the variation with sideslip.

The second point that should be noted from Figs. 24 and 22 is that the effects of incidence and sideslip on the store side force are not simply additive (this is the same conclusion as that noted earlier for the store normal force). For example, at $M = 0{\cdot}80$, $\alpha = 5{\cdot}7$ deg, $\beta = 8$ deg, $C_{Y_S} = -0{\cdot}6$ but the value that would be predicted from $(dC_Y/d\alpha)_{\beta=0}$ and $(dC_Y/d\beta)_{\alpha=0}$ would be only $-0{\cdot}35$, i.e. the side load under combined (α,β) can be appreciably greater than the sum of the loads due to α and β separately. It is important therefore that any programme of wind tunnel tests on the loads on external stores should not be pruned too severely – a full (α,β) carpet should be covered.

Finally, Fig. 24 shows that $(dC_Y/d\beta)$ and $(dC_n/d\beta)$ for the unfinned store are roughly twice as large when the store is mounted beneath the fuselage as for the underwing location (at least, at $\alpha = 5{\cdot}7$ deg). With fins on, the differences are not as great but are still substantial and in the same sense. It follows that in this respect, the apparent trend of a slight reduction in $(dC_Y/d\beta)$ as the store is moved in from say, mid semispan to 0·3 semispan – *see* Fig. 52 – is not maintained when the store is within the influence of the flow field of the fuselage. This is just one more illustration that highlights the difficulty in giving any clear answer to the question of where a store should be placed to give the smallest side loads. Even if one is only thinking in terms of aircraft with wings of about 45 deg sweepback, the answer will depend critically on the likely incidence and sideslip ranges encountered within the flight envelope. Broadly speaking, for a store mounted far out, incidence effects will be the more important while for a store mounted under the fuselage, sideslip effects may be paramount. For the more usual case for the store

mounted somewhere near mid semispan, both have to be considered since with the appropriate signs of incidence and sideslip, the effects will be additive and because of the cross-coupling noted above, rather more than directly additive. Further evidence of the major effect of the fuselage-induced effects on the loading due to sideslip is provided by Ref. 29. This presents the results of pressure distribution measurements on a store located at 0·22 times semispan at Mach numbers from $M = 0{\cdot}80$ to 1·03 for sideslip angles of 0 deg and ± 5 deg. Integrated loads on the store are given and confirm that for such a relatively far inboard store location, the changes of side force with incidence are fairly small but the changes of side force and yawing moment with sideslip are appreciable. This reference is also useful in being one of the few giving data on the side force on the pylon itself. The results show that the pylon side force varies appreciably with both incidence and sideslip. These data have been used in deriving the appropriate factors in the empirical method of Section 6.

3.8. *Effects of Pylon.*

Frequent mention has already been made of the large contributions possible from both the pylon loads and the pylon-induced effects on the store loads, particularly as regards side force. This is very significant because experience has shown that the structural design of the pylon and its attachment to the wing and to the store, are generally determined by the side forces on the store and store-pylon assembly. The side loads are important structurally because they produce large bending moments in the direction of least structural strength and also large twisting moments on the store. Since the pylons usually have to be placed in a region where the sidewash below a sweptback wing is fairly large, it is perhaps not surprising to find that even the pylon-induced effects quite apart from the loads on the pylon itself may be appreciable. A striking illustration of this is provided by the results in Fig. 14 which compares the store-alone and store plus pylon-induced values of side force for an assembly, mounted with the store centre 1·0 store diameters below the wing leading edge at 0·6 semispan, for a 45 deg sweptback wing at a Mach number of $M = 0{\cdot}90$. The data were obtained in the Langley 9 in x 12 in blow down tunnel. It will be seen that $(dC_Y/d\alpha)$ is roughly trebled by the pylon-induced effects. It is clear that for this particular application, when one also allows for the side loads on the pylon, the side force on the store alone when placed in the wing flow field with no supporting pylon represents only a very small fraction of the total side force on the assembly.

The results in Fig. 14 represent however a fairly extreme case. At the other end of the scale, the results shown in Fig. 18 for a store in the absence of a pylon were only slightly affected when a pylon was added. This result evidently came as a surprise when it was obtained and further experimental checks were made to see whether any effects of the gap between the pylon and the store were confusing the picture. These checks merely confirmed that substantially, the conclusion that the pylon-induced effects were small was true for this particular layout. Various reasons can be advanced for reconciling the apparently conflicting results for the configurations of Figs. 14 and 18. For example, the results for Fig. 18 are for low speeds whereas those in Fig. 14 are for $M = 0{\cdot}9$ and it would be expected that the pylon-induced effects would tend to increase with Mach number. Secondly, the pylon for Fig. 14 had a larger thickness/chord ratio and for this reason, the local suctions in the pylon-store junction would be greater. Also, the pylon and store for Fig. 14 were mounted in the chordwise position that would probably give the largest mean sidewash whereas the conclusions for the experiments of Fig. 18 were based on a general comprehensive survey in this respect. All these factors would play some part in the comparison but they are probably less important than the major difference which lies in the ratio of the store diameter/pylon height for the two cases. In the notation of Fig. 15, this ratio (d/b_p) was about 2·0 for the configuration in Fig. 14 but only about 0·6 for the layout of Fig. 18. This difference would have a really major effect on the results as shown by the curve for the pylon-induced effects in Fig. 15. As explained earlier in Section 2.2.1., Fig. 15 was strictly derived for $M = 1{\cdot}6$ but it is probable that similar qualitative trends would be present at subsonic Mach numbers if allowance is made for the different local values of sidewash at subsonic and supersonic speeds. The curves in Fig. 15 were obtained from Ref. 15 which explains that they are based on both theoretical analysis and experiment. Through the use of the wing tip tank theory of Ref. 25 the maximum values of (store diameter/wing semispan) of 0·3 given in that report have been

extended to values up to 1·6 to produce the curves of Fig. 15. It should be noted that the ordinate in Fig. 15 is the side force derivative divided by the A.R. of the pylon and so in absolute terms for a store of given size, the pylon and pylon-induced loads would not increase as rapidly with decreasing b_p as indicated on the graph. Nevertheless, as stressed earlier in Section 3.3., even in absolute terms, the pylon-induced effects will increase dramatically as the pylon height is reduced. Also the loads on the pylon itself do not show a net decrease with reduction in pylon height until (d/b_p) is greater than about 1·0.

It seems clear that the ratio of store diameter/pylon height is the most significant factor in determining the size of the pylon-induced effects. The effects are likely to be small if (d/b_p) is less than say 0·6 but may be all-important if (d/b_p) is say, 1·4 or more. For present-day configurations, the stores are usually mounted about one store diameter below the wing; this implies that the ratio (d/b_p) can be greater than 2·0. For the specification set out in Sections 2.2.4. and 6. for the range of application of the empirical method for estimating store side loads, the range suggested for this parameter is from roughly 1·2 to 2·0. From both these statements, it follows that pylon-induced effects are likely to be very significant for the configurations of current interest. The results shown in Fig. 14 therefore, although slightly extreme, are likely to be much more typical than the fact that the pylon-induced effects were relatively small for the layout of Fig. 18.

Three other points should be mentioned which follow as a consequence of what has just been established. First, while it is true that the empirical method presented in Section 6 for estimating side loads takes account of the pylon effects (*see* Fig. 45), the allowance can only be regarded as giving the effects for a mean representative value of (d/b_p); if this ratio is much smaller than about 1·6, the method is likely to overestimate the pylon-induced effects considerably. Second, no mention has been made of how the effects are likely to vary with pylon sweepback or pylon thickness/chord ratio. There is not sufficient data to analyse either of these parameters systematically. One would expect that reductions in the pylon thickness/chord ratio would tend to decrease the pylon-induced effects particularly at high subsonic Mach numbers. The possible effect of pylon sweepback is much more difficult to assess even qualitatively as it will probably depend significantly on the aspect ratio of the pylon. For the relatively short pylons which give the largest induced effects, it is quite possible that an unswept pylon would have lower surface velocities than one with say, 40 deg sweep and hence, the pylon-induced effects might be less with the unswept pylon. These remarks are very speculative and merely serve to emphasise that even for a given (d/b_p) and a given chordwise position, there could be a considerable variation in the pylon effects due to other geometrical variables. The third and final point is that most of the data discussed in the earlier sections when considering the effects of store chordwise position, spanwise position, etc., were obtained from measurements of store loads in the absence of a pylon. It is quite possible that some of the conclusions drawn regarding the effects of these other variables could be modified when a pylon was present. For example, the pylon effects on the store loads could be less for a far-forward store position with the pylon attached to the rear part of the store than if the store were further aft with the pylon attached in a region of relatively high suctions. Similarly, with changes in the store chordwise position, the pylon attachment to the aircraft wing might vary in chordwise position and results discussed later in Section 5.7. shows that this can be quite important at least at supersonic speeds.

Despite all these reservations, however, there are good grounds for hoping that since the range of pylon-store assemblies that can be used in practice tends to be somewhat limited through non-aerodynamic considerations, the separate conclusions about the effects of different parameters will still remain valid at least qualitatively. To quote an example, if the main aim is to keep the store side loads as small as possible without regard to the other components, the evidence from such figures as Figs. 12 and 18 for the effects of chordwise position and store depth can be combined with the evidence of Fig. 15 regarding pylon-induced effects to select an assembly where the side loads are at least likely to be satisfactory. At the very least, it may be possible to use the figures to reject arrangements which should be completely unsatisfactory. This is in fact the basis of the justification for the method put forward in Section 6. What all the reservations about interrelated effects really imply is that even with the best possible method of estimation, actual measurements of the loads for favoured installations will still be required. This philo-

sophy has been expressed before; it is merely reiterated here because it is clear that the pylon-induced effects and how these vary with a large number of parameters are perhaps the largest source of uncertainty.

3.9. *Effect of Store-aircraft Angle.*

Many experimental reports have considered the effects on the store loads of both skewing and pitching the store relative to the aircraft centreline. These are obvious methods of reducing either the store side force or store normal force and pitching moments under whatever are considered to be the most important flight conditions.

3.9.1. *Store skew.* In an attempt to reduce the large side forces due to incidence caused by the underwing sidewash, Ref. 30 presents the results of skewing the store 5 deg nose-in under a swept wing. As shown in Fig. 25, the effect was to displace the side force curves with little or no change in $(dC_{Y_S}/d\alpha)$. At $M = 0{\cdot}75$, the change in C_{Y_S} from 5 deg skew is roughly the same as that due to 3 deg of incidence. This suggests that $|d\sigma/d\alpha| \simeq 1{\cdot}6$ where σ is the mean sidewash over the store-pylon assembly. This value is rather high compared with the results in Fig. 4 where the maximum value of this ratio was a little less than 1·0. However, three factors in the layout for Fig. 25 could explain the high value: first, the store is fairly far out (0·6 semispan); second, the store is very close to the wing and third, the results are for $M = 0{\cdot}7$ rather than for low speeds. Fig. 25 also gives results for two supersonic Mach numbers as well as $M = 0{\cdot}7$ and these show that the effect of the 5 deg skew on C_{Y_S} is greater at the supersonic Mach numbers.

Another set of results showing the effects of store skew on the side loads is presented in Fig. 26. Once again, skewing the store 5 deg nose-in gives a change in C_{Y_S} that increases with Mach number but is virtually independent of incidence. In this case, 5 deg of skew gives a change that is roughly comparable with the effect of 5 deg of α at $M = 0{\cdot}6$ rising to 7 deg at $M = 1{\cdot}0$. Fig. 26 suggests that at low Mach number, the 5 deg nose-in skew might have reduced the side forces obtained within the flight range of incidence but that for this particular case, the 5 deg skew would tend to give much larger values of the store side loads over most of the incidence range at transonic speeds. Basically, this is because of the relatively large positive values of C_{Y_S} at $\alpha = 0$ deg for even the unskewed store: this trend is particularly pronounced at $M = 1{\cdot}0$.

The effects of store skew on the store side force as shown in Figs. 25 and 26 are quite straightforward but the possible effects of store skew on the store normal force as illustrated in Fig. 27 are much more surprising. The point that needs to be stressed here is that the pylon was skewed at the same time as the store and it is clear that the skewed pylon must have a very large effect on the local flow field characteristics beneath the wing. The net effect is that the store skew which was no doubt introduced to give more acceptable lateral loads is very helpful in reducing the values of store normal force. The variation of C_{N_S} with α is completely changed by the pylon-store skew. The mechanism underlying this effect is not clearly understood but once again, this is a result for a particular application which should possibly not be taken as a general conclusion. It is important to note that at zero skew, this particular layout gives a negative value for $(dC_{N_S}/d\alpha)$. Several factors have been mentioned in Sections 3.4 and 3.6. which could help to explain why $(dC_N/d\alpha)$ is negative for this particular layout. Perhaps the most important is that since there are no large wing-type lifting surfaces on this store, the dominant parameter is the difference in the local velocities over the upper and lower surfaces of the store. It is possible that skewing the pylon has modified this difference in velocities and if so, this could explain why a positive change in $(dC_N/d\alpha)$ has been obtained with the 5 deg skew. Unfortunately, no evidence has been found to show whether skew has any major effect on store normal force for a missile-type store as shown in Figs. 11 and 18 which for the unskewed condition gives a positive $(dC_N/d\alpha)$ and for which the normal force characteristics are primarily determined by the downwash field. This is clearly an area in which more experimental evidence is needed.

For the particular application of Fig. 27, the effects of skew on store normal force tend to decrease with increasing Mach number through the transonic range but again, this is a result which could be peculiar to the particular arrangement being tested. It will be noted for example that the curves for the zero-skew case also change their character with Mach number.

3.9.2. *Store tilt.* Ref. 31 gives the results of some tests on a finned store at 0·33 semispan with the store tilted 5 deg nose down. Reduction of the store pitching moments was accomplished at the expense of substantial increases in the store normal force. These results were of course peculiar to the particular store configuration tested: the more important point is that the change in store incidence gave the expected changes in the longitudinal components. Also, the change in store tilt did not result in any significant changes in the lateral force or moment characteristics. There is little point in quoting more examples here because it should usually be possible to make a fairly good estimate of the effects of store tilt in any particular case while the precise quantitative effects will depend on various detailed factors and will usually therefore be a matter for experiment.

3.10. *Effect of Mach Number.*

The available experimental data showing the effects of Mach number are not nearly as comprehensive as one would like particularly in the transonic speed range. Nevertheless, certain broad trends can be listed.

In the sub-critical range, before any shock waves are present, Fig. 9 illustrates typical effects of Mach number on the flow field characteristics as predicted theoretically. It will be seen that at zero lift, both the sidewash and downwash values increase appreciably with Mach number. It is known that the values of C_p on the surface of a sweptback wing vary roughly as $[1-M^2(\cos^2\Lambda - C_{pi})]^{-\frac{1}{2}}$ where C_{pi} is the pressure coefficient in incompressible flow. It should be noted that the increase in the peak values of downwash and sidewash at zero lift is much greater than this and coincidentally, is about the same as the simple Glauert factor $(1-M^2)^{-\frac{1}{2}}$. The explanation for the more rapid variation in the sidewash and downwash values is that effectively in terms of the wing flow field, any given point becomes closer to the wing surface as the Mach number increases. Hence, the rate of change of either sidewash or downwash with Mach number is also a function of the rate of change with depth below the wing and this is why the variation was described above as being only coincidentally similar to $(1-M^2)^{-\frac{1}{2}}$.

Fig. 9 shows that the variation of the downwash and sidewash with incidence also increases with Mach number. If the results for two Mach numbers are compared at a given C_L, the changes are less marked but the increase in the maximum values of the downwash with Mach number is still apparent while the relatively good agreement shown for the sidewash values at $M = 0$ and 0·8 for $C_L = 0{\cdot}49$ is purely coincidental (the changes in $(d\sigma/dC_L)$ with M have merely compensated for the changes in σ at $C_L = 0$). To some extent, the increase in $(d\varepsilon/d\alpha)$ with M could be somewhat less in practice than that predicted as in Fig. 9 by linear theory. This remark is based on observed differences between experiment and first-order theory for the variation of surface pressure distributions with Mach number.

To sum up the conclusions from Fig. 9, it is probably fair to say that the results are valid in suggesting that the downwash and sidewash at zero lift and hence the store C_{m_0}, C_{Y_0}, should increase with Mach number in the subcritical range; $(d\varepsilon/d\alpha)$ and $(d\sigma/d\alpha)$ should also increase with Mach number but in the case of $(d\varepsilon/d\alpha)$, the increase may not be quite as great as suggested by the results in Fig. 9. One would therefore expect to find an increase in $(dC_Y/d\alpha)$ with Mach number in the subcritical range but one cannot be quite so certain that there would be any appreciable changes in say, $(dC_m/d\alpha)$.

These conclusions are broadly borne out by the available experimental data. For example, on the basis of tests on a pylon-supported tank beneath a 40 deg sweptback wing, Ref. 19 concludes that the values of C_{m_0} should be scaled by $(1-M^2)^{-\frac{1}{2}}$ while $(dC_m/d\alpha)$ and C_N should be taken as independent of Mach number.

Figs. 20, 22, 25, 26, 27, 47, 48 and 51 all provide some indication of how the store loads vary with Mach number not merely at subcritical speeds but throughout the transonic speed range. Perhaps the two most important trends to note are the large variations with Mach number that occur in the side-force coefficient at zero lift and zero sideslip and in $(dC_Y/d\beta)$. There will obviously always be many exceptions to any general rule but it seems fair to say that the maximum values of C_Y for a given store configuration are likely to increase appreciably with Mach number in the transonic range. This makes the relative lack of tests data in this range even more embarrassing than it would otherwise have been.

A few comments can be made about the main trends shown in the actual figures, *viz*,

(1) Figs. 25, 26 illustrate that there can be quite a large increase in the values of C_{Y_0} for $\alpha = \beta = 0$ deg through the transonic range, e.g. for the unskewed store in Fig. 26, C_{Y_0} increases from about 0·25 at $M = 0{\cdot}6$ to 0·35 at $M = 0{\cdot}8$ and 0·45 at $M = 1{\cdot}0$ before falling to 0·25 at $M = 1{\cdot}2$. The changes in C_{Y_0} for the configuration in Fig. 22 are less pronounced but it should be noted that in this case, the values of C_{Y_0} are fairly small irrespective of Mach number. For the standard type of store layout assumed for the empirical method of estimating side loads in Section 6, Figs. 48 and 51 for unfinned and finned stores respectively give the variation of C_{Y_0} with Mach number; these curves were obtained from an analysis of all the available data. There seems little doubt that the trend for C_{Y_0} to increase with Mach number to a maximum somewhere near $M = 1{\cdot}0$ and then to decrease and ultimately change sign at some supersonic Mach number is correct but it should be emphasised that the available data are not really sufficient to be sure of the true quantitative variation. In particular, there is the rather odd apparent result in Fig. 48 that the pylon-induced effects on C_{Y_0} change sign somewhere in the transonic range. Several reasons could be suggested why the pylon-induced effects could vary with Mach number but the idea that they could change sign seems physically unsound. One has to admit that the pylon-induced effect proposed for supersonic speeds in Fig. 48 is entirely based on a single set of results at $M = 1{\cdot}6$. The unsatisfactory nature of Fig. 48 is a graphic illustration of the need for more data in the transonic range. (Perhaps it should be stressed that it is only the effect of Mach number on the pylon-induced effects on C_{Y_0} that is difficult to explain physically; in practice, the maximum values of C_Y for a pylon-store assembly will depend rather more on the values of $(dC_Y/d\alpha)$ and $(dC_Y/d\beta)$ and for these terms, the pylon-induced effects suggested in Figs. 45, 47, 52 and 53 appear to be at least physically plausible).

(2) Increasing Mach number through the transonic range appears to have a much larger effect on $(dC_Y/d\beta)$ than on $(dC_Y/d\alpha)$. This is shown most clearly by the results in Fig. 22. For this configuration, $|dC_Y/d\beta|$ roughly doubles between $M = 0{\cdot}8$ and 1·2, most of the increase occurring between $M = 0{\cdot}9$ and 1·0. Figs. 47 and 53 also bear out the suggestion that in the transonic range, Mach number has a larger effect on $(dC_Y/d\beta)$ than on $(dC_Y/d\alpha)$. A distinction should possibly be made here however between what happens in the 'transonic range' and what happens in the 'subcritical range'. As regards the relative lack of variation of $(dC_Y/d\alpha)$ with M, the results being discussed here with the possible exception of those in Fig. 26 strictly suggest merely that there is little variation close to $M = 1{\cdot}0$ or that the results at say, $M = 1{\cdot}2$ to 1·4 are similar to those at say, $M = 0{\cdot}8$. Other unpublished data show that significant increases in $(dC_Y/d\alpha)$ with M can occur in the sub-critical range, e.g. for stores mounted at 0·47 and 0·7 times semispan with the store centre roughly below the leading edge of a 6 per cent thick, 40 deg sweptback wing, $(dC_Y/d\alpha)$ increased by about 20 per cent between $M = 0{\cdot}6$ and about $M = 0{\cdot}85$ but then decreased again between $M = 0{\cdot}85$ and $M = 1{\cdot}0$; $(dC_Y/d\beta)$ on the other hand increased to a maximum at a Mach number much nearer $M = 1{\cdot}0$. These trends could of course depend not merely on the aircraft wing flow field characteristics but also on the shape and position of the store being tested. It may be rash therefore to draw any general conclusions but the impression from the available data is that $(dC_Y/d\alpha)$ is likely to reach a maximum somewhere near the critical Mach number of the aircraft and then to fall again before rising somewhat above $M = 1{\cdot}0$ whereas $(dC_Y/d\beta)$ may show a more substantial rise continuing to near $M = 1{\cdot}0$ followed by only small further changes (*see* Figs. 47, 53).

(3) The results in Fig. 20 illustrate that the lift contribution from the tail fins on a store can increase appreciably with Mach number at high subsonic speeds, i.e. in the lower part of the transonic range. For this example, the tail-fin contribution to $(dC_N/d\alpha)$ roughly doubles between $M = 0{\cdot}80$ and $M = 0{\cdot}96$ with a corresponding change to $(dC_m/d\alpha)$. This sort of effect could also be part of the explanation for the radical change with Mach number in the C_{N_S} versus α curves in Fig. 27 for the unskewed store. In this case, however, there could be another more important factor. As explained earlier, the negative value for $(dC_N/d\alpha)$ at low Mach numbers for this store assembly is probably largely a function of the different local velocities along the top and the bottom of the store as a result of the wing-induced flow field. In supersonic flow, the rate of change of velocity with depth below the wing – at least along the local Mach lines would be expected to be much less rapid and thus, this could be the major reason for the relatively small values of $(-dC_N/d\alpha)$ beyond $M = 1{\cdot}0$ as compared with those at say, $M = 0{\cdot}6$ to 0·8.

(4) The results in Figs. 25 and 26 show that the effect on store side force of a given amount of store skew increases with Mach number between high subsonic and low supersonic speeds.

3.11. *Interaction of two stores on one wing panel.*

The interference effects between inboard and outboard stores on the same wing panel have not received a great deal of attention. Indeed, no published information at subsonic speeds has been discovered during the literature search. Some unpublished data have however been analysed for an example in which stores were mounted at 0·47 times and 0·70 times semispan below a wing with 37 deg sweepback on the quarter-chord line and a thickness/chord ratio varying between 6 per cent and 7 per cent. Both store centres were roughly below the wing leading edge at a depth of about $0{\cdot}23c$ for the inner store and $0{\cdot}33c$ for the outer store. Measurements were made of the pylon root bending moments with the stores mounted either separately or alternatively together. To the first order, the pylon root bending moments should be proportional to the total side force on the store-pylon assembly. The results are interesting in showing that both $(dC_{Y_{SP}}/d\alpha)$ and $(dC_{Y_{SP}}/d\beta)$ for either store are reduced when the other store is present by as much as 18 to 23 per cent. Results were only obtained for two Mach numbers ($M = 0{\cdot}60$ and 0·92) but allowing for some scatter in the results, no significant trend with Mach number was observed in this limited test.

It is clear from this one example that the interference effects from one store on another can be significant and that this is an area in which further experimental information is needed.

4. *Flow Fields and Load Prediction Methods for Supersonic Speeds.*

It is clear from the literature that the position regarding the prediction of store loads at supersonic speeds is at least better than the uncertain state-of-the-art at transonic speeds. On the other hand, methods have been developed for estimating the aircraft flow-field characteristics and the various interference effects between the aircraft wing, pylon and store. Also, a large amount of experimental data on store loads at supersonic speeds is available from American reports – particularly for $M = 1{\cdot}6$ and 2·0. These experimental data are sufficient to give a general idea of how the store loads vary with the different parameters but, as is usually the case with experimental surveys, the data are somewhat more limited in scope than may appear at first sight. This is despite the fact that the stated aim of the experiments was to investigate a wide range of configurations irrespective of whether the store was mounted in a 'practical' position or not. One of the drawbacks is that most of the results are for a relatively large store which is either just a simple body of revolution or which has merely some small tail fins. As will be seen from the analysis below, rather different results might have been obtained for a smaller store or for a store with wing-type lifting surfaces.

As at subsonic speeds, the natural starting point is to consider the wing-fuselage flow fields in which the stores are immersed. Various reports can be quoted that help in this respect. For example, Ref. 32 presents equations for calculating the sidewash due to incidence, wing thickness and fuselage thickness. The detailed theoretical expressions for the sidewash due to wing incidence are quoted again in Ref. 33 which also includes charts for determining the sidewash near a semi-infinite triangular wing with any leading-edge sweep. This analysis can be applied to determine the sidewash due to incidence in most of the region below a wing of finite span and chord, irrespective of whether the wing leading edge is subsonic or supersonic. Corresponding expressions for the longitudinal and vertical velocity components and hence for the resultant velocity and the downwash due to wing incidence are contained in Refs. 34, 35, 36 and 37 while expressions for the downwash due to wing thickness are given in Refs. 38, 39 and 46. All these methods are based on linear theory; the results of such calculations are however compared with experimental data in Refs. 41 and 42. In Ref. 42 in particular, it is shown that improved estimates can be obtained if the theoretical assumptions are modified in the light of details of the flow field as revealed in schlieren photographs. The downwash and sidewash characteristics are discussed in detail below in Section 4.1.

At supersonic speeds, the influence of the wing flow field is not merely confined to the mean sidewash, downwash and velocity over the store. There is a further important factor for which there is no direct

parallel in subsonic flow. The wing static pressure field is propagated in a direction roughly corresponding to the stream Mach angle and as a result, the wing pressure field can strike the upper surface of the store ahead of where it would affect the lower surface. These induced pressure distributions can be very significant in supersonic flow because up to the point where the wing flow field intersects the store, the variation in the magnitude of the pressures with depth below the wing is relatively slight. The important point however is that for a store of finite diameter, there is an appreciable axial displacement between the induced pressure distributions on the top and bottom of the store and this can give rise to a significant 'buoyancy' normal force and pitching moment. Other components are affected but to a lesser degree. This type of wing-induced interference has to be considered in a rather different light from the sidewash and downwash effects. One cannot discuss the problem in terms of the wing-fuselage flow field without referring to the position and the size of the store, in particular, its diameter. Even the cross-sectional shape of the store could be important because this will control the way in which the induced flow field is propagated round the store surface. Also, in this context, it may be necessary to consider not simply the wing-fuselage flow field but the composite wing-fuselage-store flow field. At supersonic speeds, the wing flow field will reflect in the store upper surface and similarly, the store flow field will reflect in the wing lower surface and the reflected waves will reflect again and so on. There is therefore the possibility of at least a two-fold multiple shock-reflection system between the store and the wing lower surface and it is a matter for experiment as to whether all these factors have to be taken into account. The possible magnitude of the pressure-field interference effects is discussed below in Section 4.2. together with a discussion of the validity of the available methods for estimating these effects.

Having established the local sidewash and downwash over the store and estimated the wing-induced interference effects, the next step is to evaluate the resulting forces on the store and its supporting pylon. For the all-important side force component, Ref. 32 is again a good general reference but it does not include any evidence on the loads on the pylon itself. To get the full picture on this, one has to go to Refs. 15 and 44. All these reports contain numerous comparisons between predicted and measured store loads; other such comparisons are included in Refs. 45, 46 and 47. These methods for estimating the store loads and the comparisons with the experimental data are discussed below in Section 4.3. It is emphasized that the success obtained in estimating the side force and other lateral components is again critically dependent on whether one can estimate the pylon loads and the pylon-induced effect of the store loads correctly. This point is perhaps more important in supersonic flow that it was at subsonic speeds. Section 4.3. comments on what the comparisons imply regarding the validity of the methods for estimating the loads; it also includes some warnings about drawing too many general conclusions from the specific comparisons presented.

Alternatively, as at subsonic speeds, one can tackle the problem in a more empirical fashion. Instead of using methods which start from calculating the detailed flow-field characteristics, one can take the large mass of the available experimental data and try and produce a semi-empirical method for relating the store loads to Mach number and the different geometrical parameters. The new method presented in Section 6 for estimating side force is an example of this approach.

Section 4.4. contains a brief summary of the present position with some remarks about how the choice as to what is the best approach is affected by the changes that occur between subsonic and supersonic speeds.

4.1. *Wing-Fuselage Flow Fields at Supersonic Speeds.*

4.1.1. *Local sidewash.* Because of its importance in the prediction of pylon-store side force, underwing sidewash has received more attention than the other flow-field properties. Refs. 32 and 33 contain equations for estimating the sidewash due to wing incidence while Ref. 32 also gives methods for estimating the sidewash due to both wing and fuselage thickness. Sidewash due to fuselage incidence has also been calculated but the suggestion is made that in some cases this can be ignored (except for a store very close to the fuselage).

The methods are based on linear potential-flow theory and are therefore strictly applicable only to slender bodies and thin wings at low angles of incidence. For the sidewash due to wing incidence, the

lateral perturbation velocities due to a flat-plate lifting triangle of infinite chord are determined from equations involving free-stream Mach number, angle of incidence and wing geometry. It is explained in Refs. 32 and 33 that this enables one to calculate the sidewash for much of the region below wings having finite taper and chord. Treatment of alternatively the subsonic, sonic or supersonic leading-edge case is possible.

The equations and charts in Ref. 33 can be applied to wings of any leading-edge sweepback but the basic example for which calculated results are presented in Ref. 32 is the configuration shown in Fig. 28. This consists of a simple delta wing with a leading-edge sweepback of 60 deg mounted on a body with a fineness ratio of 10·0.

Fig. 28 presents the calculated sidewash due to wing incidence at $M = 1{\cdot}6$ and $2{\cdot}1$ for stations at 0·25, 0·5 and 0·75 times semispan at a depth of 0·1 times semispan below the wing. At $M = 1{\cdot}6$, the leading edge is subsonic while at $M = 2{\cdot}1$, it is just supersonic and therefore, the comparison between the results for the two Mach numbers is of particular interest.

For the subsonic leading edge ($M = 1{\cdot}6$), the calculated sidewash is zero ahead of the Mach cone emanating from the wing root-fuselage junction; it then increases rapidly to a maximum at a position just aft of the wing leading edge, the maximum value increasing steadily with distance out along the wing. Downstream of the maximum, the sidewash decreases but the spanwise variation in sidewash along the wing trailing edge is comparable with the variation in the maximum values just aft of the leading edge. As a result, considerable sidewash due to incidence is present over the whole chord for stations near the wing tip. If one compares these results with those obtained at subsonic speeds (Fig. 6), one finds that the main differences are:

(a) the disappearance of the sidewash ahead of the Mach cone from the wing-root leading edge,

(b) the consequent high values of $(d\sigma/dx)$ between the forward edge of this Mach cone and the wing leading edge,

(c) the relatively large sidewash present towards the rear of the outer wing.

It should be noted that the differences in the maximum values of (σ/α) in Figs. 28 and 6 should not be taken as necessarily indicating an increase with Mach number. The differences can be explained largely in terms of the change in wing leading-edge sweepback between Figs. 28 and 6; the values are roughly proportional to sin Λ. On the other hand, from what has been said earlier, this does not mean that the values of (σ/α) would not have varied with Mach number at intermediate speeds. Almost certainly, there would be an increase with Mach number in the subsonic range and a decrease at transonic speeds.

Broadly speaking, therefore, the differences between the values of (σ/α) at supersonic speeds with a subsonic leading edge and those at low speeds are in points of detail. Fig. 28 shows however that the changes that occur when the wing leading edge becomes supersonic are much more dramatic. For the supersonic leading edge, the results for $M = 2{\cdot}1$ in Fig. 28 illustrate that in the region between the wing leading edge and the Mach cone from the wing root leading edge-fuselage junction, the sidewash due to incidence is large and independent of both spanwise and chordwise position. Further downstream, within the Mach cone, the sidewash decreases rapidly and the values near the wing trailing edge are not dissimilar from those obtained at the lower Mach number. The peak values of (σ/α) obtained in the region between the leading edge and the Mach cone are 1·3 in this case as compared with values at $M = 1{\cdot}6$ which vary from 0·6 at 0·25 to 1·13 at 0·75 times semispan. It follows that the changes in sidewash that can be experienced by a pylon-store as the wing leading edge becomes supersonic would be greater for an assembly mounted below the inboard part of the wing. For the worst position, it is quite conceivable that the mean sidewash could almost double with a small increase in Mach number as the leading edge becomes supersonic. It should be stressed at this point that these remarks are all based on linear-theory calculations. In actual practice, as shown below, the changes would occur at somewhat higher freestream Mach numbers since because of the effects of the finite wing thickness, the leading-edge shock would remain detached up to a somewhat higher Mach number than suggested by linear theory. Also, by analogy with other results from linear theory, it might be expected that the peak maximum values would not be fully realized in practice and the experimental data included in Fig. 32 tend to confirm this. Never-

theless, it is probably fair to say that some substantial increase in side force should occur as the Mach cone moves downstream of the nose of the store and more particularly, downstream of the leading edge of the supporting pylon.

The sidewash due to wing and fuselage thickness is shown in Fig. 29. The lateral perturbation velocities due to body thickness were obtained from an integration of the velocities from an axial distribution of sources (Ref. 13), whilst the velocities due to wing thickness were calculated for a distribution of sources in the chord plane of the wing.

Fig. 29 shows that the sidewash due to body thickness is zero up to the Mach cone originating at the fuselage nose and also downstream of the Mach cone originating at the end of the forebody ($x/L = 0{\cdot}5$). This last result arises merely because for this particular application, the rear part of the body is a circular cylinder; if it were boat-tailed for example, some sidewash would have been induced. The maximum sidewash due to the body occurs on the Mach cone originating at approximately a third of the distance from the tip to the end of the forebody; the maximum value decreases with distance out from the body but even at 0·75 times semispan, it is still about 1·5 deg. It is clear that it is no longer valid as at low subsonic speeds to ignore the fuselage-induced sidewash for stores mounted outboard of about 0·2 times semispan. Indeed, as shown in Fig. 29, the body-induced sidewash can be comparable in magnitude to that induced by the wing thickness. As for the latter, results are plotted for two wing thickness/chord ratios, *viz*, 5 per cent and 3 per cent thick rhombic sections. The sidewash due to wing thickness begins at the Mach cone originating at the wing leading-edge body junction and then quickly reaches a maximum which for this example at $M = 1{\cdot}6$, occurs ahead of the wing leading edge. Aft of about $0{\cdot}5c$, the sidewash due to wing thickness changes sign and it is important to note that quite large negative values (i.e. inward towards the root) can occur towards the rear of the wing, e.g. $-4{\cdot}5$ deg for the 5 per cent thick section. These values would probably be less extreme for a more conventional aerofoil section shape.

It is again instructive to compare the sidewash due to wing thickness in Fig. 29 with the results at $\alpha = 0$ deg for the 6 per cent thick, 45 deg sweptback wing in incompressible flow as shown in Fig. 6. The most important difference is that the change from positive to negative sidewash occurs at the leading edge at $M = 0$ but on the Mach cone originating from the wing root maximum thickness position in supersonic flow. Further, if one believes the linear-theory predictions, the change occurs discontinuously in supersonic flow and also, the negative sidewash to the rear is greater than in subsonic flow.

These differences in the sidewash distributions at zero incidence lead to one important practical conclusion. This is that there will be quite a range of applications at supersonic speeds for which the resultant side force, C_{Y_0}, on the store would be fairly small if there were no pylon-induced effects. This is because the local sidewash would vary from being positive over the forward part of the store to negative over the rear part. At subsonic speeds, as shown earlier, the tendency was for C_{Y_0} to be significant and positive. The conclusion that C_{Y_0} apart from the pylon-induced effects should be fairly small is based on the assumption that the store is fairly large, e.g. with a length comparable to the local wing chord. It should not of course be generalized too far. It would not necessarily apply to a small store; also, if the store has its centre well ahead of the wing leading edge or if the wing is relatively untapered as compared with the delta planform of Fig. 29, C_{Y_0} could be significant and negative. On the other hand, if the store is far aft, C_{Y_0} is likely to be positive. Whatever the store position, as the Mach number increases, less of the store will be influenced by the negative sidewash at the rear and so with increasing Mach number, C_{Y_0} should tend towards a negative value; this explains the trend shown in Fig. 48.

Fig. 30 presents, for three values of incidence, the separate effects of wing incidence, fuselage thickness and wing thickness, together with the composite effect for the mid semispan station on the same delta wing at $M = 1{\cdot}6$. The composite figure shows that for an incidence of about 8 deg, the underwing sidewash values vary from about 11 deg near the wing leading edge to about -1 deg near the trailing edge (it should be remembered that σ is positive for flow outward from root to tip). The peak maximum value of about 11 deg compares with about 7 deg at the same incidence for the mid semispan station below the 45 deg swept wing in incompressible flow (Fig. 6) but this difference can be largely accounted for by the larger wing sweepback and the fact that results are being presented for a depth of $0{\cdot}115c$ below the wing rather than $0{\cdot}15c$. It is possible that for a given depth below a given wing, the maximum sidewash at

supersonic speeds (but with a subsonic wing leading edge) might be less than in incompressible flow. As noted earlier, a rapid increase could occur when the Mach number was sufficient for the wing leading-edge shock to move downstream of the leading edge.

The discussion so far has been based entirely on the results of the linear-theory calculations. To see whether these are valid or not, reference can be made to the results of experimental flow surveys. Ref. 42 contains results for three wing-body combinations, trapezoidal, 45 deg sweptback and 60 deg delta wing planforms. Measurements were made of the local Mach number, static pressure, downwash and sidewash at incidences of 0, 4 and 8 deg, for Mach numbers of 1·61 and 2·01. These four parameters are plotted in Ref. 42 against chordwise position, other variables remaining constant. Fig. 31 shows a sample of these results for the 45 deg sweptback wing at $M = 1{\cdot}61$. Downwash and sidewash values are plotted for the three test incidences for the station at 0·55 times semispan and for a depth of $0{\cdot}37c$ below the wing.

No direct comparison with theory is included in Fig. 31 but the sidewash results for zero incidence at both $M = 1{\cdot}61$ and 2·01 are compared with linear-theory predictions in Fig. 32. It will be seen that the jump in the sidewash distribution at the wing leading-edge shock occurs further forward than predicted and also, the magnitude is somewhat less. These discrepancies can be related to the effects of the finite wing thickness on the position of the wing leading-edge shock. Schlieren photographs confirmed that this shock was still detached at $M = 1{\cdot}61$ whereas according to the linear theory for a flat-plate wing, it should have been lying across the wing at this Mach number. This thickness effect can be allowed for approximately when calculating the sidewash by taking as the stream Mach number, not the true value but the lower figure that would give according to linear theory, the leading-edge shock direction as observed in the schlieren photographs. This use of a fictitious stream Mach number (1·4 rather than 1·61 in the present case) is the basis of the revised estimate labelled 'modified linearized theory' and it will be seen that the sidewash results calculated for $M = 1{\cdot}61$ then lie much closer to the measured values. No schlieren photographs were available for $M = 2{\cdot}01$ and so it was not possible to present revised estimates for this Mach number; nevertheless, it is clear that a similar revision would again lead to better agreement with experiment.

Returning to the sidewash results at incidence in Fig. 31, it seems that linear theory – or at least the modified version as proposed above – should also be a reasonable guide in predicting the values of (σ/α). There would however be some differences in points of detail, e.g. even when based on the effective fictitious stream Mach number, the predicted values of (σ/α) should be largest just behind the wing leading edge but from the measured results in Fig. 31, (σ/α) increases back to about 0·3 of the local chord and then remains reasonably uniform back to the trailing-edge shock.

In assessing these effects of incidence, two points could be relevant. First, there is the general principle that disturbances tend to be propagated at the Mach angle corresponding to the local Mach number of the flow rather than the free-stream value. The local Mach numbers would vary with wing incidence and as an example, Fig. 31 suggests that the direction of the wing leading-edge shock becomes somewhat less swept with increasing incidence. Such trends would have the effect of smoothing the sudden discontinuities that would be predicted in the chordwise distributions of (σ/α).

The second point that should be noted is that for this example at least, it would be wrong to ignore the sidewash due to fuselage incidence. This is certainly true for instance in the region ahead of the wing leading-edge shock. Here, for $\alpha = 8$ deg, (σ/α) downstream of the fuselage bow shock (which is outside the range of these plots in Fig. 31) is of the order of 0·25. The fact that (σ/α) in this region is greater for $\alpha = 8$ deg than for $\alpha = 4$ deg suggests that the sidewash may be increased by the effects of vortices shed from near the fuselage nose.

It is thus possible that when the various second-order effects and the sidewash due to fuselage incidence are taken into account, the details of the measured sidewash distributions at incidence could be explained satisfactorily. The most important net result is that the maximum value of (σ/α) is about 0·85. Bearing in mind that these results are for a position well below the wing ($0{\cdot}37c$ rather than $0{\cdot}115c$ as in Fig. 30), this maximum value is relatively large: for a corresponding position below a similar wing in incompressible flow, a value of 0·5 rather than 0·85 would be typical. The larger value at supersonic speeds could be partly

explained by the greater effects of fuselage incidence as noted above and also by the slower decay with distance below the wing, in the wing-induced flow field. In both respects, the key is the greater lateral extent of flow fields at supersonic speeds.

To sum up the evidence from Figs. 31 and 32 and the further comparisons in Refs. 41 and 42 it seems that linearized theory provides a sound basis on which to evaluate the sidewash below an aircraft-fuselage configuration at supersonic speeds. It is desirable however to allow for the effects of finite wing thickness on the direction and position of the wing leading-edge shock. Preferably, this should be done on the basis of schlieren pictures of the actual flow around the wing-fuselage configuration but if these are not available, the calculations should be made for a corrected Mach number which for a 5 per cent thick wing would be about 0·2 below the true free-stream value. In addition to this empirical change, the true sidewash distributions would probably be somewhat smoother than those calculated and the maximum values may be slightly smaller. The particular fuselage shape may also modify the distributions somewhat in detail but despite the various second-order effects, one would imagine that the calculated sidewash distributions should be satisfactory for the purpose of estimating the integrated side force and yawing moment on a store-pylon assembly and this is indeed confirmed by the comparisons to be discussed later in Section 4.3.

4.1.2. *Local downwash.* Although the application of the theory in Ref. 32 has been devoted primarily to the sidewash problem, it appears that downwash is amenable to the same type of theoretical treatment and the appropriate equations are developed in Ref. 35. Other appropriate references are Refs. 34, 37 and 49.

Typical experimental chordwise distributions of downwash are plotted in Figs. 31 and 32 to correspond with the sidewash distributions just discussed for the 45 deg sweptback wing fuselage layout. In Fig. 32, the results at zero incidence are compared with predictions both by linear theory and by the 'modified linear theory' using the fictitious stream Mach number derived as explained above in Section 4.1.1. Fig. 32 shows that at $M = 1{\cdot}61$ very good agreement is achieved between the experimental results and the modified predictions and it is likely that if it had been possible to make a similar comparison for $M = 2{\cdot}0$, the picture would have been almost as good. If the downwash distributions in Figs. 31 and 32 are compared with those for incompressible flow in Fig. 7, the main new trends evident at supersonic speeds are as follows:

(1) the disappearance of the upwash due to incidence for the region ahead of the wing leading-edge shock,

(2) the much greater significance of the downwash contribution from wing thickness. At $0{\cdot}2c$ below the wing (Fig. 32), this varies from about 4 deg near the leading edge to -4 deg near the trailing edge; at $0{\cdot}37c$ (Fig. 31), the corresponding values are ± 3 deg. At $M = 0$ for a wing of the same thickness, the values are only about $\pm 2{\cdot}5$ deg for $z = 0{\cdot}15c$,

(3) the chordwise distributions of (ε/α) even downstream of the wing leading-edge shock are of a different shape. Instead of there being a maximum somewhere along the chord as at subsonic speeds, the maximum does not occur until just ahead of the wing root trailing-edge shock which since the trailing edge is supersonic, lies downstream of the wing at this station,

(4) down of the wing root trailing-edge shock, (ε/α) is essentially zero.

All these differences between the downwash distributions at subsonic and supersonic speeds are in line with what would be expected on the basis of the effects on the loading over the wing surface. They can have quite a major effect on the likely variation of the store normal force and pitching moment with chordwise position. Several reports have tried to assess this and at first sight, there is a good deal of confusion about the conclusions. Basically, however, this is not because the results are inconsistent amongst themselves but because the wording of the conclusions can be too imprecise. It is not enough to refer to the store chordwise position in relation to the wing leading edge as at subsonic speeds. Since the wing flow field is propagated at roughly the Mach angle, the effects are really a function of $\{x-(M^2-1)^{\frac{1}{2}}z\}$* rather than simply x. Also, the conclusions could vary appreciably with store length –

*or more generally, $\{x-(M^2-1)^{\frac{1}{2}}(y+z)\}$

this will become clearer after reading Section 4.2. below. The most important point is to state how much of the store lies ahead of or behind the wing leading-or trailing-edge shocks. Bearing these points in mind, a few comments can be made about the influence of the downwash characteristics in Figs. 31, 32 for a relatively large store capable of producing a significant $(dC_N/d\alpha_1)$. Three types of store position in the flow field can be distinguished, *viz*,

(a) with the store nose ahead of the wing leading-edge shock and therefore in the region of small downwash and with the rear part of the store in the region of the large downwash downstream of this shock. For this type of position, $(dC_N/d\alpha)$ would be less than for the isolated store but large nose-up moments could be present,

(b) with most of the store lying between the wing leading-edge and trailing-edge shocks, $(dC_N/d\alpha)$ would be much less than for the isolated store, $(dC_m/d\alpha)$ would also tend to be slightly positive because of the trend for $(d\varepsilon/d\alpha)$ to increase to a maximum just ahead of the wing trailing-edge shock. It follows that the overall values of C_N and C_m at incidence for a store in this position are likely to be determined primarily by the values of C_{N_0} and C_{m_0} and in view of this, the buoyancy contributions could be more important than the downwash effects,

(c) with a further aft position with only the nose of the store lying ahead of the wing trailing-edge shock, $(dC_N/d\alpha)$ is likely to be relatively large. $(dC_m/d\alpha)$ could be negative but relatively small and for some positions, not sufficient to offset the possibility of appreciable positive C_{m_0} values – *see* below.

These conclusions are only intended to give a very general idea of the possibilities. It cannot be stressed too strongly that the right course is to estimate the flow field characteristics and then estimate the likely effect on the particular store being considered; the presence and position of any wings or fins on the store could affect the conclusions considerably.

4.2. *Static Pressure Distributions in Composite Aircraft-Store Flow Field.*

Even in subsonic flow, it is not always sufficient to calculate the flow sidewash and downwash characteristics and then to estimate the store loads on the basis of suitable mean angles together with a mean local velocity. The store normal force and pitching moment for an installation that was either just a simple body of revolution or which had merely relatively small tail fins could depend primarily on the difference between the general level of velocities over the store upper and lower surfaces; this difference would vary with incidence. In other respects however, results at subsonic speeds could often be related to the mean values of σ, α and q.

At supersonic speeds, however, it is quite essential to take into account the way in which the wing-induced static pressure field is propagated around the store surface. This affects principally the normal force and pitching moment but it does have some effect on the other components. The wing-induced static pressure field is propagated below the wing surface in a direction that loosely can be taken as corresponding to the stream Mach angle. Hence, the main features of this pressure distribution, e.g. the wing leading-and trailing-edge shocks and the intervening expansion waves strike the store upper surface some way ahead of where the store lower surface is affected. The decrease in the pressure perturbations with distance below the wing is relatively slow and so the pressure field that is induced on the upper surface of the store only decays slowly with increasing store depth. Hence this type of interference remains significant until the store is far enough below the wing for it to lie ahead of the wing leading-edge shock. As will be seen below, there are quite a number of detailed differences between the pressure distributions induced on the store upper and lower surfaces but the main factor is that noted above, *viz*, the axial displacement between these distributions. This axial displacement is clearly a function of both the stream Mach number and the size and shape of the store, in particular, its diameter. One cannot therefore consider this feature of the flow field without taking into account the dimensions of the store.

Also, unlike the characteristics discussed so far, there is now the possibility that one should consider not merely the wing-fuselage flow field but the composite wing-fuselage-store flow field. For example, the wing leading-edge shock will reflect from the store upper surface and given the right geometry and Mach number, this reflected wave can reflect again from the wing lower surface and then from the store upper surface and so on. Similarly, the store bow shock can reflect from the wing lower surface etc. To

see whether these mutual interference effects are significant or not, various experimental investigations have been made. The first stage in an NASA attack on the problem is reported in Ref. 50. This gives the results of pressure plotting measurements for a blunt-based body of revolution with a fineness ratio of 8 mounted in various positions with respect to a flat plate or reflection plane. At supersonic speeds, this can be considered to be the same problem as the body immersed in the flow field of an identical interfering body. Tests were made at Mach numbers of 1·41 and 2·0, and body incidence angles with respect to the plate of 0 deg and $\pm$ 3 deg. Comparisons were made with theoretical results obtained from both an adaptation of slender-body theory (Ref. 51) and also, an analysis based on simple buoyancy considerations. It was found that both the chord force increments and the variation and order of magnitude of the normal force increments could be predicted quite well.

The next stage of the NASA investigation is reported in Ref. 47. These results are more directly relevant in the present context. The pressures were measured over a body with a fineness ratio of 8 mounted in the two-dimensional flow field below an 8·33 per cent thick circular-arc wing of rectangular planform. Data were obtained for several wing-body positions at a Mach number of 2·01. Typical pressure distributions over both the body upper surface and the wing lower surface for a range of body chordwise positions are shown in Fig. 33a. Comparisons are made with experimental interference-free data. Sketches are included to show the various reflected-wave systems that can exist; these are only intended to be qualitative but they serve to identify the various jumps that are observed in the measured pressure distributions. It is clear that the incident waves of each system, i.e. the wing leading-and trailing-edge shocks and the body bow wave all have a major effect on the pressure distributions and should therefore be allowed for when estimating the forces and moments on the body. The pressure-rises where the reflected waves strike the appropriate surface are less marked but cannot be dismissed as unimportant. For example, the first reflection of the wing leading-edge shock as it strikes the lower surface of the wing could have a significant effect on the aircraft performance and stability (for the examples at $x = 0$ and $0{\cdot}33c$). Possibly the best general conclusion is that after any given wave has reflected twice, any subsequent intersections of this wave system can be ignored. For example, for the wing leading-edge shock system for the case where $x = 0$, the intersections A and B should be counted as significant but the effects of C and D could be ignored except when estimating detailed load distributions.

Having thus established from Fig. 33a that the induced pressure distributions can be significant, the next point is whether it is possible to estimate them with reasonable accuracy. The top two sets of graphs in Fig. 33b indicate the order of success that is achieved with alternatively linear theory and shock-expansion theory. In each case, two theoretical curves are presented with and without an allowance for the estimated upwash at the store centreline but this is clearly a second-order refinement. The important point to note is that the position of the main incident disturbances where the wing leading-and trailing-edge shocks intersect the store upper surface is given quite accurately by shock-expansion theory but not by linear theory. Even shock-expansion theory is not very good at predicting the actual magnitude of the pressure jump; somewhat surprisingly, the measured pressure jump is appreciably larger than that indicated by the theory.

Fig. 33b is also important in showing what happens to the induced pressure distribution as it is propagated round the surface of the store to the bottom meridian. It will be seen that in addition to the axial displacement noted above, the actual magnitude of the pressure perturbations is considerably reduced on the store lower surface. To some extent, this trend would be expected simply on a basis of depth below the wing and indeed, to some extent, it is predicted by shock-expansion theory but clearly, the three-dimensional nature of the store surface and thus its cross-sectional shape has an influence on the difference between the upper and lower surface pressures. It will be seen that whereas on the upper surface the pressure jumps are greater than predicted theoretically, the reverse is true on the lower surface; this accentuates the resulting normal force loadings on the body.

Fig. 33c illustrates how the integrated normal force and pitching moment on the body at $\alpha = 0$ and 5 deg varies as it is moved longitudinally through the wing flow field at two different depths below the wing. It should be noted that C_N and C_m are as usual non-dimensionalized on the basis of the body frontal

area and length but in this case, the pitching moments *are referred to the body nose*, rather than the mid-point.

Under appropriate conditions, values of C_N and C_m as high as about 0·5 and $\pm 0{\cdot}4$ respectively are obtained. The integrated loads can therefore be quite appreciable. Further, it is clear that for this application, the forces and moments are almost entirely due to the buoyancy effects rather than to the downwash. Comparison of the results for the two body depths illustrates how the interference effects propagate rearward with increasing depth and also, how they only decay relatively slowly (it should be noted particularly that the two sets of results are for store depths of 1 and 4 store diameters respectively). Within the likely range of store vertical positions therefore, it would almost be possible to consider the interference effect as depending merely on $\{x-(M^2-1)^{\frac{1}{2}}z\}$ or some refinement of this that would correspond better with shock-expansion theory.

The main qualitative trends shown in Fig. 33c are as follows:

(1) as the body is moved into the wing flow field from ahead of the leading-edge shock, C_N becomes negative and C_m can become strongly nose-up,

(2) with further movement, these trends are reversed and maximum positive values of C_N and negative values of C_m are recorded when the body is centrally situated within the wing interference field,

(3) with further movement, the trends are again reversed giving negative values of C_N and the possibility of large positive values of C_m.

In this case, there is not a great deal of difference between the results at $\alpha = 0$ deg and 5 deg but it should be noted that this will not always be the case. The body being tested here had no wing-type lifting surfaces and also, its length was equal to the wing chord. The comparisons to be shown later, e.g. in Figs. 37 – 39 are for a body that is appreciably longer than the wing chord and in this case, the buoyancy effects being discussed here may be rather less significant while the downwash effects referred to earlier may be greater.

The theoretical curves in Fig. 33c were obtained by integrating the pressures predicted by shock-expansion theory. These gave slightly better results than predictions based on linear theory. They undoubtedly indicate the main trends with body position remarkably accurately, although for any given position, the predicted values of C_N and C_m can be seriously in error. These quantitative errors are no doubt due to the fact that the body was assumed to be placed in the wing flow field estimated without allowing for the store effects. Therefore the weakening of the pressure disturbances as they are propagated round the surface and the effect of any reflected waves on the upper surface pressure distribution – two of the phenomena noted above – have not been allowed for in these estimates. It is possible therefore that the accuracy of the method of estimation could be improved but at the expense of considerable labour and bearing in mind that the integrated loads are the difference between two relatively large quantities, improved accuracy in the final integrated values might even then not be achieved. It is reasonable to suggest that the accuracy achieved by the simplified shock-expansion theory as applied in Fig. 33c would be quite enough to decide which store positions might have completely unacceptable jettisoning characteristics. Determination of the values of C_N and C_m for favoured positions will probably always remain a matter for experiment.

The discussion of these induced pressure effects have so far been related merely to the pitch plane. The effects in the lateral plane should obviously be much less pronounced. Ref. 32 discusses their possible magnitude and shows that, in the absence of a pylon, this particular type of interference can increase the store side force by factors varying from 2 per cent for a store at a depth of $2d$ below the wing, 8 per cent for a depth of $1d$ and between 13 and 20 per cent for a depth of $0{\cdot}5d$. These values correspond with figures of 20, 30 and 40 per cent when a pylon is present, and so clearly for the store vertical positions likely to be used in practice, the pylon-induced effects to be discussed below in Section 4.3. are much the more important.

4.3. *Estimation of Loads Including Pylon-induced effects and Pylon Loads.*

Having evaluated the local flow-field characteristics over the store at supersonic speeds, the general practice in most of the NACA references is then to calculate the store loads by either slender-body theory

or linear theory and then to add the buoyancy effects referred to above in Section 4.2. and finally, the pylon-induced effects. Some experimental results indicate that the variation of store side force with incidence is non-linear and this suggests the need for including in the theoretical estimates not merely the load in potential flow but also the viscous cross-flow term. The method of Ref. 52 appears to be adequate in this respect. Comment is also made that strictly, one should not use a linearised theory for calculating the load in potential flow but also the viscous cross-flow term. The method of Ref. 52 appears to be adequate results for the isolated stores are available, it may be preferable to use these as a basis. In other words, one would predict theoretically the appropriate local sidewash and velocity over the store but then use the experimental results for the isolated store to calculate the loads due to the local flow field.

In practice, however, these uncertainties as to what theory to use for calculating the loads on the store should not be very important. As already suggested, the normal force and pitching moment on the store may often be dominated by the buoyancy effects discussed above in Section 4.2. while the side force and yawing moment are likely to be dominated by the pylon-induced effects. Ref. 32 presents a method for estimating the pylon-induced effects. It is based on the fact that the problem of determining the side force on a store connected to a wing by a pylon is similar in some respects to the problem of determining the lift force on wing-tip tanks and the report takes the transformations of Ref. 25 which treats wing-tip tanks and adapts these to the present problem. It is shown that good agreement with experimental results is obtained in this way for the pylon-induced effects for quite a wide range of different installations. Ref. 32 does not however include a method for estimating the direct loads on the pylon itself and so subsequent NACA Reports have usually tended to use the curves presented in Ref. 15 for estimating both the pylon loads and the pylon-induced effects on the store loads. These are the curves reproduced in Fig. 15 of the present Report and already discussed in Sections 2.2.1. and 3.8. As noted earlier, there is a little ambiguity in the use of the symbol σ in Fig. 15. Ref. 15 quotes β in place of this σ where β is as usual, the angle of sideslip but in almost all the comparisons in Ref. 15, $\beta = 0$ deg and the side force on the store is due to the sidewash, σ. It seems legitimate therefore to interpret the curves in Fig. 15 as indicating the variation of $(\partial C_Y/\partial\sigma)$. Strictly, these curves were derived for $M = 1{\cdot}6$ but within limits, it should be possible to use them over quite a range of Mach number and different pylon-wing installations provided that the appropriate values of σ are fed into the estimates.

The implications of the curves in Fig. 15 were discussed in detail in Section 3.8. but a few points are worth repeating here. First, the pylon-induced effects can only be dismissed as trivial if (d/b_p) is less than about 0·6 whereas for practical installations, it is much more likely that (d/b_p) will be in the region of 2·0. Second, even the loads on the pylon itself for a given pylon chord and a given mean sidewash tend to increase as the depth of the pylon is reduced – at least, until (d/b_p) is near 1·0. In practice, the mean sidewash over the pylon would also increase as the pylon depth was reduced and so the trend for the pylon load to increase would be maintained until (d/b_p) was significantly greater than 1·0, i.e. until it was approaching the value for typical store installations. It follows that both the pylon-induced effects and the pylon loads are likely to be very significant for practical installations.

A further example in support of this conclusion is presented in Fig. 34. This is taken from Ref. 44 and shows the relative theoretical contributions to the store/pylon side force at $M = 1{\cdot}61$ for an assembly beneath a 45 deg sweptback wing. In this case, the store is mounted at 1·4 times store diameters below the wing on a swept forward pylon with the store mid-point lying a little way ahead of the local wing leading edge. Fig. 34 shows that for this example, if it were not for the effects of the pylon, the side force on the store even at $\alpha = 10$ deg would be quite small, i.e. $C_Y = -0{\cdot}15$ but allowing for the pylon-induced effects on the store, this value becomes about $-0{\cdot}9$ while the total side force allowing for the load on the pylon itself is given by about $C_{Y_{SP}} = -2{\cdot}1$. The effects of the pylon in this instance are therefore very dramatic but before hastily drawing the conclusion that one need only calculate the pylon effects, a few qualifications need to be made. It could be argued on the one hand that the store side force for this example in Fig. 34 is smaller than it might be in general, while on the other hand, the pylon load is larger than it should be for a good installation. In support of these statements,

(1) the estimated store side force in the absence of pylon effects (but including the viscous term) is undoubtedly rather small. $|dC_{Y_{S_A}}/d\alpha|$ is only about 0·017 per degree which by comparison with a large

number of results in Refs. 32 and 44 for a range of different store chordwise and spanwise positions, is towards the low end of the possible range; values varying from about 0·013 per degree up to about 0·038 per degree are recorded for different installations. This conclusion is not surprising and can easily be explained by the chordwise position of the store in the example in Fig. 34. Even the store mid-point is ahead of the wing leading edge and as a result, as can be seen from the sidewash distribution in Fig. 31, the nose of the store lies ahead of the wing-root leading edge shock and is therefore in a region where there is no wing-induced sidewash,

(2) on the other hand, the swept pylon is situated just in the region where the sidewash is likely to be at its maximum, i.e. just behind the wing leading-edge shock. The mean sidewash over the pylon is therefore relatively large and so the pylon loads are greater than they would have been if the pylon had been mounted further aft. A comparison showing the effect of pylon position as measured experimentally is included in Fig. 42,

(3) finally, there is the question of the pylon geometry. Admittedly, (d/b_p) is not as high as 2·0 as suggested above but it is 1·12 and this is certainly in the range likely to give large pylon loads and pylon-induced effects (Fig. 15) and further, and perhaps more important, the pylon aspect ratio is about 0·4 whereas values as low as 0·2 are more representative. (N.B. Fig. 15 is a plot of the side force derivative divided by A_p).

These points have been made to indicate that Fig. 34 probably represents a somewhat extreme example. Nevertheless, even if one multiplied the store loads by 2 and the pylon effects by 1/2, the point would still remain that clearly the pylon effects play a large part in determining the store-pylon side loads. It is therefore encouraging to find from the comparisons in Refs. 44 and 32 that on the whole, the prediction methods appear to be reasonably reliable in estimating these effects for quite a wide range of store positions.

Fig. 35 presents a typical illustration of the final accuracy achieved in estimating store/pylon side force including the pylon effects by the methods outlined above. This figure compares experimental results with theoretical predictions for the same store/pylon assembly mounted at three alternative positions along the span of the 45 deg sweptback wing-fuselage configuration. Of particular interest is the comparison between the two sets of theoretical curves which are based on different estimates for the local sidewash characteristics. In the first, the sidewash is calculated according to linearised theory while in the second, the estimate of the sidewash due to incidence is modified to take account of the evidence of the schlieren photographs which show that owing to the effects of the finite wing thickness, the wing leading-edge shock is not lying across the wing as it should be according to linearised theory but is still detached as it would be at a lower stream Mach number.* As explained earlier, the modification to the calculation consists of assuming that the stream Mach number was 1·4 instead of the true value of about 1·6 since the position of the shock in the schlieren photographs corresponds roughly to the predicted position for $M = 1{\cdot}4$. It will be seen from Fig. 35 that if the modified theory is used, the variation of $C_{Y_{SP}}$ with incidence is predicted with reasonable accuracy for all three spanwise stations but that this is not true of the absolute values of C_Y. For the inboard station, $(-C_Y)$ is underestimated and for the outboard station, overestimated by about 0·3 and 0·4 to 0·5 respectively. There is still a possibility however that the theoretical estimates could be improved as compared with those presented in Fig. 35. It was noted that in the modified estimates, the sidewash due to incidence was recalculated to suit $M = 1{\cdot}4$ but no change was made to the sidewash due to wing and body thickness. There is really no justification for this distinction; indeed, Fig. 32 shows that the modified approach leads to much better agreement between calculated and measured values for the sidewash at zero incidence and that this is far from a trivial point. One can show that the revised calculation would increase the mean sidewash over the pylon/store nose at the inboard station and decrease the mean sidewash at the outboard station;

*Fig. 35 also contains a third set of predicted curves derived according to the new empirical method in Section 6. These give good agreement with the measured results but this is not too surprising since these were some of the results that were analysed in producing the method. This comparison is however irrelevant in the present section of the report.

these changes are in the sense needed to improve the agreement between the calculated and measured values of C_Y for these positions. Without actually performing the calculations one cannot say whether the resulting agreement would have been entirely satisfactory but it seems likely that this would have been the case.

It appears therefore that provided one accepts the conclusions of Section 4.1.1. when estimating the sidewash and is not content with a simple linear-theory estimate, the methods should be satisfactory when predicting the store/pylon side force due to incidence at zero sideslip. We must also however consider the side force due to sideslip. For this term, the most simplified approach would be to estimate the loads due to a uniform sidewash angle equal to the angle of sideslip and to ignore the fact that with varying sideslip, the angle of sweepback of either wing panel and hence the local sidewash distribution over the store/pylon changes. On this simplified approach, the loads due to sideslip would depend on the store/pylon geometry but not on the details of the flow field. Fig. 36 presents a comparison however which shows that this simplified method is far from satisfactory. This comparison is for the same store/pylon configuration at the same three alternative spanwise positions as those considered earlier in Fig. 35 when discussing the effects due to incidence. Experimental results are presented for the variation of total side force with β at $\alpha = 4$ deg. While it is true that these experimental results confirm that to the first order, the side loads due to sideslip do not depend drastically on the particular configuration, the essential point to note is that the theoretical prediction overestimates the variation of $C_{Y_{SP}}$ with β by roughly 80 per cent. Ref. 44 includes experimental results for about eight different configurations with variations in store spanwise and chordwise position, pylon position and store shape; when all these results are compared, there are some significant variations in $(dC_Y/d\beta)$ with configuration but in all cases, the experimental values lie well below the theoretical prediction.

It is clear therefore that some refinement to the method of prediction is necessary. The obvious suggestion is that one should estimate the sidewash distribution over the store/pylon under the sideslipped wing panel and then base the loads on the resultant flow angularity $(\sigma + \beta)$. If this is what is needed to achieve agreement between the predicted and measured values in Fig. 36, this implies that as the sweepback of the rearward wing panel increases with sideslip, the mean sidewash over the store/pylon is reduced. At first sight, this seems a somewhat surprising result because clearly, increasing sweepback would increase the maximum sidewash in the field. This suggests that the more important factor is that with increasing sideslip, the store/pylon effectively moves further aft of the wing leading-edge shock and moves therefore into a region of reduced sidewash.

The last paragraph may have raised doubts as to whether the omission of the variation of σ with β in the theoretical predictions of Fig. 36 is in fact the real reason why these predictions were at fault. Fig. 37 provides some reassurance on this point. This shows the combined effects of incidence and sideslip for the store mounted in the outboard position. It will be seen that the absolute value of $(dC_{Y_S}/d\alpha)$ increases with β; this makes it fairly certain that at least (σ/α) over the store/pylon varies with β. There is still however an apparent anomaly. These results suggest that (σ/α) *increases* with β whereas the earlier comparison in Fig. 36 suggested that σ *decreased* with β. This apparent inconsistency can only be resolved if one concludes that the mean sidewash over the store/pylon at low incidence decreases with β and this is indeed quite plausible since it is the sidewash due to thickness that could reduce appreciably or even change sign if the store became well behind the wing leading-edge shock. In other words, Figs. 36 and 37 could be consistent and could both be interpreted as providing evidence that one should not estimate the effects of sideslip without allowing for the changes with β in the mean sidewash over the store/pylon. What is equally clear however is that no simple correction could be devised for this; there seems no alternative short of the detailed calculation of the sidewash field below the sideslipped wing panel.

Before leaving this subject, there is one other important conclusion to be drawn from Fig. 37. This is that in estimating the loads due to combined incidence and sideslip, it is clearly unsatisfactory to estimate the loads due to incidence at zero sideslip and those due to sideslip at zero incidence and then just add them together. This practice could seriously underestimate the loads under combined (α, β).

4.4. *General Comments on Available Methods.*

The detailed discussion in Sections 4.1. to 4.3. has been concerned with the prediction methods that are based on the calculated (or measured) flow field characteristics over the store/pylon at supersonic speeds. Earlier in the Report, it was concluded that the corresponding methods for subsonic speeds were laborious to apply and also the results achieved were somewhat disappointing. Admittedly, the methods predicted the correct trends in the variation of the store loads with the different geometrical parameters but quantitatively, the accuracy was somewhat poor; in particular, the store side force was often underestimated by a considerable factor even if the measured rather than the calculated sidewash distributions were used. The general impression that has been gained from a study of the results at supersonic speeds however is that the methods may be somewhat easier to apply than at subsonic speeds and also, the accuracy achieved may be considerably better.

As regards the ease of application, the flow field characteristics for 45 deg sweptback and 60 deg delta wings have been computed in some detail and hence, it may be possible to interpolate or extrapolate from existing results rather than have to carry out detailed calculations for the particular configuration being considered. Even if this is not the case, the charts for calculating the local sidewash as given in Ref. 33 together with the other references for the downwash and pressure distributions as quoted earlier should be helpful. Also, from what has been said already, it is clear that in predicting the side loads, the really important point is to estimate accurately the local sidewash over the pylon (and over any vertical fins on the store) while for predicting the longitudinal components, the important point is to estimate accurately the pressure distributions induced along the top and bottom meridian lines on the store.

As regards the accuracy achieved by these detailed methods of prediction, the comparisons presented in Refs. 32 and 44 and other reports and illustrated for example in Fig. 35 show that there is some hope of obtaining reasonably accurate estimates at supersonic speeds provided that certain important points are borne in mind. These have been mentioned in the previous Sections but it may be convenient to list them again here, *viz*,

(1) the local sidewash and downwash distributions should be calculated by a modified linearised theory in which allowance is made for the effects of wing thickness in modifying the flow field particularly in the region just ahead of the wing leading edge. Preferably, this should be done on the basis of schlieren pictures of the actual flow around the wing-fuselage configuration but if these are not available, the calculation should be made for a corrected fictitious Mach number which, for a 5 per cent thick wing at $M = 1{\cdot}6$ to $2{\cdot}0$, should be about $0{\cdot}2$ below the true free-stream value,

(2) in estimating the sidewash, the contributions due to wing incidence, wing thickness and fuselage volume should all be included. Also, despite the fact that in the literature there is a tendency to dismiss the sidewash due to fuselage incidence, this may not be a valid assumption in all cases. In particular, if the wing leading-edge shock lies downstream of the leading edge of the pylon supporting the store, and if the fuselage is not parallel ahead of the wing root leading edge, this contribution may be quite significant,

(3) in calculating the pressure distributions induced along the top and bottom meridian lines of the store, linear theory may possibly be adequate in estimating the overall normal force and pitching moment induced on the store by the buoyancy effects but for preference, shock-expansion theory should always be used. This is certainly the case if the detailed loading along the store is required. For estimating the normal force and pitching moment, the pressure distribution induced along the bottom meridian can be taken as that existing at that level in the wing flow field in the absence of the store but again, this may not be satisfactory when estimating the detailed loading or the chordwise force,

(4) it is debatable whether any improved accuracy would result from an attempt to allow for the multiple wave reflections that can exist between the store upper surface and the wing lower surface. Certainly, after any given wave has reflected at least once in each surface, further reflections of this wave can in general be ignored,

(5) in estimating the side loads, the pylon-induced effects and the pylon loads must always be included and the curves in Fig. 15 using the appropriate values of σ should be reliable to the first order provided the Mach number is not too far removed from $M = 1{\cdot}6$. It may be desirable to produce similar curves for a range of Mach number and a range of store length and position relative to the pylon,

(6) in estimating the store/pylon side force due to sideslip, it is necessary to allow for the variation of σ with β and so an estimate must be made of the sidewash field under the sideslipped wing of increased (or decreased) sweepback.

If the above points are borne in mind, it seems that it should be possible to obtain reasonably reliable results by these detailed methods. Even though they may not be quite as laborious as the corresponding methods at subsonic speeds, it is still obviously desirable to have some other means of obtaining a rapid approximate answer. It is useful to note in this connection that there are far more experimental measurements available for $M = 1{\cdot}6$ to $2{\cdot}0$ than for transonic speeds. Hence when wanting to estimate the loads on a particular configuration, there is a greater likelihood that one can find some test data for some fairly similar arrangement. The data contained in Refs. 45, 46, 53, 54, 55 and 56 should be useful and in particular, the contour plots showing the variation of store loads with store chordwise and spanwise position at a given incidence. Some examples of these contour plots are reproduced in Figs. 38a to e for both a 45 deg sweptback and a 60 deg delta wing configuration. These contour plots present a fairly regular appearance and this gives grounds for hoping that an empirical method for estimating store loads based on an analysis of experimental data has some chance of giving reliable results. On the other hand, the detailed analysis of these contour plots in Section 5.1. below shows that they are somewhat more complex than appears at first sight and also, it must be admitted that they are merely for zero incidence. Allowance for the effects of incidence, sideslip and changes in Mach number could alter the picture considerably.

To meet the need for a rapid method of estimating store/pylon side force, the new empirical method presented in Section 6 has been developed for use up to say, $M = 2{\cdot}0$ or more strictly, in the range for which the aircraft wing leading edge remains subsonic. It is hoped that this method should prove useful for the range of configurations set out in Section 2.2.6. or at the start of Section 6. Fig. 35 provides an example where values of $C_{Y_{SP}}$ predicted by this method are in good agreement with experiment and this illustrates that the factors and formulae of the method are a fair representation of the experimental data from which the method was derived. Despite this encouragement, it is still possible that the method as presented will not be entirely satisfactory at supersonic speeds. For example, for the sake of simplicity, it treats Mach number and the store position variables separately whereas as we have seen, they are in fact closely interrelated. It is hoped that in due course, more experimental results will become available and it will then be possible to have a more independent check on whether the method is valid.

To sum up, it seems that the detailed methods based on estimates of the wing-fuselage flow fields appear to have a good chance not merely of predicting the qualitative trends but also in certain cases, of giving good quantitative estimates of the store loads at supersonic speeds. Even so, there is still a place for a more empirical approach based on an analysis of the available experimental data and the method in Section 6 is an example of this approach. It seems possible however that a simple method such as that in Section 6 may not be quite as successful at supersonic speeds as at lower speeds because of the close interrelation of different variables. This applies particularly near the Mach number at which the wing leading-edge shock moves downstream of the wing leading edge.

5. *Experimental Measurements on Store Loads at Supersonic Speeds.*

As noted above in Section 4, a considerable amount of experimental data on store loads is available for supersonic speeds and particularly for $M = 1{\cdot}6$ and $2{\cdot}0$. Extensive investigations into the effects of store position were made for both the 45 deg swept back and the 60 deg delta wings referred to above. Even so, the range of the experimental data is not quite as great as appears at first sight. For example, much of the data is for a relatively large store mounted on a relatively large pylon; also, most of the data are for stores that are either simple bodies of revolution or which have merely some relatively small tail fins; data for stores with wing-type lifting surfaces are not so common. Also, few tests include any measurements of store rolling moment.

It is clear that the store loads at supersonic speeds depend on the same variables as at subsonic speeds but their effects are even more interrelated. To quote just one example of this, one can consider the effects of store chordwise position which is always perhaps the most important single variable. At subsonic

speeds, these effects cannot easily be separated from those of incidence or of store size and shape but on the other hand, store spanwise and vertical position and Mach number merely effect the quantitative values without substantially altering the qualitative trends. At supersonic speeds, however, all these variables are interrelated and changes in any one of them may modify even the qualitative effects of store chordwise position. In practice, at supersonic speeds, it may often be more useful to think in terms of the composite parameter $\{x-(M^2-1)^{\frac{1}{2}}\, y-(M^2-1)^{\frac{1}{2}}z\}$.

Despite these reservations, comparisons showing the effects of different variables should still be useful if interpreted carefully and with due regard to the flow field characteristics discussed earlier. Such comparisons are discussed below; the results should clearly not be generalized too far but it is hoped that at least, they will not be misleading in suggesting the main trends.

In the comparisons selected for inclusion in the Report, one should always be careful to note whether the data being studied are for the loads on the store alone in the presence of the wing/fuselage or whether they include the pylon-induced effects or whether they are the total loads including those on the pylon itself.

5.1. *Effect of Store Chordwise and Spanwise Position.*

It is convenient to treat these two variables together because as noted above, the store loads at supersonic speeds for a given store depth below the wing should not vary much as the store is moved along the local Mach lines in the flow field. This assertion can be checked by referring to the large amount of experimental data contained in Refs. 45, 46, 53, 54, 55 and 56. These give 6-component measurements at $M = 1{\cdot}61$ and $2{\cdot}01$ on sting-supported stores (with no pylon) mounted in a large variety of positions beneath both a 45 deg sweptback and a 60 deg delta wing. In all these references, the incidence of the wing-fuselage was varied from 0 deg to 4 deg, but the store remained at $\alpha = 0$ deg (*see* Section 5.5.).

A typical set of contour plots of all the store load coefficients (except rolling moment) is reproduced as Fig. 38a to e. These are for $\alpha = 0$ deg, $M = 1{\cdot}61$, for stores at a vertical position of $0{\cdot}77$ store diameters below both the sweptback and delta wing planforms. The contour lines in Fig. 38 are the loci joining the positions of the store mid-point which give constant values of the appropriate store load coefficient. According to the argument put forward earlier, these contour lines should correspond roughly to the local Mach lines in the flow field. It is clear from Fig. 38 that over much of the field, this is certainly true – at least to the first order. Directly under the wing however or more strictly, in the region between the wing leading-edge and trailing-edge shocks, some variation with spanwise position is evident and also, the contour lines near the wing trailing edge tend to be influenced rather more by the wing geometry than in other parts of the flow field.

In addition to Fig. 38, several other Figures give illustrations of the effects of store chordwise and spanwise position. For example, Fig. 33c shows the effect on $C_{N_{SA}}$ and $C_{m_{SA}}$ as the store is moved in a chordwise sense through the wing flow field. The effects of chordwise and spanwise position of stores mounted beneath a 45 deg sweptback wing on the variation of the store loads with incidence at zero sideslip is shown in Figs. 39a and b. These results include the pylon-induced effects but not the pylon loads; the corresponding picture for the effect of spanwise position on the side force including the pylon loads is given in Fig. 35 and has already been mentioned when discussing the accuracy of the different theoretical methods of prediction.

The evidence from all these figures will now be discussed considering each component in turn, *viz*,

(1) *Store axial force or drag* (*Fig.* 38*a*).

The maximum adverse interference effects on store drag are observed when the store is mounted well inboard and roughly below the wing mid-chord, i.e. allowing for the vertical position, the store is probably then just a little aft of the wing leading-edge shock. For the particular store considered in Fig. 38, under these conditions, the interference effects increase $C_{D_{SA}}$ by about 60 per cent for both the delta and the 45 deg sweptback wing. As the store is moved rearward towards the trailing edge and outward towards the tip, the values of $C_{D_{SA}}$ decrease towards what they would be for the store in isolation. With the store aft of the wing trailing edge, the drag is reduced below the interference-free values, i.e. the interference is favourable.

These trends are qualitatively in agreement with what would be predicted on the basis of the pressure distributions induced on the store by the wing as illustrated in Fig. 33b. For example, the favourable-interference case with the store located far aft corresponds with the third column of pictures in Fig. 33b. For such a store position, the suctions over the forward-facing parts of the store are increased due to the wing expansion field while the suctions over the rearward facing surfaces are reduced owing to the influence of the wing trailing-edge shock; both these factors contribute to the reduction in store drag.

Many other examples of the interference effects on store drag can be found in the literature and these results are of course important from the performance view-point. The chordwise force is however unlikely to be critical as a load on the store and so it will not be discussed further here.

(2) *Store lift or normal force* (*Figs.* 38*b*, 33*c and* 39).

The principal effects of store chordwise position on normal force have already been mentioned in Section 4.2. with reference to Fig. 33c. It will be seen that as the store moves into and out of the wing flow field, $C_{N_{SA}}$ becomes negative but in between, when it is virtually completely immersed within the wing flow field, significant positive values of $C_{N_{SA}}$ can be recorded even at $\alpha = 0$ deg owing to the buoyancy effects. The spanwise position and depth help to determine where the store 'enters or leaves the wing-flow field'. Similar trends to those in Fig. 33c can be seen in Fig. 38b. $C^*_{L_{SA}}$ increases rapidly from a negative to a positive value as the store mid-point moves downstream of the wing leading edge; the decrease further aft as the store mid-point moves through the wing trailing-edge shock is even more abrupt. The maximum values of $C_{L_{SA}}$ recorded in Fig. 38b vary from about 0·32 for inboard positions to about 0·22 near the tip of the sweptback wing or 0·10 near the tip of the delta wing. This marked decrease with distance out along the span, particularly for the delta planform, is simply a direct geometrical consequence of the wing taper or, more strictly, of the ratio of the local wing chord to the store length. Clearly, if the local wing chord is relatively small, little of the store will be affected by the wing-induced pressure distribution. The maximum values of $C_{N_{SA}}$ in Figs. 33c and 38b appear reasonably consistent; the value for $z_s = 1{\cdot}0d$ in Fig. 33c is almost 0·4 but here, the wing chord is equal to the store length while in Fig. 38, this ratio does not approach 1·0 except near the extreme root of the delta wing.

In Fig. 33c the results for $C_{N_{SA}}$ at $\alpha = 0$ deg and 5 deg are fairly similar and one might be tempted to conclude that the buoyancy effects already present at $\alpha = 0$ deg are likely to give the most important contribution to C_N at incidence. Figs. 39a and b show however that this is far from a general conclusion and indeed, for some store positions, the precise opposite could apply. If it is possible to draw any general conclusions, they would be as follows:

(a) for stores located wholly within the wing flow field, the values of C_N at $\alpha = 0$ deg can be large owing to the buoyancy effects but the variation with α should be relatively small because of the relatively large $(d\varepsilon/d\alpha)$,

(b) for stores mounted at least partly ahead of or partly behind the wing flow field, the values of C_N at $\alpha = 0$ deg would be relatively small but the variation of C_N with α can be large as shown for two of the examples in Fig. 39, viz, the most rearward store position in Fig. 39a and the furthest inboard position in Fig. 39b. In each case, i.e. for both the forward and the rear positions, it is conceivable that there are two contributory factors. First, the parts of the store which are either ahead of the wing leading-edge shock or behind the wing trailing-edge shock, i.e. the nose of the store for a forward position or the tail of the store for a rear position, are not subject to the wing downwash field. Second, the chordwise region in which the buoyancy effects tend to give a positive contribution to C_N probably increases somewhat with incidence – at the forward end because the wing leading-edge shock will become somewhat more detached with increasing incidence and at the rear end because of a change with incidence in the wing-induced pressure distribution on the store. These trends in the buoyancy effects can be seen in Fig. 33c but unless the store is fairly small relative to the local wing chord, it is probably the lack of downwash outside the wing-induced flow field that is the more vital factor,

---

*In these results, since $C_{A_{SA}}$ was measured, $C_{N_{SA}}$ was corrected to $C_{L_{SA}}$.

(c) from Fig. 39 it will be seen that for the store positions which give large values of $(dC_N/d\alpha)$, the $C_N - \alpha$ curves are notably non-linear. To some extent, this could be due to the store moving into different parts of the flow field with increasing incidence but it also suggests – as might be expected – quite a large cross-flow component to the store lift.

Clearly, positions which give large values of C_{N_S} may be undesirable from the point of view of store jettisoning. It is difficult to draw general conclusions as to which store positions should be best in this respect. This is partly because the answer could depend greatly on the relative size of the store to the local wing chord. For relatively small stores, the buoyancy effects would be more important and hence chordwise positions in the middle of the wing-flow field may be undesirable. For larger stores, or for outboard positions on a tapered wing, far forward or far aft positions may be unacceptable. Within the likely practical range of chordwise positions, the literature tends to advise strongly against the rearward end of the range and it is certainly true that in Fig. 39, the largest values of C_N at high incidence are obtained with the far aft store shown in Fig. 39a. For this case, C_{N_S} has become about 0·7 by $\alpha = 12$ deg.

(3) *Store pitching moment* (*Figs.* 38*c*, 33*c and* 39).

As might be expected, the changes in store pitching moment with chordwise and spanwise position have a distinct affinity to the changes in normal force. Fig. 33c shows that as regards the buoyancy effects, the usual trend is for positive values of C_m to accompany negative values of C_N and *vice versa*. The change at the rear from a negative to a positive value takes place for a very small change in store chordwise position. Quantitatively, it is the negative values of C_m at intermediate positions which are the largest at $\alpha = 0$ deg in Fig. 33c and this is borne out by the contour plots in Fig. 38c. Again, there is reasonable correlation between these two sets of results when one allows for the size of the store relative to the local wing chord.

It seems likely however that the critical values of C_m will be determined largely by the variation of C_m with α rather than by the values at zero incidence. Fig. 39 shows that the usual trend is for C_m to become more positive with increasing incidence. This is particularly noticeable in Fig. 39 for the configurations where the store is relatively far forward, e.g. the three positions in Fig. 39b and the furthest forward position in Fig. 39a. For these cases, values of C_{m_S} of the order of 0·25 are reached at $\alpha = 12$ deg. Fig. 33c shows however that it is not merely for the far forward positions that large positive values of C_m may be expected; there could be a similar tendency for positions where the store mid-point is near or perhaps just ahead of the wing trailing-edge shock. It will be noted in this latter case that the buoyancy and downwash effects are additive in giving these nose-up pitching moments. Large positive values of C_m were not obtained with the furthest aft position shown in Fig. 39a but this is not necessarily inconsistent with Fig. 33c: this aft position in Fig. 39a is perhaps just too far forward to show the effect and as noted above, the transition from a negative to a positive value of C_m in this region can occur for a very small change in chordwise position.

From the point of view of store jettisoning, it is probable that the nose-up values of C_m would be the more embarrassing and for this reason, the forward or relatively far aft positions are unattractive. Hence, to the extent it is possible to draw any general conclusion, one can possibly say that there would be some preference for a fairly central chordwise position and a fairly far outboard station, i.e. a central position to avoid the large incidence effects and an outboard station which for a tapered wing, should minimise the positive C_N (and negative C_m) from the buoyancy effects. This can only be regarded as a very loose general conclusion, e.g. a 'central' position means in respect of the wing flow field which itself is propagated further aft with increasing Mach number.

(4) *Store side force* (*Figs.* 38*d*, 39 *and* 35).

Fig. 38d shows that over the length of the wing span, the contour lines for $C_{Y_{S_A}}$ at $\alpha = 0$ deg closely follow the local Mach lines. For these examples at $M = 1{\cdot}6$, C_{Y_0} is negative for store positions well ahead of the wing leading edge, is positive for positions close to the wing leading edge with a maximum near the mid semispan station, then becomes zero or negative near the wing trailing edge and finally significant and positive well aft of the trailing edge. These changes could be correlated with the sidewash distributions

shown earlier in Figs. 30 and 31, but the important point to note is that everywhere in the field, these values of C_{Y_0} for the store-alone are quite trivial compared with the values of $|C_Y|$ that are obtained when a pylon is present. This is particularly true when one compares them with the values obtained at incidence including the pylon-induced effects (Fig. 39) and even more so when including the loads on the pylon itself (Fig. 35). For example, for any likely store position in Fig. 38, the value of $C_{Y_{SA}}$ at $\alpha = 0$ deg lies between $\pm 0{\cdot}12$ whereas at $\alpha = 12$ deg, $|C_{Y_S}|$ is likely to be of the order of 1·0 while $|C_{Y_S}|$ can be more than 2·0. To some extent, this is because of the Mach number that has been chosen for the example of Fig. 38; for reasons explained earlier in Section 4.1.1., for any given store position, C_{Y_0} for the store alone decreases with Mach number in the supersonic range and for many applications should be near zero at about $M = 1{\cdot}4$.

It follows therefore that the values of C_{Y_S} and $C_{Y_{SP}}$ are related primarily to the mean sidewash over the pylon and so as regards this component, comparisons which show the effect of chordwise and spanwise position are largely indicating the effects of changes in position of the pylon rather than the store.

For most of the examples in the literature, the pylon is usually mounted from the forward part of the local wing section and as a result, it is usually situated in a region of relatively large sidewash. This is certainly true for example of the three configurations at different spanwise positions shown in Fig. 39b. For this example, one would expect that the mean sidewash over the pylon at incidence would increase with distance out along the span (*see* Fig. 29) and this is therefore the explanation of the increase in $|C_{Y_S}|$, e.g. at $\alpha = 12$ deg, C_{Y_S} varies from $-0{\cdot}8$ at the inboard station to about $-1{\cdot}4$ at the outboard position. This increase with distance out along the span would be expected to apply until the wing leading edge became supersonic; then, there should be a material increase in $|C_{Y_S}|$ for inboard pylon positions with less variation across the span.

Fig. 39a showing the effects of chordwise position is of particular interest. It will be seen that the values of $|C_{Y_S}|$ obtained for the intermediate position are substantially the same as those for the forward position and at first sight, this may seem surprising because for the intermediate position, the pylon has been moved to the rear of the local wing section. One has to think in terms however not merely of where the pylon intersects the local wing section but of where its plan area is in relation to the wing flow field. On this basis, in the forward position, the pylon being swept forward lies partly ahead of the wing leading-edge shock and partly therefore in a region where there is no wing-induced sidewash. For the intermediate position, the pylon is unswept and the lower part of the pylon is probably in the region of the greatest sidewash just aft of the wing leading-edge shock. It is therefore quite plausible that the side loads can be high for both these installations. It is only for the rear position with its sweptback pylon lying wholly downstream of the region of greatest sidewash that a material reduction in $|C_{Y_S}|$ would be expected and this is borne out by the results in Fig. 39a: at $\alpha = 12$ deg, $|C_{Y_S}|$ for this rear installation is only 0·4 as compared with slightly more than 1·0 for the other two positions. A further example showing the effect of pylon position is given in Fig. 42 and will be discussed later in Section 5.7.

The overall conclusions from these comparisons as regards store/pylon side force is therefore that the values depend primarily on the pylon position and that to keep them as small as possible, a rear sweptback pylon mounted well inboard is desirable. This recommendation conflicts with that made earlier as to the store position desirable to avoid large values of C_N and C_m but there are possibilities for compromise. For example, the values of C_Y depend primarily on pylon position whereas C_N and C_m depend on store position and therefore, a store mounted fairly far forward on a rear sweptback pylon could be the basis of a compromise. This is a case however where general statements can obviously be misleading and perhaps not very useful; the important point is to appreciate what are the primary factors involved and then to decide on the best installation in the light of the requirements for the specific case.

(5) *Store yawing moment* (*Figs.* 38*e*, 39).

The first point to note about the values of store/pylon yawing moments is that the pylon effects should be much less important than they were in the case of side force. This is because the pylon-induced loading is concentrated fairly near the moment reference centre and so does not contribute proportionately to the yawing moments. It follows therefore that the contour plot of $C_{n_{SA}}$ for $\alpha = 0$ deg in Fig. 38e is more significant in relation to the total loads than is the corresponding plot of $C_{Y_{SA}}$ in Fig. 38d.

The contour lines in Fig. 38e clearly follow the local Mach lines and indeed over the forward part of the field ahead of the wing mid-chord position, the variation along these lines is probably less than for any other component. The values of $C_{n_{S_A}}$ vary from being negative (i.e. nose outward) for store positions near the wing leading edge through zero near the wing mid-chord position to being positive near the wing trailing edge, these positive values becoming more pronounced with distance out along the span. These trends can be related to the sidewash distributions at zero incidence as shown in Figs. 29 and 31. The negative values of C_n for the forward positions arise when the forward part of the store is subject to the maximum fuselage-induced sidewash. The positive values for rear positions arise when the store mid-point is somewhere near the forward edge of the Mach cone originating from the wing maximum thickness ridge – as shown in Fig. 29, the sidewash due to wing thickness changes sign in this region and thus, the loading over the forward and rear parts of the store would then tend to compensate as regards C_Y but be additive in respect of C_n.

Again, for many practical installations, the more important trends could be those due to incidence. The largest absolute values of C_n at incidence are likely to be obtained with fairly well forward store positions such that only the rear part of the store is subject to the wing-induced sidewash due to incidence. The three store positions in Fig. 39b and the forward position in Fig. 39a are examples for which $(dC_{n_S}/d\alpha)$ is significant and positive for this reason. By $\alpha = 12$ deg, C_{n_S} is of the order of 0·1. For the more rearward positions in Fig. 39a, $(dC_{n_S}/d\alpha)$ tends to be negative and this again is what would be predicted from a study of the sidewash distributions. This means that for a moderately rearward but not too far aft store position, the yawing moment at incidence should be relatively small. It seems therefore that C_{n_S} should be fairly small for the store/pylon arrangements being suggested as a compromise at the end of (4) above. For the more forward positions that are common in practice however, significant nose-in values of yawing moment could accompany large outward values of side force.

5.2. *Effect of Vertical Location.*

Evidence on the effects of store vertical location is contained in Figs. 33c and 40. As noted earlier, since the wing-flow field is propagated rearward roughly in the direction of the local Mach lines (but more precisely as predicted by shock-expansion theory), the variation of the store loads with height should be a smooth function of some variable such as $\{x-(M^2-1)^{\frac{1}{2}}z\}$ whereas with respect to simply z, there could be some abrupt discontinuities, e.g. when the store becomes sufficiently far below the wing at a given chordwise position to be ahead of the wing leading-edge shock. This applies particularly to the case of the longitudinal components which depend on the buoyancy and downwash effects on the pressure distribution over the store. The point should be less significant as regards store/pylon side force since these loads depend more on the mean sidewash over the pylon.

Fig. 33c compares the values of $C_{N_{S_A}}$ and $C_{m_{S_A}}$ at store depths of $1{\cdot}0d$ and $4{\cdot}0d$. This figure is a good illustration of the point made in the last paragraph. Clearly, cross-plots of C_N or C_m against z might appear somewhat random and inconsistent but the variation allowing for the chordwise displacement with depth of the wing-flow field is quite sensible. Perhaps the most important point to note about this variation is that it is relatively slow and the maximum values of C_N and C_m recorded at $z_s = 4{\cdot}0d$ are at least 70 per cent of those for $z_s = 1{\cdot}0d$. This is a case where the buoyancy effects are the more important; for installations or conditions where the downwash effects are the more important, the decrease between $z_s = 1{\cdot}0d$ and $z_s = 4{\cdot}0d$ might be more noticeable; also, for such a case, there could be marked changes with depth for $z_s < 1{\cdot}0d$.

The suggestion that the store loads could increase significantly for store depth less than $1{\cdot}0d$ applies particularly in the case of store/pylon side force. Fig. 40 extracted from Ref. 26 illustrates this effect by comparing the values of $C_{Y_{S_A}}$ (i.e. no pylon) at store depths of 0·5, 1·0 and $1{\cdot}5d$ below a 45 deg sweptback wing at $M \doteq 1{\cdot}62$ and 1·96. This figure shows that at high incidence, $|C_{Y_{S_A}}|$ is more than doubled when the store spacing is reduced from $1{\cdot}5d$ to $0{\cdot}5d$. All the changes evident in Fig. 40 could undoubtedly be related to changes in the local sidewash distribution over the store. This is true not merely of the values of $(dC_{Y_{S_A}}/d\alpha)$ but also of the changes in $(C_{Y_0})_{S_A}$. For example, for all store depths, $(C_{Y_0})_{S_A}$ is following the usual supersonic trend of becoming more negative with increasing Mach number. It was noted earlier

that this trend was related to the fact that with increasing Mach number, the negative sidewash in the rear part of the wing-flow field at zero incidence would tend to pass further downstream and hence possibly aft of the store which would then only be influenced by the positive sidewash in the forward part of the field. On this explanation, one might expect that for a given chordwise position, the Mach number at which $(C_{Y_0})_{SA} = 0$ would be lower for stores at a small depth below the wing and this is in fact what can be deduced from the results in Fig. 40.

Fig. 40 shows the variation of C_Y with store depth in the absence of a pylon. With a pylon present, the trend for the values of C_Y to increase as the store depth is reduced would be even more pronounced. This point was discussed earlier in Section 4.3. on the basis of the curves in Fig. 15. The pylon-induced effects on C_Y should be fairly trivial for a store depth greater than about $2{\cdot}5d$ but increase rapidly as the store is brought closer to the wing. Even the absolute loads on the pylon itself can increase as the pylon depth is reduced despite the smaller surface area of the pylon; if the sidewash were uniform, this increase in the pylon load would continue until the store was about $1{\cdot}5d$ below the wing; allowing for the variations in sidewash, the trend could continue in many cases until the store was as close as $1{\cdot}0d$. It should be emphasised that these are only very general statements. The precise variation of the pylon loads and pylon-induced effects with store depth will depend critically on the changes in mean sidewash over the pylon and hence would be a function of the pylon position, size and sweepback.

5.3. *Effect of Store Size and Shape.*

The changes in store force and moment coefficients based on store frontal area and length as the store size is reduced are likely to depend primarily on two factors. First, as the store size is reduced in relation to the local wing chord, the buoyancy effects on C_N and C_m should become larger in general. Second, for a small store, there is the greater likelihood that most or all of the store/pylon will be situated in a region of uniform sidewash and downwash. If the store is very favourably located, this last point could of course be beneficial as regards the magnitude of the store loads but it much more likely that in general, the effects on C_N and C_Y would be adverse, with possibly favourable but secondary effects on C_m and C_n. Allowing for the two factors, it is probable therefore that for most store/pylon installations, the force and moment coefficients (except for yawing moment) would be larger for a small store than for a large store. It is very difficult to say whether this tendency would be more pronounced at supersonic than at subsonic speeds: several opposing arguments could be put forward. Indeed, the quantitative effects of changes in store size and shape are extremely difficult to assess without knowing all the details of the wing-fuselage flow field in which the stores are immersed.

Ref. 54 gives a comparison of the drag, lift and side force on both a large and a small store of the same fineness ratio, one of length $1{\cdot}33c$ and the other, $1{\cdot}82c$. Fig. 41 abstracted from this reference shows the variation of the forces with chordwise position for the stores mounted at three alternative spanwise positions. While similar trends are evident for the two sizes of store, it is clear that the magnitude of the store force coefficients for any given position can be very different. Also, in general, the results bear out the expectation that the maximum values of C_{N_S}, C_{Y_S} and C_{A_S} will be larger for the small store; on the other hand, it is perfectly possible to find store positions for which the reverse is true. Broadly speaking, for the comparisons shown in Fig. 41, the smaller store will give the higher values of C_N and C_Y for positions where the store mid-point is ahead of about $0{\cdot}7c$ while the reverse is true for the further aft positions. This can be explained satisfactorily on the grounds that as the store is moved aft, the position of the store mid-point at which the nose of the store moves out of the wing flow field is further forward for a small store. By analogy, it would seem that for far forward store positions outside the range covered in Fig. 41, the trends could again reverse in favour of the small store.

To summarise therefore the effects of store size, the maximum store force coefficients recorded at the worst chordwise positions are likely to increase as the store size is reduced but the range of chordwise positions over which these forces are large will also become less. Hence the conclusion in any specific case can only be estimated even qualitatively by visualising where the store is in relation to the wing flow field.

The addition of fins and wings to the stores will generally result in large changes in all load coefficients but no simple general guidance can be offered in this respect because it depends on where the store wings and fins are in relation to the aircraft wing flow field. As noted earlier, some systematic data are available for the effects of adding tail fins but systematic studies on the loads on stores with wings are less common at supersonic speeds.

5.4. *Effect of Aircraft Geometry.*

The store loads at supersonic speeds are affected by the same variables in the aircraft geometry as at subsonic speeds but the ways in which these variables may exert an influence are in some cases rather different. The principal variables are probably the wing sweepback, the wing taper, the wing thickness/chord ratio and maximum thickness position, the ratio of fuselage diameter to wing span, the shape of the fuselage forebody and finally, whether the wing-fuselage junction is specially waisted to suit area-rule considerations.

Some of the principal effects of wing sweepback and wing taper will have become apparent from the various results that have been presented for wings of alternatively 45 deg sweepback and moderate taper and of 60 deg delta planform. Clearly the sweepback of the forward part of the wing is important not merely in determining as at subsonic speeds the values of sidewash due to wing thickness and incidence but also as being the principal parameter which determines at what Mach number, the wing leading-edge shock moves downstream of the wing leading edge (as noted earlier, a radical change in the sidewash distribution over the span and chord occurs when this happens).

Wing taper can also affect the results in various ways. As at subsonic speeds, it can affect the spanwise lift distribution and hence the downwash and sidewash characteristics but in relation to the longitudinal load components on the store, it can do more than this: for a given size of store below a strongly tapered wing, the buoyancy effects on C_{N_S} and C_{m_S} will be relatively large for store inboard locations and relatively small for outboard locations. Another way in which taper can influence the results is that it could determine the type of flow pattern over the wing. For the examples considered in this report, the wing leading edge has usually been subsonic but the trailing edge, supersonic. For an untapered wing, however, with a subsonic leading edge, the trailing edge would also be subsonic and if the wing and body were also shaped to give a subcritical-type flow pattern even at a supersonic flight speed, the wing pressure distributions and hence the downwash characteristics etc. would be different from those discussed here; they could bear more resemblance to those at subsonic speeds.

The wing thickness/chord ratio and thickness distribution will affect the sidewash due to thickness (Fig. 29) and also the buoyancy effects (Fig. 33). As noted already, there may be a special significance in the position of the maximum thickness in determining where the sidewash due to wing thickness changes sign.

The fuselage effects and in particular, the influence of the forward fuselage shape can be much more important in supersonic flow because of their much greater lateral extent. It was suggested earlier that it might be possible to ignore the fuselage effects in subsonic flow for store locations outboard of say, 0·25 times semispan but this is certainly not justifiable in supersonic flow. Fig. 29 illustrates for example that the sidewash due to fuselage thickness only decays relatively slowly with distance out along the span and for the standard 60 deg delta wing-fuselage example, the effects at 0·75 times semispan are still rather more than half those at 0·25 times semispan. Similarly, the effects of any special fuselage shaping introduced for example to suit area-rule considerations could have a profound influence even for outboard store locations. Unfortunately, the only example of the effect on store loads of modifying the wing-fuselage junction line that was discovered in the literature search is that already discussed in Section 3.8. and illustrated in Fig. 21. These results are for $M = 1{\cdot}2$ and in this case, indenting the fuselage opposite the wing reduced the magnitude of C_Y and C_n for a store mounted at 0·25 times semispan.

The position and shape of the fuselage nose can influence the store loads in other ways. At high Mach number, or if the store is in a far forward position, the fuselage bow shock could intersect the store. If so, the nose of the store ahead of this shock would be in a region of zero sidewash. Also, the store side

force (and yawing moment) could include a significant buoyancy term, due to the propagation of this shock across the store. This is analogous to the buoyancy effect on store normal force, due to the propagation of say, the wing leading-edge shock, as described in Section 4.2.

5.5. *Effect of Aircraft Incidence.*

The effects of aircraft incidence on the store loads at supersonic speeds have already been discussed in some detail when considering the effects of store position in Section 5.1. Figs. 35, 39 to 42 all provide some illustrations of the effects of incidence; all these figures except for Fig. 42 have been discussed already; Fig. 42 will be discussed in Section 5.7. below.

In view of the close interrelation between the effects of incidence and store position, there is no point in repeating here the detailed discussion of Section 5.1. beyond noting that for some store positions, the effects of incidence can be very large while for others, they can be quite trivial. It is perhaps worth including a few comments however on whether the variation of the store loads with incidence is likely to be linear and in giving some idea of the extreme maximum values of the store-load coefficients which can be obtained at high incidence with some store positions.

As shown in Fig. 39, the most pronounced non-linear variation is often in the store normal force. $(dC_{N_S}/d\alpha)$ is often much larger at high incidence than at low incidence and so for this component, it may be unwise to extrapolate trends observed merely at low incidence. To some extent, a similar non-linear characteristic might be found for the store in isolation but this is clearly not the whole answer. For example, for the furthest forward store position in Fig. 39a, $(dC_{N_S}/d\alpha)$ changes sign above about $\alpha = 6$ deg and the implication is that with increasing incidence, the store is effectively moving into a different part of the wing-flow field. For many store positions, the values of the store normal-force coefficients at high incidence will be somewhat less than the isolated store values – because of the downwash effects. On the other hand, for a store completely immersed in the wing flow field, the values of C_{N_S} at low and moderate incidences could be appreciably greater than the isolated store values because of the buoyancy effects.

Provided that the store is not too close to the wing (i.e. for $z_s \geqslant 0{\cdot}7d$) the store pitching-moment coefficients (referred to the store mid-point) are generally linear with incidence over the range ± 10 deg. In general, the maximum value at $\alpha = \pm 10$ deg for a store without any large fins or wings should not exceed about $\pm 0{\cdot}30$, but since this conclusion is based on only a limited amount of experimental evidence, it may not apply in all cases. The addition of tail fins could have a large effect, possibly altering the sign of $(dC_m/d\alpha)$.

Most experimental results suggest that the variation of store/pylon side force with incidence remains closely linear.* As noted in Sections 5.1. and 5.7., the magnitude of the variation of C_Y with incidence depends critically on the position and size of the pylon.

The largest variations in C_{n_S} with incidence are likely for arrangements in which the store mid-point is well forward of the wing leading edge and the store is mounted on a swept forward pylon. For such positions, $(dC_n/d\alpha)$ should be positive (Fig. 39), i.e. the trend is for the yawing moment to become more nose inward as the incidence is increased. In general, the maximum yawing moment coefficient (referred to the store mid-point) at $\alpha = \pm 10$ deg is not likely to exceed $\pm 0{\cdot}20$ for a store without fins or wings. Again it should be noted that large increases in C_n may follow the addition of tail fins, particularly if the fins are located in a region of high sidewash.

Store axial force can also vary rapidly with incidence but again, the magnitude of the variation is a function of the spanwise and chordwise position of the store. For stores mounted well forward near the wing leading edge, the usual trend is for the store axial force to decrease with incidence – at least for spanwise locations between 0·25 and 0·85 times semispan. For store positions near mid-chord, on the other hand, $(dC_{A_S}/d\alpha)$ is near zero while for locations near the trailing edge, it is usually positive.

All these remarks in this Section are rather loose general statements which may not apply in all cases. To estimate what could be the incidence-effects in any particular application, one should either try and

*A non-linear trend as predicted for the cross-flow effects is observed in some cases.

find a similar installation somewhere in the literature or one should try and analyse the particular application on the basis of the physical principles and methods discussed in Section 4 and illustrated in some detail in Section 5.1.

5.6. *Effect of Aircraft Sideslip.*

The most significant changes with sideslip are the increases in store/pylon side force which are usually accompanied by appreciable decreases in the store normal force (as at subsonic speeds). Typical illustrations of the effects of sideslip on side force at supersonic speeds are included in Figs. 36, 37 and other examples may be found in Ref. 4.3. The results in Figs. 36, 37 have been discussed in some detail in Section 4.3. in relation to theoretical estimates. The main conclusions regarding store/pylon side force are as follows:

(a) at supersonic speeds above about $M = 1{\cdot}4$, C_{Y_0}, $dC_Y/d\alpha$ and $dC_Y/d\beta$ should all be negative – even if C_{Y_0} is positive, it would only be small in comparison with the other terms. Hence there is little doubt that for these speeds, the side loads should be greater for the store below the rearward wing panel. At lower speeds, this conclusion might not always apply because C_{Y_0} – at least, $(C_{Y_0})_{SA}$ and $(C_{Y_0})_S$ – could be positive and appreciable. Allowing for inertia effects, it is likely that the rearward panel will always provide the critical conditions.

(b) Fig. 37 shows that the loads under combined incidence and sideslip are not simply additive but can be appreciably greater than the sum of those due to incidence at zero sideslip and those due to sideslip at zero incidence. This means that it is important in any experimental investigation to include a full (α,β) coverage and similarly, as noted in Section 4.3., any theoretical method must take account of the variation with sideslip in the mean sidewash over the store/pylon. Incidentally, it should not be assumed from Fig. 37 that the sidewash necessarily increases with sideslip; indeed, as noted earlier, there is some suggestion that the reverse may be true at low incidences,

(c) Fig. 36 shows that the store spanwise position has only a fairly small effect on the variation of $C_{Y_{SP}}$ with β. The results in Ref. 44 show that store chordwise position has a somewhat larger effect although even in this case, it is still true to say that the effect of store position on $(dC_Y/d\beta)$ is much less than the effect on $(dC_Y/d\alpha)$. This is indeed true of all the variables except as might be expected, the addition of tail fins to the store,

(d) to quote some typical figures, Fig. 37 shows that at $\alpha = 8{\cdot}2$ deg, $M = 1{\cdot}61$ for the store mounted well forward and well outboard below the 45 deg sweptback wing-fuselage configuration, C_{Y_S} varies from about $-0{\cdot}6$ at $\beta = 0$ deg to about $-2{\cdot}0$ at $\beta = 10$ deg or about $+0{\cdot}35$ at $\beta = -10$ deg. Earlier it was suggested that for store/pylon arrangements in which the pylon was mounted well forward on the wing in a region of relatively high sidewash, the values of side force at an incidence of about 10 deg might be in the region of $-1{\cdot}0$ for C_{Y_S} and $-2{\cdot}0$ or more for $C_{Y_{SP}}$. Including the effects of 10 deg of sideslip, corresponding values would be about $-2{\cdot}2$ for C_{Y_S} or $-4{\cdot}2$ for $C_{Y_{SP}}$.

5.7. *Effect of pylon.*

Much has already been said about the effects of pylon and the way in which for many installations, the side force will be determined largely by the pylon-induced effects on the store and the loads on the pylon itself. It is also found experimentally that the pylon can have powerful secondary effects on the normal force and axial force of the store although these points have been given less systematic treatment. It may be useful to summarise here the effects of the pylon on side force at supersonic speeds although these have already been discussed in some detail in Sections 4.3., 5.1. and 5.2.

The standard curves used for estimating the pylon-induced effects and the pylon side loads are those given in Fig. 15. For a typical installation, the value of (d/b_p) should be in the region of 2·0, i.e. a store depth of about $1{\cdot}0d$. For such a value, both the pylon-induced effects and the pylon loads are likely to be appreciable. For example, the pylon-induced effects can only be dismissed as trivial for values of (d/b_p) less than about 0·6. Also, even the loads on the pylon itself tend to be at a maximum near $d/b_p = 1{\cdot}5$, i.e. it is only for pylons shorter than this that the reduction in pylon length becomes the overriding factor.

Fig. 34 provides an illustration of how the pylon-induced effects and the pylon loads can dominate the variation of store/pylon side force with incidence. Admittedly, this is a somewhat extreme example since the forward part of the store is in a region of relatively small sidewash while the pylon is situated where the variation of sidewash with incidence is likely to be at its maximum. Also, the pylon aspect ratio in Fig. 34 is about 0·4 whereas a value of 0·2 might be more typical of current practice. Even so, the comparisons in Fig. 39 suggest that it is only for fairly far aft pylons that the pylon effects are likely to be reduced to small proportions.

The evidence of Fig. 39 on this point is however somewhat confused by the fact that the pylon and store positions are changed simultaneously. Fig. 42 which has not so far been discussed is clearer in that this presents a comparison in which only the pylon position is changed. This figure which is also taken from Ref. 44 compares the variation of C_Y with α for installations in which the pylon is alternatively mounted from the forward part and from the rear part of the wing section but where in both cases, the store mid-point is $0{\cdot}25c$ aft of the local wing leading edge. The top figure compares the values of C_{Y_S}, i.e. it does not include the loads on the pylon. It will be seen that moving the pylon aft reduces $(dC_{Y_S}/d\alpha)$ by about 17 per cent and the value of C_{Y_S} at $\alpha = 10$ deg by about 23 per cent. There would be two reasons for these reductions, *viz*, the aft pylon would be in a region of smaller sidewash and secondly, since the flow is supersonic, less of the store would be influenced by the presence of the pylon. The effects on $C_{Y_{SP}}$ in the lower figure are even more striking. The value of $(dC_{Y_{SP}}/d\alpha)$ is reduced by about 23 per cent but there is also a very large change in the value of $C_{Y_{SP}}$ at $\alpha = 0$ deg, from $-0{\cdot}3$ to $+0{\cdot}3$. The net result is that the value of $C_{Y_{SP}}$ at say, $\alpha = 10$ deg is reduced by about 43 per cent.

It is clear that in this particular example, the largest single term in the reduction of $C_{Y_{SP}}$ from moving the pylon aft is the reduction or more strictly, the change in sign of the pylon side load at zero incidence. Such an effect could have been predicted from the sidewash distribution at zero incidence as plotted in Fig. 31. This large change in $(C_{Y_0})_{SP}$ could vary greatly with Mach number. One could argue that it might well be less both at lower speeds and at higher speeds. For example, at lower Mach numbers, the mean sidewash over the forward pylon might be less while at higher Mach numbers, the mean sidewash over even the rear pylon might become positive. Despite the fact that Fig. 42 may therefore be a somewhat extreme example of the effect of pylon position on $(C_{Y_0})_{SP}$) as regards Mach-number effects, this is not necessarily true in other respects. For example, if the store had been located further aft, the pylon mounted on the rear part of the wing could have been swept back and this could well have given a larger reduction in the value of $|dC_{Y_{SP}}/d\alpha|$.

To sum up, it has been stated earlier that at $\alpha = 10$ deg, $\beta = 0$ deg, the values of $|C_{Y_{SP}}|$ of the order of 2·0 to 2·5 may be expected; Fig. 42 shows that with a favourable pylon location, there are grounds for hoping that these values could be reduced to between 1·0 and 1·5 (N.B. the results in Fig. 42 are for a store depth of $1{\cdot}4d$ – as noted earlier slightly higher values of $|C_{Y_{SP}}|$ might have been obtained with a depth of $1{\cdot}0d$).

5.8. *Effect of Store-aircraft Angle.*

The effects of store skew and tilt relative to the aircraft datum are similar at supersonic speeds to those observed at subsonic speeds. No additional data are available however beyond those already discussed in Sections 3.9. and illustrated in Figs. 25 to 27. Fig. 25 in particular contains results showing the effects of 5 deg skew on the variation of $C_{Y_{SA}}$ with α for $M = 1{\cdot}41$ and 1·96 in comparison with results for $M = 0{\cdot}75$. It will be seen that for all three Mach numbers, the effects are roughly independent of incidence and the increment in $C_{Y_{SA}}$ due to 5 deg skew varies from about 0·25 at $M = 0{\cdot}75$ to about 0·45 at both supersonic Mach numbers. It is clear therefore that a nose-in skew of say, 5 deg could be very useful in partially relieving the large negative values of C_Y to be expected with most store/pylon arrangements at supersonic speeds.

5.9. *Effect of Mach Number.*

The effects of Mach number on the store loads at supersonic speeds are particularly difficult to assess in general terms since they are so interrelated with the aircraft wing-fuselage geometry and with the

position of the store/pylon. In addition to the changes between subsonic and supersonic speeds in the sidewash and downwash characteristics as described in Section 4.1., there are the additional buoyancy effects which appear at supersonic speeds owing to the wing flow field being propagated rearward roughly in the direction of the local Mach lines. Indeed, until the wing leading edge becomes supersonic, perhaps the principal reason for the store loads to vary with Mach number at supersonic speeds is the fact that the wing-fuselage flow field is propagated in a direction which is Mach-number dependent. There are however a lot of other factors as described in Section 4 and as these do not all act in the same sense, their combined effect on the store loads will vary from one application to another.

Rather than trying to draw any general conclusions therefore, it may be more useful to take a typical case and to analyse for example how and why the store side force has varied with Mach number. Fig. 43 is a good illustration since results are available for the full speed range from $M = 0{\cdot}7$ to $M = 1{\cdot}96$.* Results are presented for the variation of store side force, with and without a pylon, over the incidence range from -5 deg to 10 deg for a store located at 0·6 semispan beneath a 45 deg sweptback wing with the mid-point of the store situated at the local wing leading edge. It will be noted that the overall answer is that the largest absolute values of C_{Y_S} at say, $\alpha = 10$ deg, are obtained at the highest test Mach number of $M = 1{\cdot}96$. Results discussed earlier suggest that this trend would have been even more pronounced if Fig. 43 had included the pylon loads, i.e. if $C_{Y_{SP}}$ had been plotted rather than C_{Y_S}.

Basically, the increase in $|C_Y|$ between high subsonic and supersonic speeds is mostly due to the variation in C_{Y_0} with Mach number: in the subsonic range, C_{Y_0} becomes steadily more positive but beyond $M = 1{\cdot}0$, this variation is reversed and C_{Y_0} eventually changes sign and becomes more negative with increasing Mach number. This trend also appeared in back-figuring the experimental data to produce the empirical method of Section 6 for estimating store/pylon side force – *see*, for example Figs. 48 and 51. Generally, ignoring the pylon loads, the reversal in sign of $(C_{Y_0})_{SS}$ occurs somewhere near $M = 1{\cdot}4$ but the effect of the pylon loads is to make $(C_{Y_0})_{SP}$ even more strongly negative. The decrease in C_{Y_0} in the transonic and low supersonic range can be related to the change between subsonic and supersonic speeds in the sidewash distribution due to wing thickness: in incompressible flow the change from positive to negative sidewash occurs at the wing leading edge but in supersonic flow, it occurs on the Mach-cone originating from the wing root maximum thickness position. The continued trend towards more negative values of C_{Y_0} at higher supersonic Mach numbers would be expected since the negative sidewash field will progressively pass to the rear of the store/pylon. This type of variation of C_{Y_0} with Mach number should apply for any store arrangement but the magnitude of the variation and the Mach number at which C_{Y_0} is zero would of course vary with the size, shape and position of the store and its pylon.

The variation of $(dC_Y/d\alpha)$ with Mach number in Fig. 43 is not so clear-cut. The trend is for the absolute value to increase to a maximum near $M = 1{\cdot}0$ and then decrease to a minimum near $M = 1{\cdot}4$ and subsequently increase again. The significant point here is probably that the store is in an extremely far forward position. As a result, the nose of the store ceases to be influenced by the sidewash due to wing incidence at a relatively low supersonic Mach number and this probably accounts for the decrease in $|dC_{Y_{SA}}/d\alpha|$ between $M = 1{\cdot}0$ and $1{\cdot}4$. The rapid increase between $M = 1{\cdot}4$ and $M = 1{\cdot}6$ in the pylon-induced contribution to $|dC_{Y_S}/d\alpha|$ suggests that the mean (σ/α) over the pylon is then increasing rapidly. Two possible explanations could be put forward for the increases in $|dC_{Y_{SA}}/d\alpha|$ between $M = 1{\cdot}4$ and $M = 1{\cdot}96$. First, the side load on the forward part of the store could increase because of the sidewash due to the forward fuselage (Fig. 31). Then, as the fuselage bow shock approached and finally intersected the store, there could be appreciable buoyancy contribution to $C_{Y_{SA}}$ and $C_{n_{SA}}$ (analogous to the effect of the wing flow field on $C_{N_{SA}}$ and $C_{m_{SA}}$ – *see* Section 4.2.). In the present case, it is thought that the fuselage bow shock should intersect the store nose at about $M = 1{\cdot}8$. Ultimately, at some Mach number beyond the test range, i.e. beyond $M = 1{\cdot}96$, $|dC_{Y_{SA}}/d\alpha|$ and $|C_{Y_{SA}}|$ should decrease again as more of the store lies ahead of the fuselage bow shock and hence is unaffected by the aircraft flow field. These suggestions are a little speculative but if true, they imply that the trends with Mach number in $(dC_Y/d\alpha)$ as shown in

*It is possible that at low supersonic Mach numbers, the results may have been influenced by wave reflections from the tunnel walls but these should not have affected the general trends.

Fig. 43 are occurring at somewhat lower supersonic Mach numbers than would be the case for a store mounted with its mid-point near or behind the wing leading edge.

It is hoped that this brief discussion of the results in Fig. 43 will help in understanding some of the changes that can occur with increasing Mach number in the supersonic range. At higher Mach numbers, when the aircraft wing leading edge becomes supersonic, rather more radical changes may occur particularly for stores mounted well inboard. Fig. 28 shows that the sidewash due to incidence over the forward part of the inner wing could then increase appreciably, thus giving a large further increase in $|dC_{Y_{SP}}/d\alpha|$ for an arrangement with a forward pylon.

The changes with Mach number in the values of C_N are possibly less important in practice than the changes in C_Y but it should be noted that they are possibly more radical. Considering a store without fins or wings, the value of C_{N_0} at subsonic speeds will usually tend to be positive but at supersonic speeds, it can be either positive or negative according to where the store is situated in relation to the wing-flow field and is quite likely to be larger in magnitude. The value of $(dC_N/d\alpha)$ at subsonic speeds for such a store is almost certain to be negative whereas at supersonic speeds, for certain store positions as shown in Fig. 39, it can be quite large and positive. This distinction is partly due to a change in the isolated store characteristics but other contributory factors could be the lack of downwash behind the wing trailing-edge shock and an increase with incidence in the buoyancy contribution to C_N for certain parts of the field. This last point could be particularly important for stores mounted near the root of a well tapered wing. For the same reasons, there could be changes in the pitching moment characteristics with Mach number which would be even more difficult to predict in a general fashion.

The discussion above has been entirely based on results for underwing stores. Ref. 27 presents the results of a store-loads investigation from $M = 0{\cdot}80$ to $M = 1{\cdot}43$ for an underfuselage store. The changes with Mach number in the measured store load coefficients in this case were relatively slight.

5.10. *Interaction of Two Stores on One Wing Panel.*

Ref. 44 presents experimental results at $M = 1{\cdot}61$, showing the interference effect of an inboard store at 0·55 semispan on the aerodynamic loads on an outboard store at 0·85 semispan, on the same wing panel. As shown in Fig. 44, at zero sideslip, the addition of the inboard store gives only small changes in the axial force, pitching moment and yawing moment on the outboard store but there were appreciable effects on normal force and side force particularly at incidence. At $\alpha = 10$ deg, C_{N_S} was increased by the mutual interaction by 0·25 while C_{Y_S} was reduced by about 25 per cent. The reduction in C_{Y_S} comes from a positive increment at zero incidence of about 0·15 and a reduction in $|dC_{Y_S}/d\alpha|$ of about 12 per cent. All these changes in C_{N_S} and C_{Y_S} suggest that the presence of the inboard store is serving to reduce the mean sidewash over the outboard store/pylon; in other words, primarily, the inboard store/pylon can be considered to act as a 'fence' which shields the outboard store. As noted in Section 3.11., similar results have been obtained in another investigation at subsonic Mach numbers.

Ref. 44 also includes evidence on the interference effects with the model sideslipped. The differences in C_N and C_Y due to the influence of the inboard store increase with β, i.e. are greater when the stores are under the rearward wing panel. One has to be a little careful here: the differences are greater or in other words, the interference reduces $|dC_Y/d\beta|$ in the same way as it reduces $|dC_Y/d\alpha|$ but as a ratio, the effect of the interference is less pronounced, e.g. for $\alpha = 8{\cdot}2$ deg, $\beta = 10$ deg, the interference reduces $|C_{Y_S}|$ by about 15 per cent as compared with the 25 per cent figure quoted above for $\beta = 0$ deg. This implies that as might have been expected, the interference effects between the stores is somewhat less pronounced on $|dC_Y/d\beta|$ than on $|dC_Y/d\alpha|$. Under sideslipped conditions, in addition to the effects on C_N and C_Y, the addition of the inboard store also gives material changes in the values of C_A on the outboard store; the changes in C_m and C_n remain fairly small. The changes in C_A are in the sense of the axial force being reduced at positive β (i.e. stores under rearward wing panel) and increased at negative β.

6. *New Empirical Method for Estimating Store Pylon Side Force.*

The discussion in the earlier parts of the Report has shown that there is no method available for estimating the store/pylon side force that is relatively quick and easy to apply. Since this is probably the most

important load component, there is a real need for such a method of estimation provided that it can be developed to give moderate accuracy. It is clear from the previous discussion that there can be no hope of producing an empirical method to be a completely adequate substitute for wind-tunnel testing but provided one does not set one's sights too high, something useful can perhaps be achieved. This means that one should not try and develop an empirical method which allows for the effects of all possible variables; if one tried to do this, the method would not only become very complicated and so defeat the object of the exercise but also almost certainly it would tend to become inaccurate. Enough has been said to show that if one is trying to achieve a really accurate method of prediction allowing for all variables, one must not start from an empirical approach but from calculating or measuring the characteristics of the flow field in which the stores are immersed. Even then, the methods of this type that have been developed appear to be only capable – at least, at subsonic speeds – of predicting the general qualitative trends.

In setting limited aims for the empirical method, the first and most important point to note is that one must decide on a range of store/pylon size and position that can be taken as typical of current and future practice and one must accept the fact that if one tries to extrapolate the method outside this range, this is likely to lead to a considerable loss in accuracy. To give an illustration of this point, it is clear from the earlier discussion that any method of prediction has to take account of the effects of store chordwise and spanwise position. If one assumes however the method only need apply to stores of roughly comparable size, the co-ordinates of the store mid-point will suffice to define its position but a radical change in store size would mean that for a given position of the mid-point, the nose of the store or its tail fins could be in a region of vastly different sidewash. Hence, if one has to admit large variations in store size, further parameters have to be introduced and so on.

In addition to defining within fairly close limits the range of store/pylon geometry for which the method is going to be applicable, it is clear that the true detailed changes with Mach number can only be defined in a very broad manner. This applies both in the transonic range for which the main difficulty is the relative lack of available experimental data and also in the supersonic range where as noted above in Section 5.9., the changes in side force with Mach number may be far from smooth or monotonic as the different parts of the wing-fuselage flow field pass over the store/pylon with increasing Mach number.

Despite these obvious difficulties however it has been found possible to devise a relatively simple method for estimating store/pylon side force which appears to give a reasonable fit to the experimental data that have been analysed. The satisfactory correlation with the data that form the starting point of the analysis merely implies that a suitable set of parameters has been chosen to fit these data; the more crucial test will come later when predictions by the method are compared with new experimental data that were not available at the time the method was derived. Even so, the order of agreement that has been achieved so far was thought sufficiently encouraging to justify presenting the method in this Report. Almost certainly, analysis of later experimental data will show the need to revise some of the figures that are presented and there is quite a possibility that new results will show that no simple method such as this can work in the transonic and low supersonic Mach-number range. Apart from this, however, it is hoped that new data will confirm that the basic framework of the method is sound. If this proves to be the case, it may be possible to extent the method to other components although it should be said at the outset that detailed arguments could be put forward as to why side force could be easier to predict than the rest. The details of the method are presented in the succeeding Sections.

6.1. *Range of Application of Method.*

The aim has been to cope with the wing-store-pylon configurations that are likely to be of most interest in the immediate future.* This was taken to imply that the method should be suitable

(a) for aircraft wing designs ranging from say, 30 deg to 40 deg sweptback wings of moderate taper to say, 60 deg delta planforms,

---

*The range of likely configurations was based on suggestions from Weapons Department, R.A.E. Farnborough.

(b) pylons with a thickness/chord ratio of say, 5 or 6 per cent, a maximum thickness of 3 in to 4 in, a depth below the wing of 10 in to 12 in and a chord of the order of half the local wing chord,

(c) stores of streamline shape with a diameter of say, 14 in to 20 in, a length of from 115 in to 160 in, a fineness ratio of order 7·5 to 8·5 and with or without small tail fins with a span of about 1·4 times the store maximum diameter with a fin gross aspect ratio in the region of 1·4 and a fin leading-edge sweepback of about 45 deg.

This specification implies that the range of the important geometrical parameters when non-dimensionalised by the mean chord of the wing is as follows:

	Swept wings	Delta wings
$l_s/\bar{c}$	0·80 to 1·10	0·50 to 0·80
$d_{max}/\bar{c}$	0·10 to 0·15	0·06 to 0·09
z_s/d	Near 1·0	Near 1·0

As regards store position, the method is designed to cope with a range of spanwise positions from say, 0·25 to 0·8 times wing semispan, for a range of chordwise positions of the store mid-point from well ahead to well behind the wing leading edge and despite the preference for a store depth of about $1{\cdot}0d$ noted above, for a range of store depth from 0·5 to $3{\cdot}0d$ below the wing.

Restricting the range of geometry to the figures quoted above implies that some of the possible variables can be eliminated. Perhaps the most important point to note however is that certain basic assumptions have been made regarding the type of pylon that would be used. It has been assumed that for all store positions, the pylon would be rigidly attached to the wing in the region of the wing maximum thickness and that it would be swept forward, unswept, or swept back according to the chordwise position of the store. In other words, no allowance is made for possible changes in the position of the pylon-wing junction with the chordwise position of the store. This is an important reservation because as seen in Section 5, the store/pylon side force at supersonic speeds can be largely a function of the pylon geometry and for example, for a given store chordwise position, appreciable changes in C_Y can result from moving the pylon from the front to the rear of the local wing section. The results shown in Fig. 42 provide the only direct evidence on this point; in all other investigations, changes in pylon geometry were accompanied by changes in store position as assumed for the present method. It was not thought worthwhile therefore to try and introduce any refinement to allow for changes in pylon-wing position since in practice, structural and other considerations will probably dictate that as assumed here, the pylon is attached in the region of the wing maximum thickness.

It must be admitted that the reports containing experimental results on store/pylon arrangements within the range of geometry as specified above are relatively few in number and so to establish the formulae of the method it has been necessary to extend the range of geometry in certain directions, e.g. the length of a relevant size store has had to be extended up to 1·8 times the mean chord of the wing (as noted earlier, much of the experimental data at supersonic speeds are for relatively large stores). One final point on store geometry is that it has been assumed that the store has no tilt or skew relative to the aircraft centreline.

Strictly, the numerical values in the figures are intended to apply for stores mounted beneath 45 deg sweptback wings and it is suggested that for small differences in sweepback from this value, the estimates of C_{Y_0} and $(dC_Y/d\alpha)$ should be factored by the appropriate values of sin Λ where Λ is the quarter-chord sweepback.

The method provides formulae for estimating the loads on the store in the presence of the wing but with no pylon, the side loads including the pylon-induced effects on the store, and the total store/pylon loads.

The method is intended to provide estimates over the full speed range from low speeds up to about $M = 2{\cdot}0$. With the wing geometry as specified above, this implies that the method is intended to cover the

supersonic Mach-number range in which the wing leading edge remains subsonic – allowing for the effects of the finite wing thickness. At higher Mach numbers, particularly for inboard store locations, the method may become unreliable. It would certainly be unwise to use it without further verification for estimating the loads on stores mounted beneath relatively unswept wings.

6.2. *Notation.*

The notation used in Figs. 45 to 53 remains as defined in the List of Symbols with the factors K_{m_1}, and K_{m_2} etc. being empirical factors defined in the equations later in this section. It should be noted that α is the angle of incidence (degrees) relative to the freestream, positive nose up while β is the angle of sideslip (degrees) relative to freestream, positive nose to port.

6.3. *Variation of Side Force with Incidence.*

The available experimental results show that the variation of store/pylon side force with incidence (and indeed with sideslip) remains substantially linear with change in store location, Mach number, and other minor parameters. This suggests the use of an empirical 'straight line law' modified by factors which take account of the effects of these parameters as measured experimentally.

6.3.1. *Store with no tail fins.* The following rule gives a close approximation to the side force experienced by a relevant size store, pylon mounted adjacent to a 45 deg swept wing, with no tail fins.

$$(C_Y)_\alpha = \left[C_{Y_0} K_{m_3} + K_{m_1} . K_{m_2} . (\alpha) \left(\frac{dC_Y}{d\alpha} \right) \right] K_{m_4} \tag{1}$$

Values of $\left(\frac{dC_Y}{d\alpha} \right)$ vary with spanwise location of the store as shown in Fig. 45 for the store alone (S.A.), store plus pylon induced(S.), and total store plus pylon (S.P.) cases. Regions inboard of about 0·20 semispan and outboard of about 0·85 semispan are excluded from this analysis. Factor K_{m_1} allows for the variation of $(dC_Y/d\alpha)$ with the chordwise location of the store mid-point (Fig. 46) and factor K_{m_2} allows for the variation of this quantity with Mach number (Fig. 47). Note that the variation of K_{m_2} with Mach number is doubtful at transonic speeds and that the values of K_{m_2} at supersonic speeds are not valid if the bow shock wave ahead of the fuselage nose intersects the store directly.

Values of C_{Y_0} are substantially unaffected by spanwise position of the store but vary with Mach number as shown in Fig. 48 for the store alone, store plus pylon induced, and total store plus pylon cases. Again the variation of C_{Y_0} with Mach number is doubtful at transonic speeds. Indeed, as noted earlier, it is difficult to explain physically why the pylon-induced effects change sign somewhere in the transonic range. This is perhaps one of the most doubtful points in the curves for the method. No information on the total store plus pylon values are available other than at $M = 1{\cdot}61$. Fig. 49 shows that the value of C_{Y_0} is dependent upon the chordwise location of the store mid point and allowance for this is made by the inclusion of factor K_{m_3}.

The magnitude of the store/pylon side force coefficient is closely dependent upon the vertical location of the store centreline, and increases rapidly as the store approaches the wing. In an attempt to allow for this Fig. 50 has been prepared and plots the variation of factor K_{m_4} with store vertical location in store diameters.

Equation (1) is applicable to the estimation of the variation with incidence of $C_{Y_{SA}}$, C_{Y_S} and $C_{Y_{SP}}$ for a store with no fins beneath a 45 deg swept wing. For other wing sweeps it is sufficiently accurate to multiply $(C_Y)_\alpha$ by the ratio ($\sin\Lambda/\sin 45$ deg).

6.3.2. *Estimated effect of tail fins.* The addition of tail fins to a store can produce large changes in the store/pylon side-force coefficients. The available experimental results indicate that the presence of fins between $x_s = 0{\cdot}5$ and $x_s = 1{\cdot}5$ approximately produce a change in C_{Y_0} with only small changes in $(dC_Y/d\alpha)$. It is therefore recommended that the values of C_{Y_0} for a store with relevant size fins in the above chordwise locations should be obtained from Fig. 51 instead of Fig. 48 and that all the other parameters in equation (1) remain unaltered.

If the fins are located in close proximity to the local wing leading edge the above recommendation is not advisable since Figs. 6 and 31 indicate that they will then be in a region of large sidewash.

6.4. *Variation of Store/Pylon Side Force with Sideslip* ($\alpha = 0$).

The remarks contained in this Section refer to stores on the rearward wing panel where positive sideslip produces negative (outboard) side forces. Stores on the forward wing panel are subjected (in general) to positive (inboard) side forces with positive sideslip. The underwing sidewash at zero incidence produces values of C_{Y_0} given in Fig. 48 for the fins off case (Fig. 51 for fins on); these values are added to the side force produced by positive sideslip. Note that the values of C_{Y_0} change sign at $M = 1{\cdot}4$ (approx.) for the store plus pylon induced case, and at $M = 1{\cdot}6$ (approx.) for the store alone case.

6.4.1. *Store with no tail fins.* The amount of experimental evidence on the variation of store/pylon side force with sideslip is limited, but the following empirical rule gives a close approximation to the side force experienced by a relevant size store/pylon mounted adjacent to a 45 deg swept wing, with no tail fins.

$$(C_Y)_\beta = \left[C_{Y_0} K_{m_3} + K_{m_5}(\beta) \left(\frac{dC_Y}{d\beta}\right) \right] K_{m_4} \tag{2}$$

Values of $\left(\frac{dC_Y}{d\beta}\right)$ vary slightly with spanwise location as shown in Fig. 52 for the store plus pylon induced and the total store plus pylon cases. No information is available for the store alone case. Factor K_{m_5} is included to allow for the variation of $(dC_Y/d\beta)$ with Mach number; large doubtful changes are evident at transonic speeds (Fig. 53). No experimental results are available from which the variation of C_Y with store vertical location may be obtained, but it seems reasonable to include factor K_{m_4} in equation (2) to allow for this. The variation of $(dC_Y/d\beta)$ with chordwise location appears to be negligible.

Values of C_{Y_0} and K_{m_3} may be obtained from Figs. 48 and 49.

6.4.2. *Estimated effect of tail fins.* For store tail locations aft of about the local wing mid-chord point, the addition of relevant size tail fins is shown principally by an increase in $(dC_Y/d\beta)$ and a smaller variation of this quantity with Mach number. This is illustrated in Fig. 53 which shows the variation of factor K_{m_5} with Mach number for the fins on and fins off cases.

A good approximation to the variation of store/pylon side force with sideslip for a store with fins may be obtained by using equation (2) and substituting the fins-on value of K_{m_5} from Fig. 53.

6.5. *Variation of Store/Pylon Side Force with Combined Incidence and Sideslip.*

The available experimental evidence suggests that it is not sufficiently accurate to estimate the combined effects of incidence and sideslip as the sum of the separate effects of incidence given by equation (1), and of sideslip given by equation (2). It appears that the values of $(dC_Y/d\beta)$ given in Fig. 52 increase by about 25 per cent when incidence and sideslip are applied together.* Until further experimental results are available, a more accurate empirical rule for use with combined incidence and sideslip would be:

*Note that equations (1) and (2) both contain the C_{Y_0} term (i.e. the value at $\alpha = \beta = 0$) hence straight addition of equations (1) and (2) would in any case be in error since C_{Y_0}. K_{m_3}. K_{m_4} would be included twice.

$$(C_Y)_{\alpha\beta} = (C_Y)_\alpha + 1{\cdot}25\, K_{m_5} . K_{m_4} . (\beta) \left(\frac{dC_Y}{d\beta}\right) \tag{3}$$

In this respect it is necessary to consider the direction of the side force due to incidence and due to sideslip. Positive sideslip (nose to port) gives outwardly directed side forces on stores beneath the rearward (port) wing panel, and inwardly directed side forces on stores beneath the forward (starboard) wing panel. Positive incidence (nose up) gives outwardly directed side forces on stores beneath either wing panel. Hence the maximum side forces produced by combined incidence and sideslip occur on port wing stores when both angles are of the same sign, and on starboard wing stores when the angles are of opposite sign.

6.6. *Specimen Calculation and Comparisons with Experiment.*

A specimen calculation on the store/pylon combination of ref. 27, Fig. 20, is now given to show the steps in the empirical method.

Calculation of typical side force values.

Data: Ref. 27, Configuration as Fig. 20.

45 deg swept wing, aspect ratio 4·0, taper ratio 0·15
NACA 64A206, $a = 0$, from $y_s = 0$ to $y_s = 0{\cdot}50$
NACA 64A203, $a = 0{\cdot}8$ (mod), from $y_s = 0{\cdot}50$ to $y_s = 1{\cdot}0$
Dihedral = 0 deg, waisted fuselage
Store length $(l_s) = 1{\cdot}41c$, Fineness ratio = 8·5, with fins
$y_s = 0{\cdot}25^b/2 \qquad x_s = 0{\cdot}625c \qquad z_s = 0{\cdot}85d \qquad M = 0{\cdot}80.$

From Figs. 45 to 53 inclusive the following values are evident for the STORE PLUS PYLON INDUCED CASE at $M = 0{\cdot}80$.

$(dC_Y/d\alpha) = -0{\cdot}050$ from Fig. 45 $\qquad K_{m_3} = 1{\cdot}080$ from Fig. 49

$K_{m_1} = 0{\cdot}670$ from Fig. 46 $\qquad K_{m_4} = 1{\cdot}300$ from Fig. 50

$K_{m_2} = 1{\cdot}250$ from Fig. 47 $\qquad (dC_Y/d\beta) = -0{\cdot}043$ from Fig. 52

$C_{Y_0} = 0{\cdot}285$ from Fig. 51 $\qquad K_{m_5} = 2{\cdot}30$ from Fig. 53

(1) At $\beta = 0$, $(C_Y)_\alpha = [(C_{Y_0})\, K_{m_3} + K_{m_1}\, K_{m_2}\, (\alpha)\, (dC_Y/d\alpha)]\, K_{m_4}$

$= [(0{\cdot}285)\, 1{\cdot}080 + 0{\cdot}670.\ 1{\cdot}250\, (-0{\cdot}050)\, \alpha]\, 1{\cdot}30$

$$\underline{(C_Y)_\alpha = 0{\cdot}40 - 0{\cdot}0544\, \alpha} \tag{1}$$

(2) At $\alpha = 0$, $(C_Y)_\beta = [(C_{Y_0})\, K_{m_3} + K_{m_5}\, (\beta)\, (dC_Y/d\beta)]\, K_{m_4}$

$= (0{\cdot}285)\, 1{\cdot}08 + 2{\cdot}30\, (-0{\cdot}043)\beta]\, 1{\cdot}30$

$$\underline{(C_Y)_\beta = 0{\cdot}40 - 0{\cdot}129\beta} \tag{2}$$

(3) At combined $\alpha\beta$, $(C_Y)_{\alpha\beta} = (C_Y)_\alpha + 1{\cdot}25\, K_{m_5}\, K_{m_4}\, (\beta)\, (dC_Y/d\beta)$

$= 0{\cdot}40 - 0{\cdot}0544\alpha + 1{\cdot}25\, (-0{\cdot}129\beta)$

$$(C_Y)_{\alpha\beta} = 0{\cdot}40 - 0{\cdot}0544\alpha - 0{\cdot}161\beta \tag{3}$$

Fig. 55 plots the experimental variation of C_{Y_S} with β at both $\alpha = 0$ deg and $\alpha = 5{\cdot}6$ deg. Using the above equations the empirical values are as follows:

At $\alpha = 0$ deg, $\beta = 0$ deg, $C_{Y_S} = 0{\cdot}40$ from (1), (2) or (3)

At $\alpha = 0$ deg, $\beta = 8$ deg, $C_{Y_S} = -0{\cdot}63$ from (2)

At $\alpha = 5{\cdot}6$ deg, $\beta = 0$ deg, $C_{Y_S} = 0{\cdot}10$ from (1)

At $\alpha = 5{\cdot}6$ deg, $\beta = 8$ deg, $C_{Y_S} = -1{\cdot}19$ from (3)

Reference to Fig. 55 shows good agreement with experiment over the sideslip range from 0 deg to 10 deg.*

Further comparisons between experimental and empirical store side force values are given in Figs. 54 and 56 at $M = 1{\cdot}61$ for a large store without fins, pylon-mounted beneath a 45 deg swept wing. Fig. 54 shows the comparison of store plus pylon induced values for the store mounted at 0·55 semispan, whilst Fig. 56 shows the comparison for the total store plus pylon values for the same store mounted at 0·85 semispan. Again, good agreement between measured and predicted values are evident. This is also confirmed by two other examples given earlier in Figs. 17 and 35. For example, Fig. 35 illustrates that the variation of $C_{Y_{SP}}$ with incidence ($\beta = 0$) for three spanwise locations is closely predicted, while Fig. 17 is another example at low Mach number which incidentally shows that the new empirical method for store side force is superior to that contained in Ref. 17.

7. *Concluding Remarks.*

This report has contained a large number of conclusions both about the validity and accuracy of the various methods available for estimating the aerodynamic loads on external stores adjacent to wing-fuselage configurations and also on what the experimental data indicate as regards the variation of these loads with different parameters at subsonic, transonic and supersonic speeds. These conclusions have been summarised at appropriate points in the text and it would be redundant to repeat them all here. Instead, it may be more useful to conclude by reviewing the scope of the report and the extent to which it may have succeeded in its aims.

The first step in producing this Report was to review the available literature on aerodynamic loads on external stores, carried principally on pylons in underwing locations. Although this search produced a list of 371 references, in the interests of brevity only those which are directly relevant have been included in this version of the Report.

The next aim was to review the methods at present available for estimating the aerodynamic loads. It has been found that broadly speaking, these methods fall into two categories. First, there are the fairly elaborate methods which start from either the measured or the predicted wing-fuselage flow field characteristics. It is found that these are usually rather laborious to apply – perhaps particularly at subsonic speeds – and even in the end, they do not necessarily lead to good quantitative load estimates. In particular, the results achieved at subsonic speeds are disappointing in that although the correct qualitative trends are indicated, the quantitative values of normal force and side force are often underestimated by a factor of 2 or more. At supersonic speeds, rather better success is obtained and provided one bears in mind the various points listed in Section 4.4., the whole problem appears to be rather more tractable. Throughout the speed range, this type of approach starting from the wing-fuselage flow field characteristics is the best way of tackling the problem; even if the methods do not lead to good quantitative predictions, an understanding of the flow field characteristics is vital to any appreciation of how the store loads vary with store position, Mach number etc. The main features of the flow fields both at subsonic and supersonic speeds and how they can affect the loads have therefore been analysed and described in considerable detail in the Report and it is hoped that this discussion will help in interpreting any set of experimental load measurements.

*In these and other comparisons, results are presented for stores on the rearward wing panel at positive β.

The second type of method for predicting the loads is to take the results of actual experimental measurements and to analyse them to give factors dependent on different geometrical parameters, incidence, sideslip and Mach number. The R.A.E. developed such methods for estimating the loads on stores at low speeds but the usefulness of these methods is now severely limited: they strictly only apply to a range of store geometry which does not include some of the current practical installations; they do not include any allowance for pylon loads and they are relatively weak in estimating the most important component, i.e. the store side force. To meet the urgent need for a reasonably reliable and quick method for estimating this component, a new method has been derived and is presented in Section 6 of the report.

The hope is that the new empirical method for estimating store/pylon side force will apply to store/pylon/aircraft geometries that are regarded as typical of current practice and over the full speed range up to about $M = 2{\cdot}0$ (or strictly, for the range in which the aircraft wing leading edge is subsonic). Comparisons are included to illustrate that the method gives reliable results when compared with the experimental data from which it was derived. This confirms that the choice of the different parameters in the method is suitable in respect of these data but a more crucial test will come later when predictions by the method are compared with experimental data not yet available. Even without this check, there seems sufficient grounds for optimism to justify presenting the method. The chief doubt relates to how well the method predicts the trends with Mach number: in the transonic range, these are very uncertain because of the severe shortage of experimental data while at supersonic speeds, it is impossible in any simplified method to reproduce all the various Mach-number effects which are very dependent on store/pylon size and position. When more experimental data are available, it may be found necessary to revise some of the curves presented in Figs. 45 to 53 for use with the method; this is particularly true at transonic speeds and it is even possible that the additional data will show that a simplified method of this sort would never be entirely satisfactory in this range.

The final aim has been to show with the help of selected illustrations how the store loads vary with the major parameters at subsonic, transonic and supersonic speeds. The effects of many of these parameters are closely interrelated and so it is often difficult to draw any general conclusions. It is frequently stressed that one must not try and generalise from any set of results without thinking in terms of what are the relevant changes in the wing-fuselage flow field that are involved in the generalisation. Despite these difficulties, it is hoped that the Report will have conveyed some idea of how the loads are likely to vary with store chordwise, spanwise and vertical position, pylon size and position, store skew relative to the aircraft centreline, incidence, sideslip, Mach number and the more important features of the aircraft-fuselage geometry such as wing sweepback, taper and thickness and fuselage size and shape. In particular, it is shown how the pylon-induced effects and the loads on the pylon itself play a major part in determining the store/pylon side force, particularly at supersonic speeds.

Of the other variables, leaving aside the obvious effects of incidence, sideslip, Mach number and store depth, it seems that store chordwise position is probably the most important single variable. For many applications, the store mid-point will often be somewhere near the wing leading edge but it is shown that this type of position is likely to lead to large absolute values of both C_Y and C_N at high incidence (and sideslip) and other positions could be found to give smaller aerodynamic loads. Other points that are worth noting here are that in trying to estimate the maximum aerodynamic loads likely for any given installation, one should not ignore the negative g or negative incidence case for which the local dynamic pressure over the store can perhaps be almost twice as great as at high positive incidence. Also, in estimating the loads under combined (α,β), it is not sufficient to estimate the loads due to incidence at zero sideslip and those due to sideslip at zero incidence and simply add them together: this practice could lead to a serious underestimate of the combined loads.

To sum up, it is hoped that this Report will help in three major respects, *viz*,

(1) in reviewing the available methods for estimating the loads and in presenting a new rapid empirical method for estimating store/pylon side force for a limited but important range of configurations,

(2) in indicating the main qualitative trends in the variation of the store loads with the major parameters in the aircraft/store geometry and with incidence, sideslip and Mach number,

(3) and in contributing to a real understanding of the problem.

Further experimental data are needed to provide additional checks to the new empirical method for estimating store/pylon side force. Even if these substantiate the method with only minor revisions, it seems clear that for store side force and indeed for other components, wind tunnel tests will always be required to provide accurate quantitative results. This is particularly true at high subsonic and transonic speeds.

8. *Acknowledgement.*

The Authors wish to acknowledge the assistance of Mr. E. J. McAdam in the search for relevant reports and in correlating the material from these reports.

LIST OF SYMBOLS (*see* also Fig. 1)

For stores on either wing panel:

N	Normal force, positive upwards
Y	Side force, positive inwards
A	Axial force, positive rearwards
m	Pitching moment, positive nose upwards
n	Yawing moment, positive nose inwards
1	Rolling moment, positive inboard side down
C_N	Store normal-force coefficient $= N/qF$
C_Y	Store side-force coefficient $= Y/qF$
C_A	Store axial-force coefficient $= A/qF$
C_m	Store pitching-moment coefficient $= m/qF1_s$
C_n	Store yawing-moment coefficient $= n/qF1_s$
C_1	Store rolling-moment coefficient $= 1/qF1_s$
F	Store maximum frontal area
1_s	Store length
q	Free stream dynamic pressure
ε	Angle of downwash, positive downwards
σ	Angle of sidewash, positive outwards
α	Angle of incidence, positive upwards
β	Angle of sideslip, positive nose to port
α_1	Resultant flow angularity in pitch plane $= (\alpha-\varepsilon)$ deg
β_1	Resultant flow angularity in yaw plane $= (\beta+\sigma)$ deg
$(C_Y)_\alpha$	Store/pylon side-force coefficient at incidence α deg ($\beta = 0$ deg)
C_{Y_0}	Store/pylon side-force coefficient at $\alpha = \beta = 0$ deg
$\frac{dC_Y}{d\alpha}$	Rate of change of store/pylon side-force coefficient with incidence (per degree)
$(C_Y)_\beta$	Store/pylon side-force coefficient at sideslip β deg ($\alpha = 0$ deg)
$\frac{dC_Y}{d\beta}$	Rate of change of store/pylon side-force coefficient with sideslip (per degree)
$(C_Y)_{\alpha\beta}$	Store/pylon side-force coefficient at combined incidence α deg and sideslip β deg
K_{m_1}, K_{m_2}, etc.	Empirical factors in side-force estimation
$C_{Y_{SA}}$	Store side-force coefficient in the presence of the wing-fuselage combination with no pylon (designated store alone).

C_{Y_S}	Store side force coefficient in the presence of the wing-fuselage combination and the pylon (designated store plus pylon induced).
$C_{Y_{SP}}$	Total side-force coefficient of the store/pylon assembly (designated total store plus pylon)
C_{Y_P}	Pylon side-force coefficient in the presence of the store (designated pylon plus store induced) $= C_{Y_{SP}} - C_{Y_S}$
A_p	Pylon aspect ratio $= b_p/c_p$
b_p	Pylon span (exposed) $= z_s-(d/2+t/2)$
b	Wing span
c	Local wing chord at store station
c_0	Root chord of wing
c_T	Tip chord of wing
c_p	Pylon chord
$\bar{c}$	Aerodynamic mean wing chord
d	Maximum diameter of store
D	Maximum diameter of fuselage
M	Mach number
S	Wing gross area
t	Wing maximum thickness
x_F	Chordwise distance from fuselage nose to wing $c/4$ apex
x_p	Chordwise distance from fuselage nose to wing $c/4$ apex
x_p	Chordwise distance from store nose to pylon leading edge (on store centreline).
x_s	Chordwise position of store mid point relative to the local wing leading edge
x_w	Chordwise distance from store nose to local wing leading edge
y_s	Spanwise position of store mid point expressed as a fraction of the wing semispan from the fuselage centreline
z_s	Vertical distance of store centreline from wing chord plane.
Λ	Wing quarter-chord sweep
Λ_p	Pylon leading-edge sweep

REFERENCES

No.	*Author(s)*	*Title, etc.*
1	W. J. Alford, Jr.	Theoretical and experimental investigation of the subsonic flow fields beneath swept and unswept wings with tables of vortex-induced velocities. NACA Report 1327, 1957.
2	H. Glauert	*The elements of aerofoil and airscrew theory*. 2nd ed., C.U.P., 1948.
3	H. J. Allen and E. W. Perkins	Characteristics of flow over inclined bodies of revolution. NACA RM A50L07, March, 1951.
4	H. Multhopp	Methods for calculating the lift distributions of wings (subsonic lifting-surface theory). A.R.C. R. & M. 2884, January, 1950.
5	D. Kuchemann	A simple method for calculating the span and chordwise loading on straight and swept wings of any given aspect ratio at subsonic speeds. A.R.C. R. & M. 2935, August, 1952.
6		Royal Aeronautical Society. Method for the rapid estimation of theoretical spanwise loading. Royal Aeronautical Society Transonic Data Memorandum No. 6208.
7	M. Zlotnick and S. W. Robinson, Jr.	A simplified mathematical model for calculating aerodynamic loading and downwash for wing-fuselage combinations with wings of arbitrary planform. NACA TN 3057, January 1954.
8	W. Letko and E. C. B. Danforth, III	Theoretical investigation at subsonic speeds of the flow ahead of a slender inclined parabolic-arc body of revolution and correlation with experimental data obtained at low speeds. NACA TN 3205, July 1954.
9	F. K. Schmidt	Calculations of the airflow in the vicinity of fuselages. Air Material Command Technical Report No. F–TS–2615–RE, May 1948.
10	H. Multhopp	Aerodynamics of the fuselage. NACA TM 1036, December 1942.
11	W. J. Alford, Jr., H. N. Silvers and T. J. King, Jr.	Preliminary low-speed wind tunnel investigation of some aspects of the aerodynamic problems associated with missiles carried externally in positions near airplane wings. NACA RM L54J20, December 1954.
12	W. J. Alford, Jr.	Effects of wing-fuselage flow fields on missile loads at subsonic speeds. NACA RM L55E10A, June 1955.

REFERENCES—*continued*

No.	*Author(s)*	*Title, etc.*
13	W. J. Alford, Jr., H. N. Silvers and T. J. King, Jr.	Experimental aerodynamic forces and moments at low speed of a missile model during simulated launching from the mid-semispan location of a 45 deg sweptback wing-fuselage combination. NACA RM L54K11A, February 1955.
14	W. J. Alford, Jr.	Experimental static aerodynamic forces and moments at low speed on a canard missile during simulated launching from the mid-semispan and wing-tip locations of a 45 deg sweptback wing-fuselage combination. NACA RM L55A12. April 1955.
15	P. J. Bobbitt, H. W. Carlson and A. O. Pearson ..	Calculations of external-store loads and correlation with experiment. NACA RM L57D30A, July 1957.
16	N. K. Walter	The estimation of the aerodynamic loads on external stores. R.A.E. TN Aero. 1715, January 1946.
17	J. F. Holford	The low speed aerodynamic loads on tanks mounted on struts under swept-back wings. R.A.E. TN Aero. 2205, November 1952.
18	W. J. G. Trebble and J. F. Holford	Low speed wind tunnel measurements and estimations of the pitching and yawing moments of tanks mounted on struts under 40 deg swept and straight wings. R.A.E. TN Aero. 2394, October 1955.
19	Staff of R.A.E. High Speed Wind Tunnel	Tests in the R.A.E. 10 ft × 7 ft High Speed Wind Tunnel on drop tanks fitted to two swept-back wings. Part II: Comparison of various under-wing drop-tank arrangements. A.R.C. R. & M. 2951. July 1952.
20	R. Fail and J. F. Holford ..	Preliminary note on low speed tunnel model tests of pressure distribution, jettisoning and drag of tip tanks on an unswept wing. R.A.E. TN Aero. 2085. November 1950.
21	R. Fail and J. F. Holford ..	Preliminary note on low speed tunnel model tests of pressure distribution and jettisoning of strut tanks on a 40 deg swept-back wing. R.A.E. TN Aero. 2095. March 1951.
22	R. Fail	Further low-speed tunnel tests of jettisoning of strut tanks on a 40 deg swept-back wing. R.A.E. TN Aero. 2095a. December 1951.

No.	*Author(s)*	*Title, etc.*
23	J. F. Holford	Preliminary note on low speed tunnel tests of pressure distribution and jettisoning of strut tanks on a 40 deg swept-back wing. Addendum: further pressure plotting tests. R.A.E. TN Aero. 2095b. June 1952.
24	J. Weber	Theoretical load distribution on a wing with a cylindrical body at one end. A.R.C. R. & M. 2889. June 1952.
25	D. E. Hartley	Theoretical load distributions on wings with cylindrical tip-tanks. A.R.C. CP 147. June 1952.
26	L. D. Guy and W. M. Hadaway	Aerodynamic loads on an external store adjacent to a 45 deg sweptback wing at Mach numbers from 0·70 to 1·96, including an evaluation of techniques used. NACA RM L55H12. November 1955.
27	D. E. Wornom..	Transonic aerodynamic characteristics of a 45 deg swept-wing-fuselage model with a finned and unfinned body pylon-mounted beneath the fuselage or wing, including measurements of body loads. NACA Memo 4–20–59L. May 1959.
28	T. J. King, Jr.	Investigation at high subsonic speeds of some effects of sideslip on the aerodynamic loads on finned and unfinned bodies mounted from the wing of a swept-wing-fuselage model. NACA RM L56A24. April 1956.
29	J. M. Hallissy, Jr. and L. Kudlacik	A transonic wind-tunnel investigation of store and horizontal-tail loads and some effects of fuselage-afterbody modifications on a swept-wing fighter airplane. NACA RM L56A26. April 1956.
30	L. D. Guy	Loads on external stores at transonic and supersonic speeds. NACA RM L55E13B. July 1955.
31	W. J. Alford, Jr. and H. N. Silvers	Investigation at high subsonic speeds of finned and unfinned bodies mounted at various locations from the wings of unswept and swept-wing-fuselage models, including measurements of body loads. NACA RM L54B18. April 1954.
32	P. J. Bobbitt, F. S. Malvestuto, Jr. and K. Margolis	Theoretical prediction of the side force on stores attached to configurations traveling at supersonic speeds. NACA RM L55L30B. March 1956.
33	P. J. Bobbitt and P. J. Maxie	Sidewash in the vicinity of lifting swept wings at supersonic speeds. NACA TN 3938. February 1957.

No.	*Author(s)*	*Title, etc.*
34	R. T. Jones	Thin oblique airfoils at supersonic speeds. NACA Report 851. 1946.
35	J. N. Nielsen and E. W. Perkins	Charts for the conical part of the downwash field of swept wings at supersonic speeds. NACA TN 1780. December 1948.
36	H. Mirels and R. C. Haefeli ..	Line-vortex theory for calculation of supersonic downwash. NACA TN 1925. August 1949.
37	P. A. Lagerstrom and .. .. M. E. Graham	Downwash and sidewash induced by three-dimensional lifting wings in supersonic flow. Douglas Aircraft Company Inc. Report No. SM–13007. April 1947.
38	H. Lomax and M. A. Heaslet	A special method for finding body distortions that reduce the wave drag of wing and body combinations at supersonic speeds. NACA Report 1282. 1956.
39	K. Margolis and M. H. Elliott	Formulas pertinent to the calculation of flow-field effects at supersonic speeds due to wing thickness. NASA Memo 4–3–59L. May 1959.
40	J. N. Mielsen and W. C. Pitts	General theory of wave-drag reduction for combinations employing quasi-cylindrical bodies with an application to swept-wing and body combinations. NACA TN 3722. September 1956.
41	D. J. Geier and H. W. Carlson	Measurements of static forces on externally carried bombs of fineness ratio 7·1 and 10·5 in the flow field of a swept-wing fighter-bomber configuration at a Mach number of 1·6. NACA RM L56K30. January 1957.
42	H. W. Carlson	Measurements of flow properties in the vicinity of three wing-fuselage combinations at Mach numbers of 1·61 and 2·01. NASA TM–X–64. October 1959.
43	P. J. Bobbitt, H. W. Carlson and A. O. Pearson	Calculation of external-store loads and correlation with experiment. NACA RM L57D30A. July 1957.
44	O. A. Morris, H. W. Carlson and D. J. Geier	Experimental and theoretical determination of forces and moments on a store and on a store-pylon combination mounted on a 45 deg swept-wing-fuselage configuration at a Mach number of 1·61. NACA RM L57K18. January 1958.

No.	*Author(s)*	*Title, etc.*
45	N. P. Smith and H. W. Carlson	The origin and distribution of supersonic store interference from measurement of individual forces on several wing-fuselage-store configurations. I–Swept-wing heavy-bomber configuration with large store (nacelle), lift and drag; Mach number 1·61. NACA RM L55A13A. March 1955.
46	H. W. Carlson and D. J. Geier	The origin and distribution of supersonic store interference from measurement of individual forces on several wing-fuselage-store configurations. V–Swept-wing heavy bomber configuration with large store (nacelle). Mach Number 2·01. NACA RM L55K15. February 1956.
47	J. P. Gapcynski and H. W. Carlson	The aerodynamic characteristics of a body in the two-dimensional flow field of a circular-arc wing at a Mach number of 2·01. NACA RM L57E14. July 1957.
48	A. Ferri..	*Elements of aerodynamics of supersonic flows.* Macmillan Co. 1949.
49	M. A. Heaslet and H. Lomax	The calculation of downwash behind supersonic wings with an application to triangular planform. NACA TN 1620. June 1948.
50	J. P. Gapcynski and H. W. Carlson	A pressure-distribution investigation of the aerodynamic characteristics of a body of revolution in the vicinity of a reflection plane at Mach numbers of 1·41 and 2·01. NACA RM L54J29. January 1955.
51	B. Moskowitz	Approximate theory for calculation of lift of bodies, afterbodies and combinations of bodies. NACA TN 2669. April 1952.
52	H. J. Allen	Estimation of the forces and moments acting on inclined bodies of revolution of high fineness ratio. NACA RM A9I26. November 1949.
53	N. F. Smith and H. W. Carlson	The origin and distribution of supersonic store interference from measurement of individual forces on several wing-fuselage-configurations. II–Swept-wing heavy-bomber configuration large store (nacelle). Lateral forces and pitching moments; Mach number 1·61. NACA RM L55E26A. July 1955.
54	N. F. Smith and H. W. Carlson	The origin and distribution of supersonic store interference from measurements of individual forces on several wing-fuselage-store configurations. III–Swept-wing fighter-bomber configuration with large and small stores; Mach number 1·61. NACA RM L55H01. September 1955.

No.	*Author(s)*	*Title, etc.*
55	O. A. Morris	The origin and distribution of supersonic store interference from measurement of individual forces on several wing-fuselage-store configurations. IV–Delta-wing heavy-bomber configuration with large store. Mach number 1·61. NACA RM L55I27A. December 1955.
56	N. F. Smith	The origin and distribution of supersonic store interference from measurement of individual forces on several wing-fuselage-store configuration. VI–Swept-wing heavy-bomber configuration with stores of different sizes and shapes. NACA RM L55L08. March 1956.
57	H. A. Hamer and T. C. O'Bryan	Flight measurements of the loads and moments on an external store mounted under the wing of a swept-wing fighter-type airplane during rolling and yawing maneuvers. NACA RM L55G22. September 1955.
58	J. R. Thompson, T. C. O'Bryan and M. C. Kurbjun	A limited analysis of buffeting experienced in flight by a North American F–86A–1 airplane with and without external fuel tanks. NACA RM L54J22. September 1955.
59	G. S. Campbell	A finite step method for the calculation of span loadings of unusual planforms. NACA RM L50L13. July 1951.

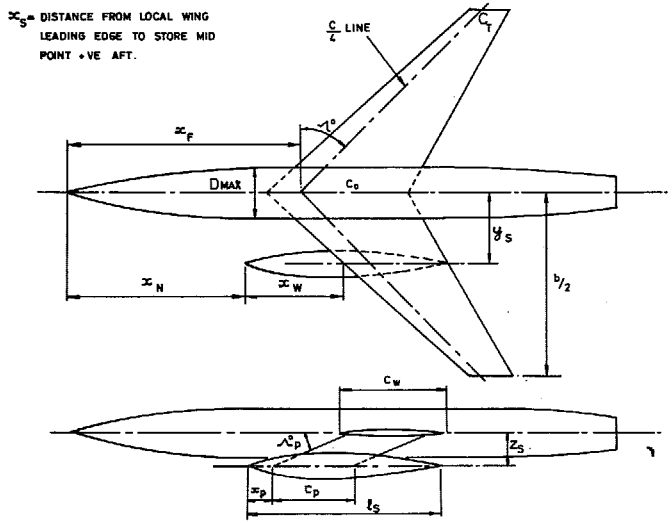

FIG. 1a. Nomenclature for external stores.

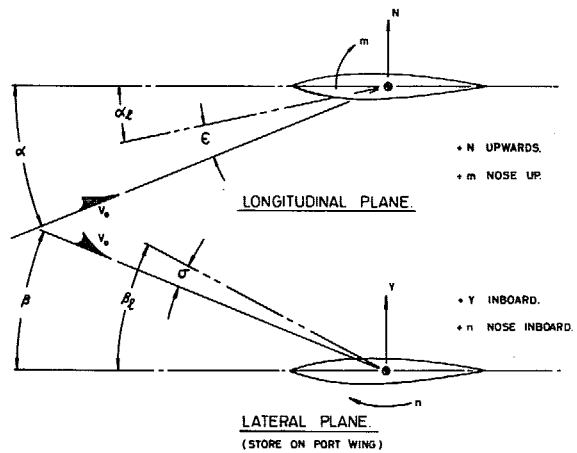

FIG. 1b. Positive directions of forces, moments and angles for typical store.

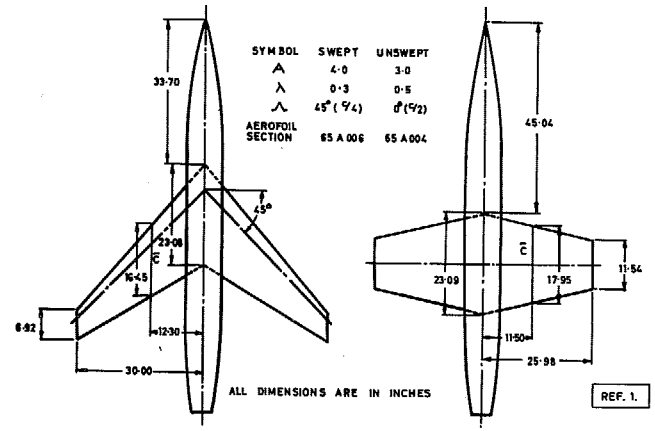

FIG. 2. Geometrical details of wing-fuselage test models used in experimental flow-field determination.

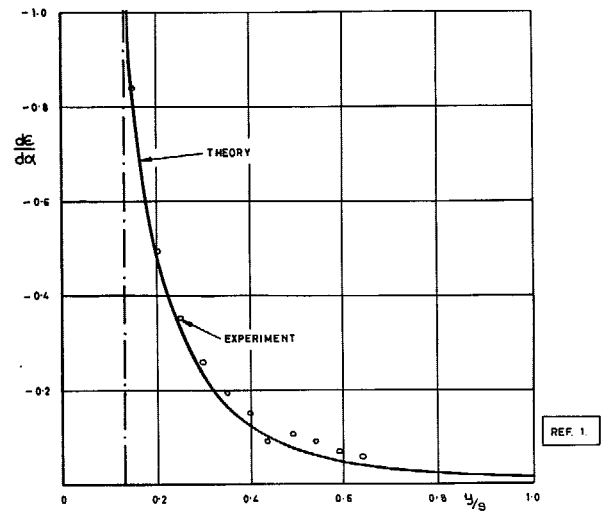

FIG. 3. Upwash induced by circular fuselage, $M = 0$ for swept-wing configuration in Fig. 2.

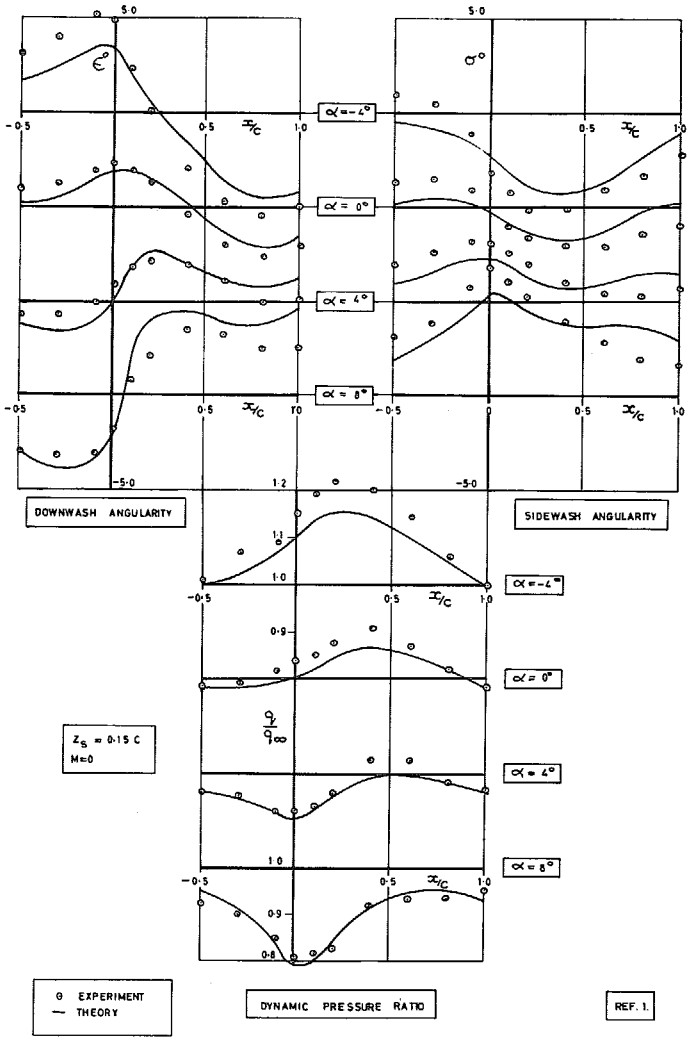

FIG. 4. Comparison of theoretical and experimental flow fields, 45 deg swept wing, mid semi-span location.

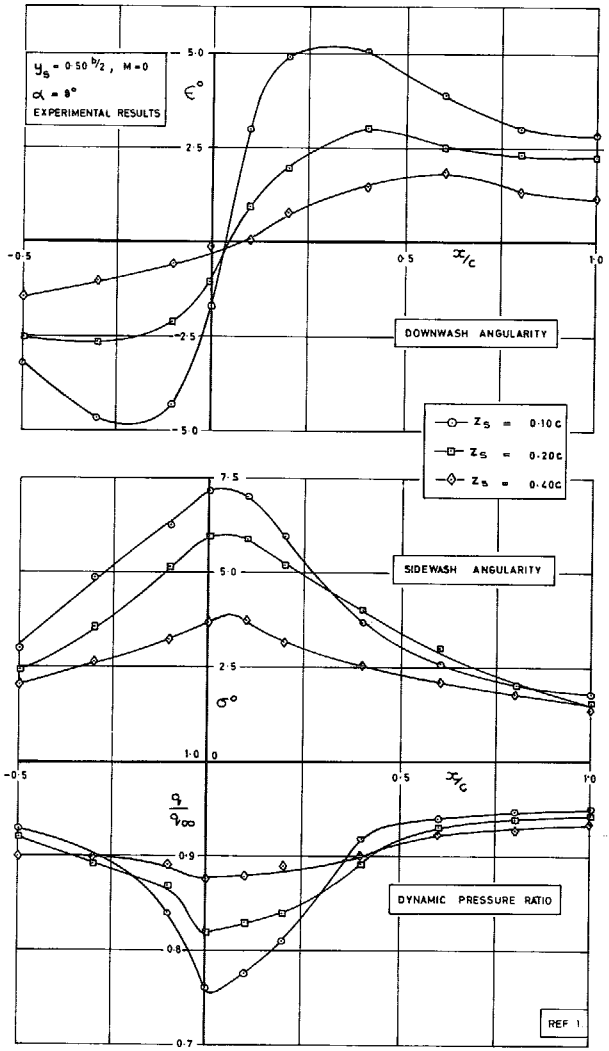

FIG. 5. Effect of vertical location on the flow-field characteristics beneath a 45 deg swept wing.

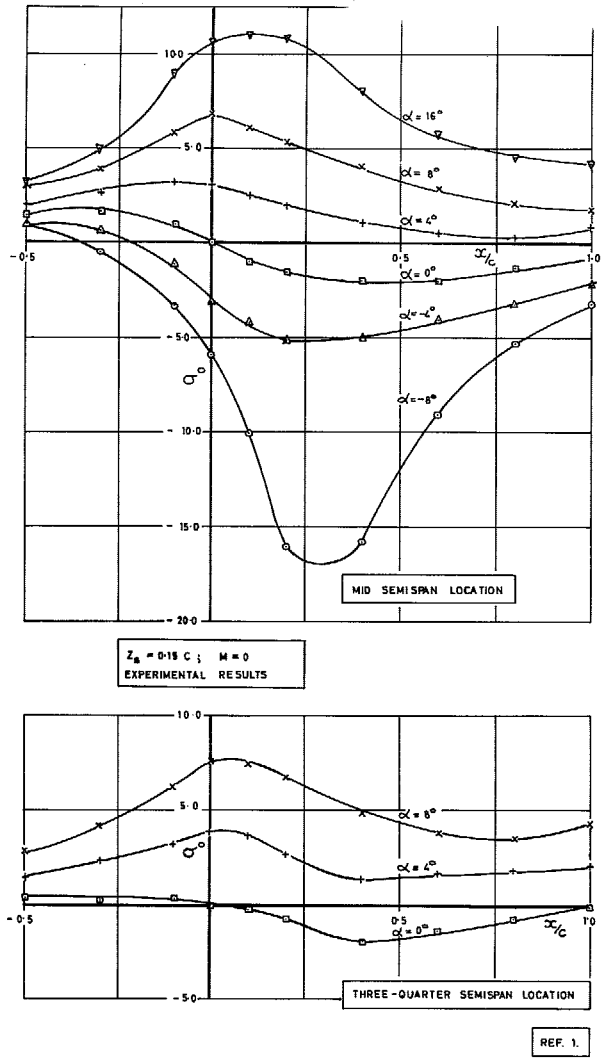

FIG. 6. Effect of incidence on the sidewash angularity beneath a 45 deg swept wing.

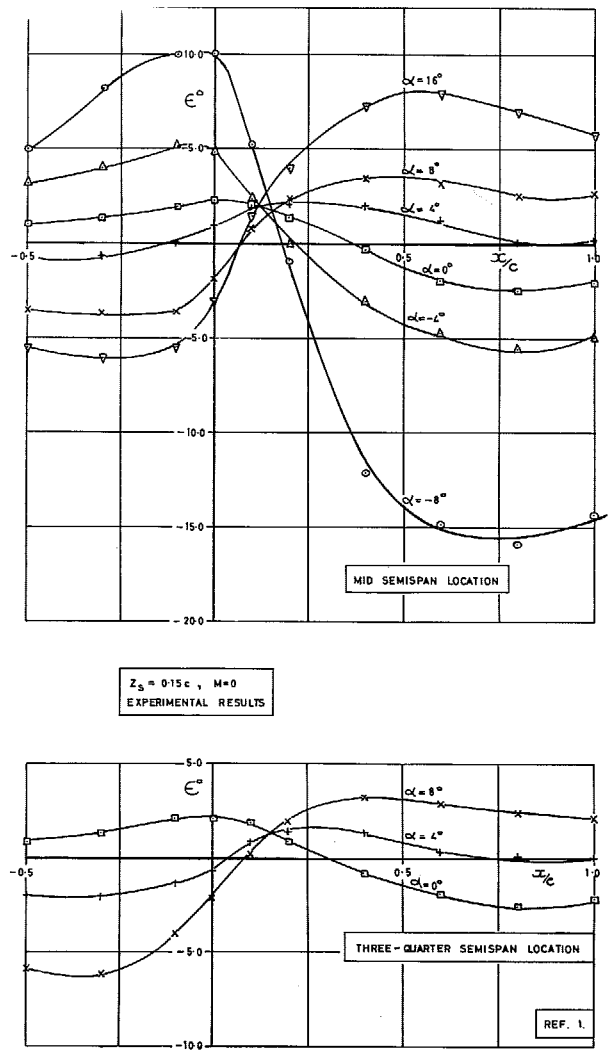

FIG. 7. Effect of incidence on the downwash angularity beneath a 45 deg swept wing.

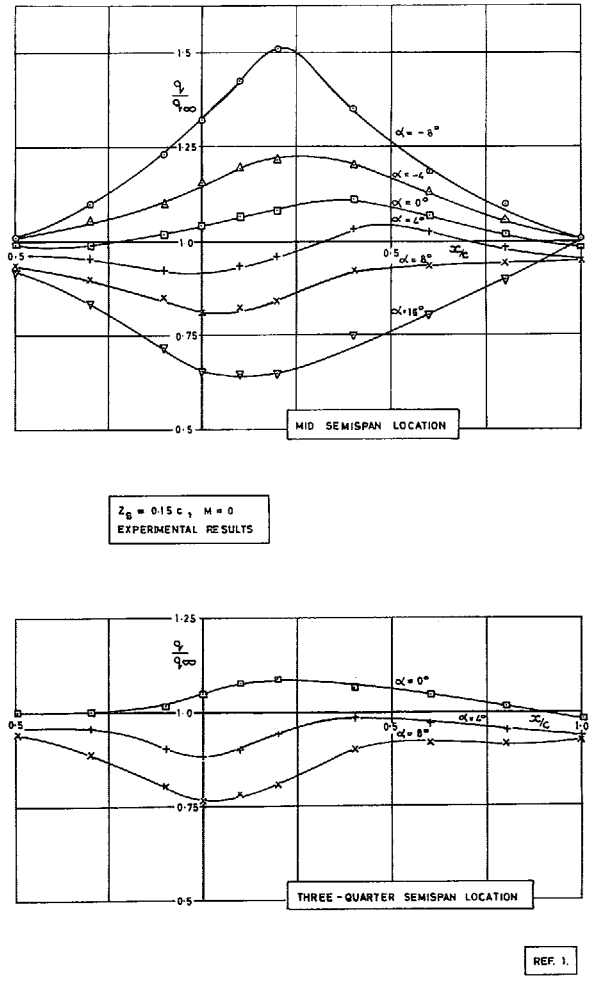

FIG. 8. Effect of incidence on the dynamic pressure ratio beneath a 45 deg swept wing.

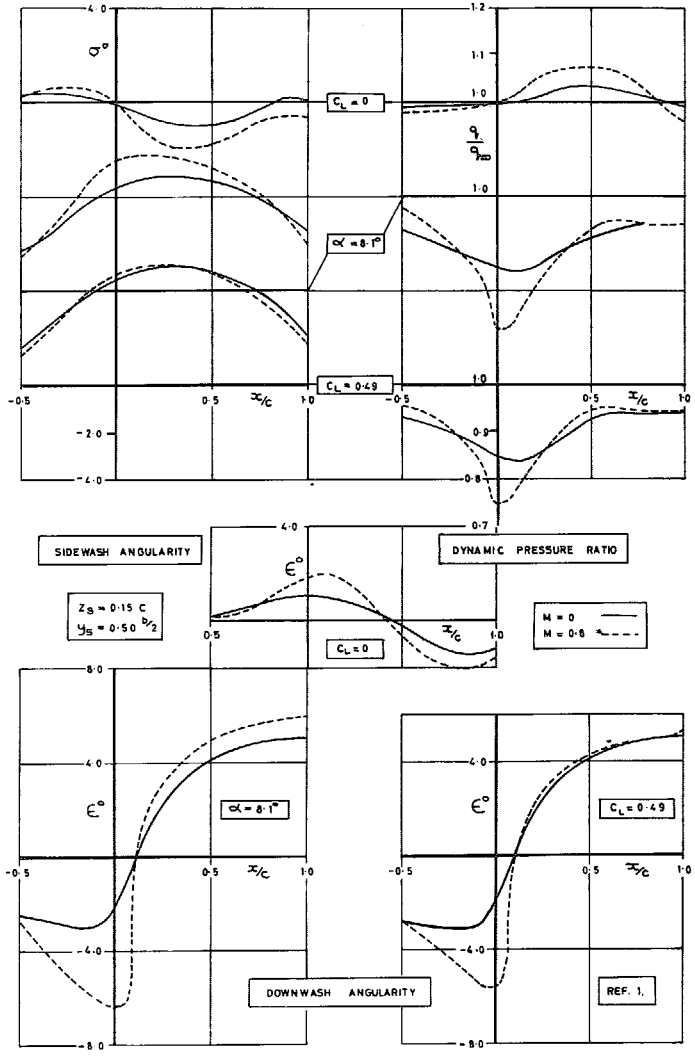

FIG. 9. Theoretical effect of Mach number on the flow-field characteristics beneath a 45 deg swept wing.

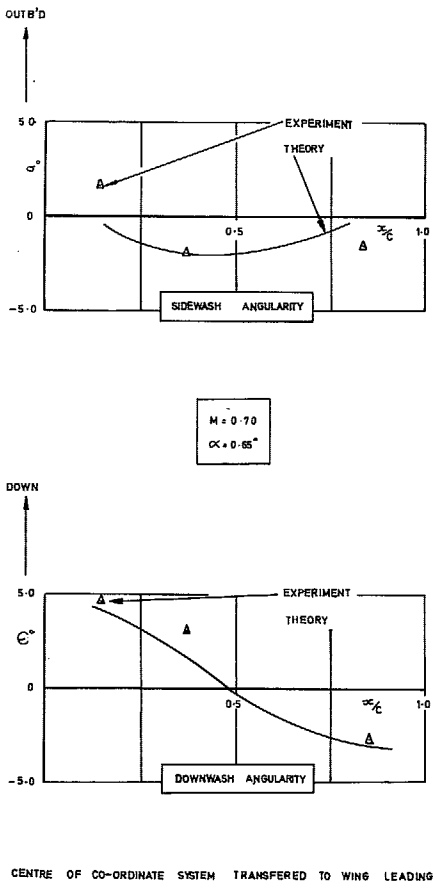

FIG. 10. Comparison of theoretical and experimental flow fields beneath a 35 deg swept wing.

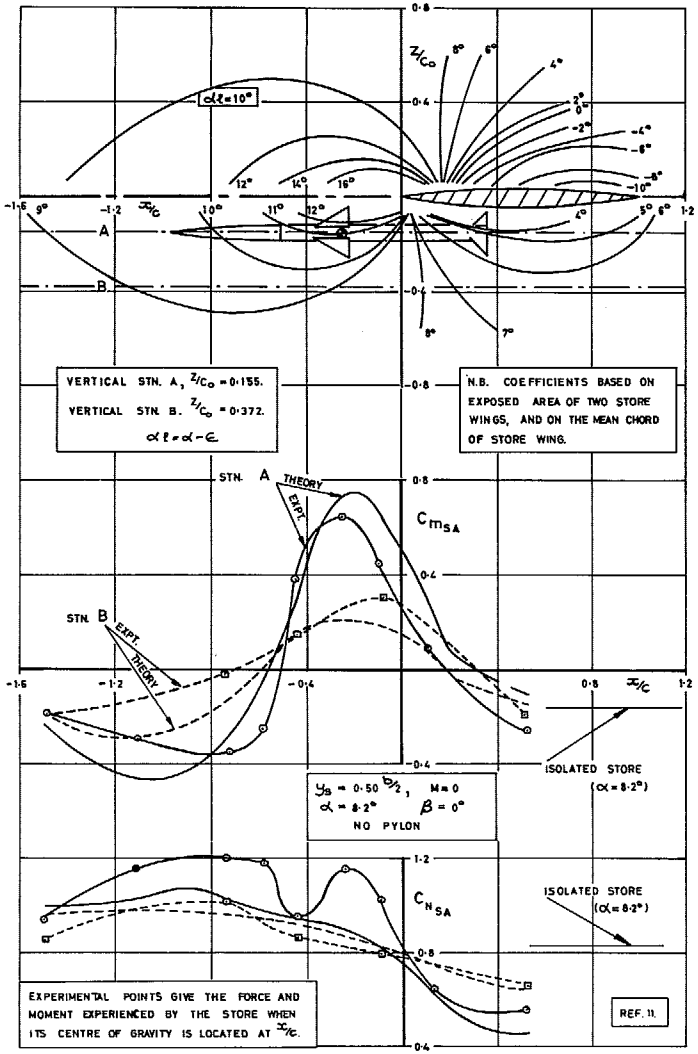

FIG. 11. Experimental downwash contours and store forces and moments beneath a 45 deg swept wing.

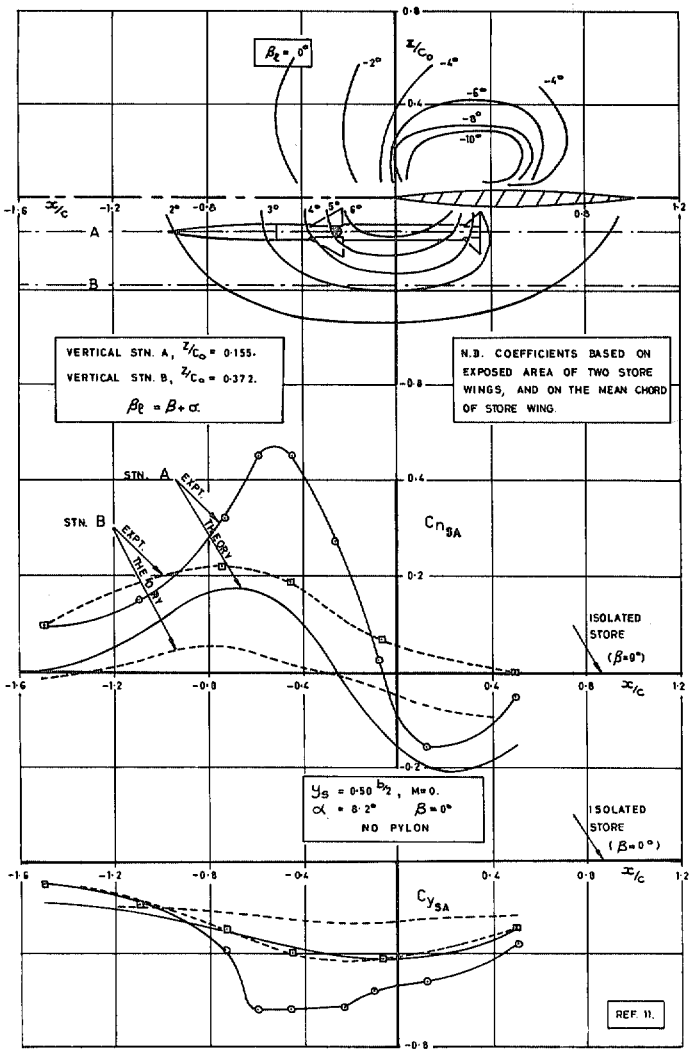

FIG. 12. Experimental sidewash contours and store forces and moments beneath a 45 deg swept wing.

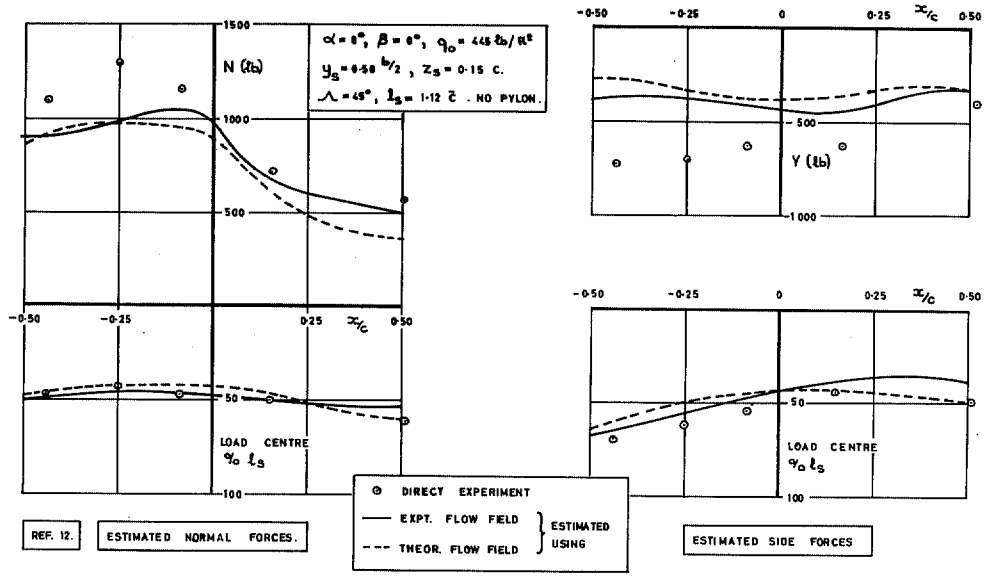

FIG. 13. Comparison between measured and estimated store normal and side forces.

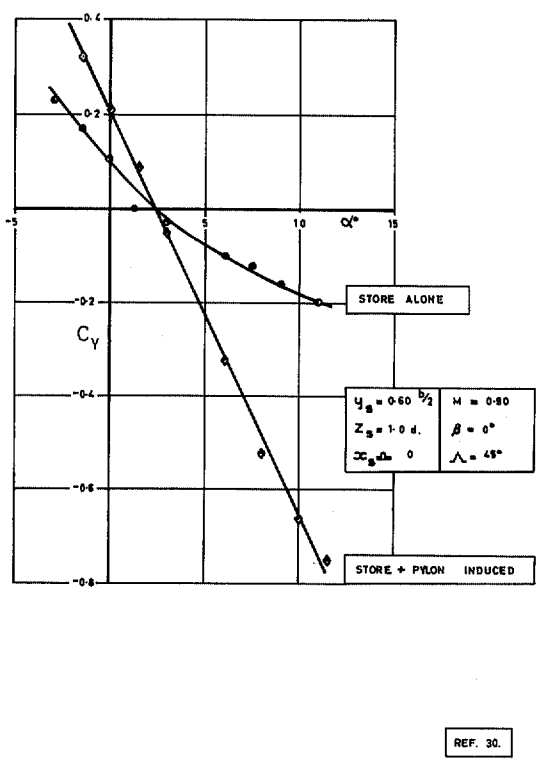

FIG. 14. Effect of pylon on store side-force coefficients (*see* also Fig. 43).

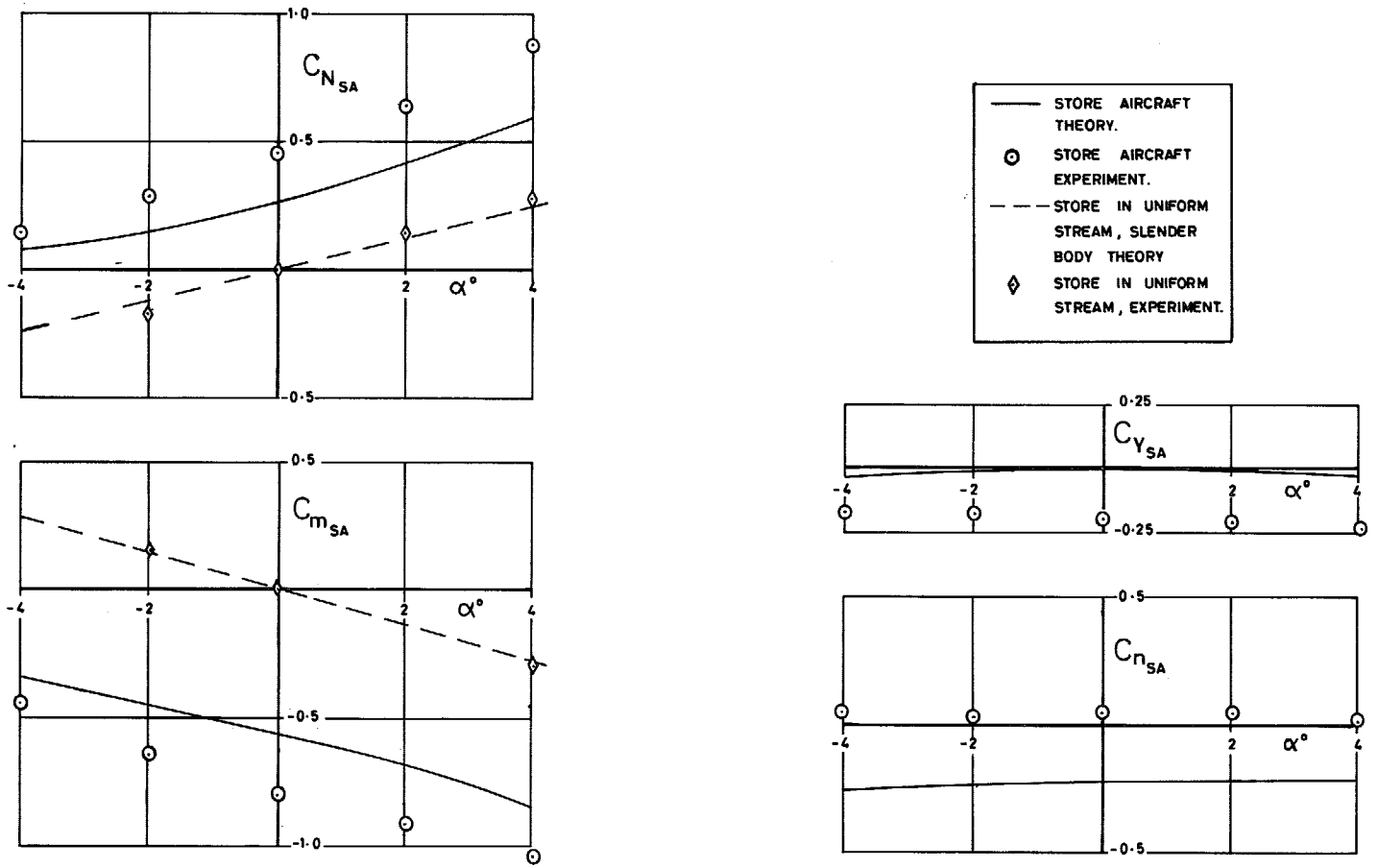

FIG. 16. Comparison of theoretical and experimental forces and moments on a finned store beneath a 35 deg swept wing at $M = 0{\cdot}70$.

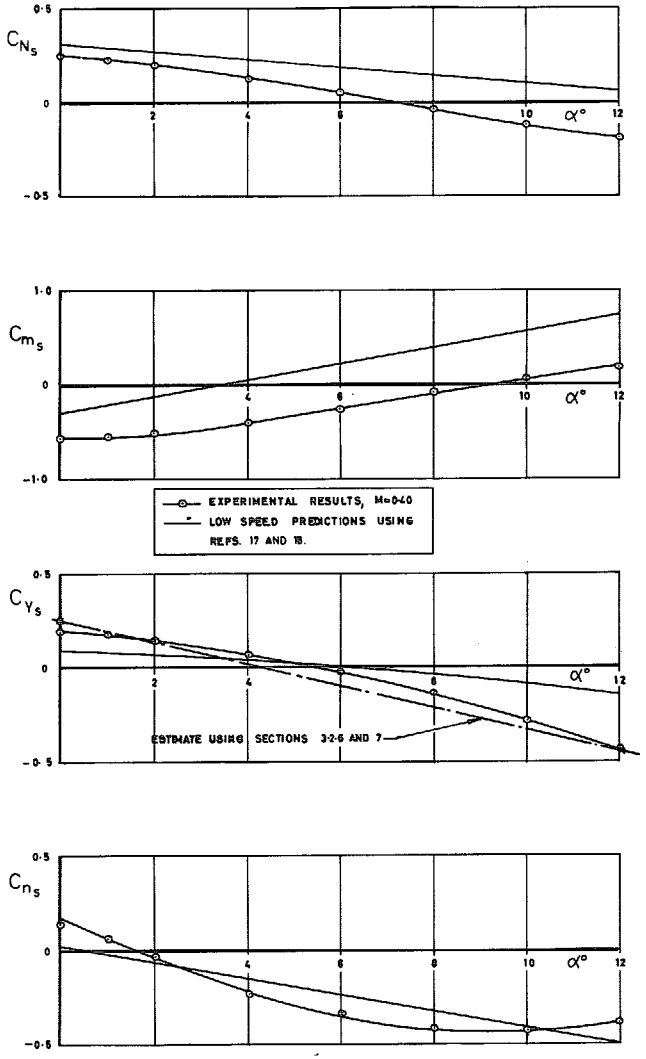

FIG. 17. Comparison between experimental and estimated store coefficients. Configuration as Fig. 26.

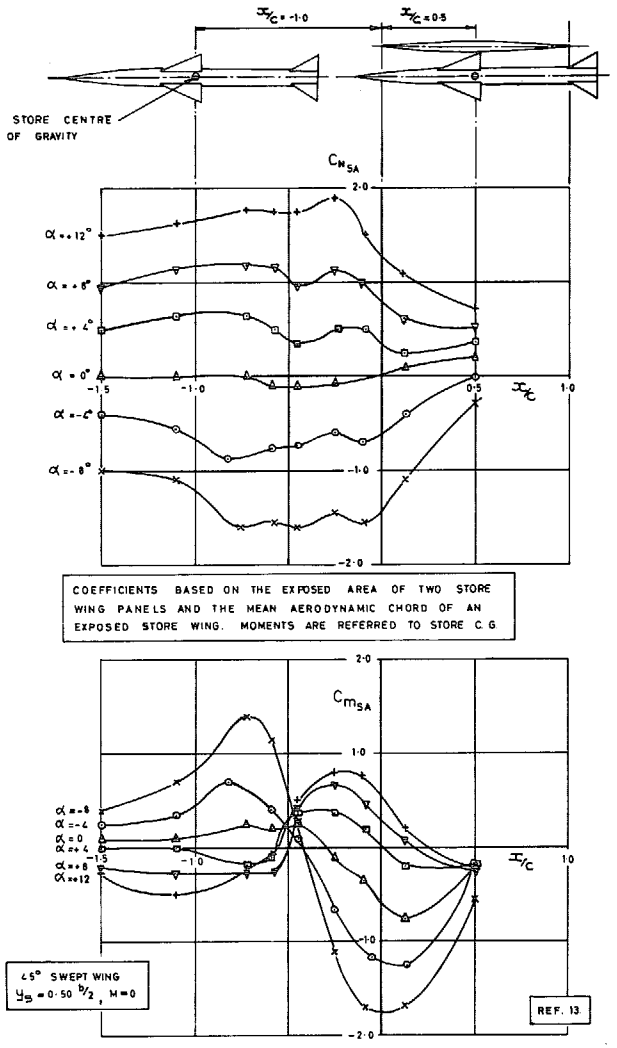

FIG. 18a. Variation with chardwise location of store normal force and pitching moment.

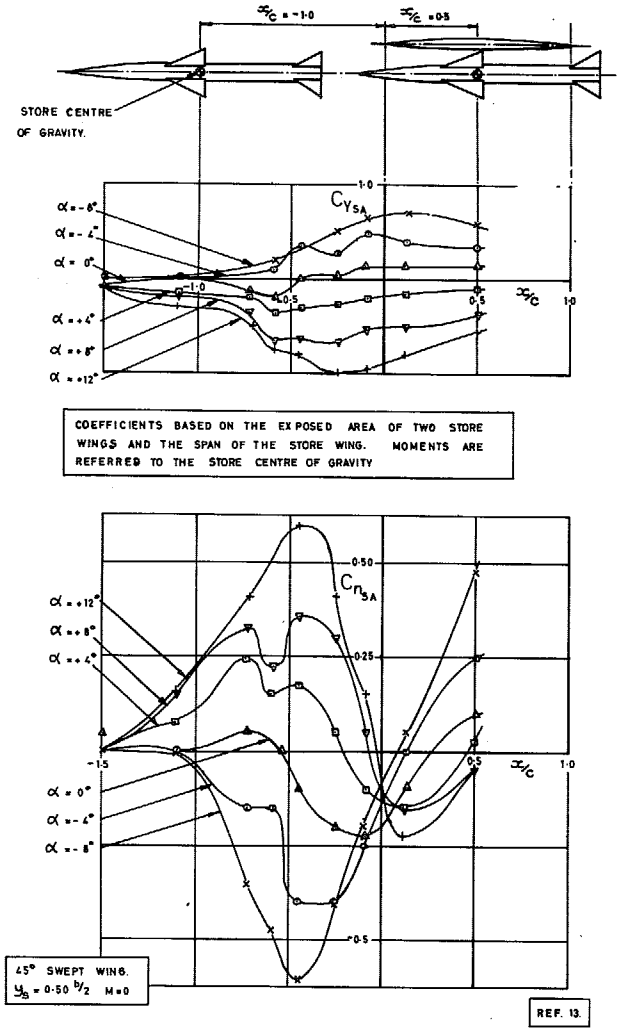

FIG. 18b. Variation with chordwise location of store side force and yawing moment.

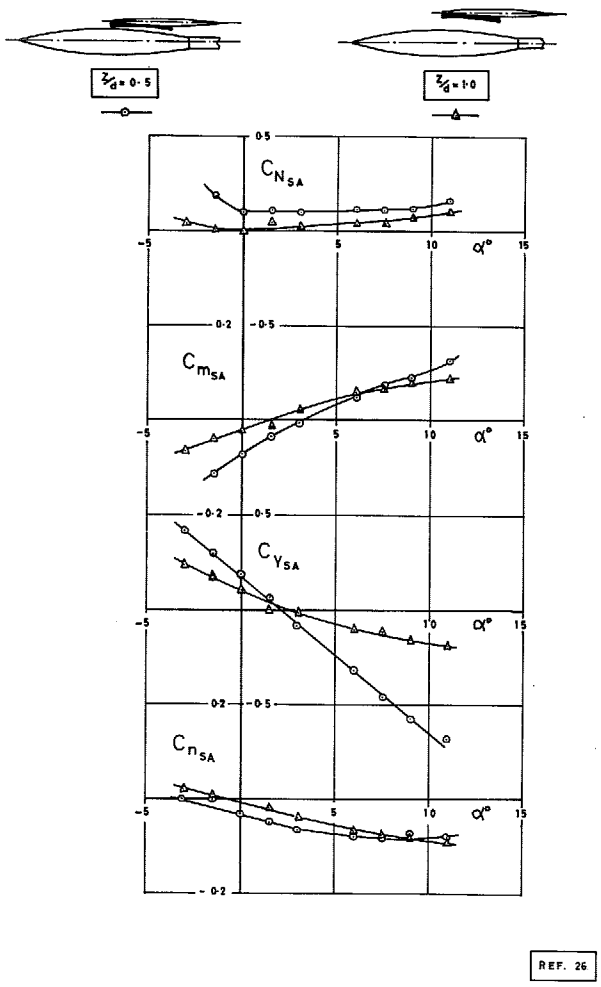

FIG. 19. Effect of store vertical location beneath a 45 deg swept wing on store loads at $M = 0{\cdot}90$.

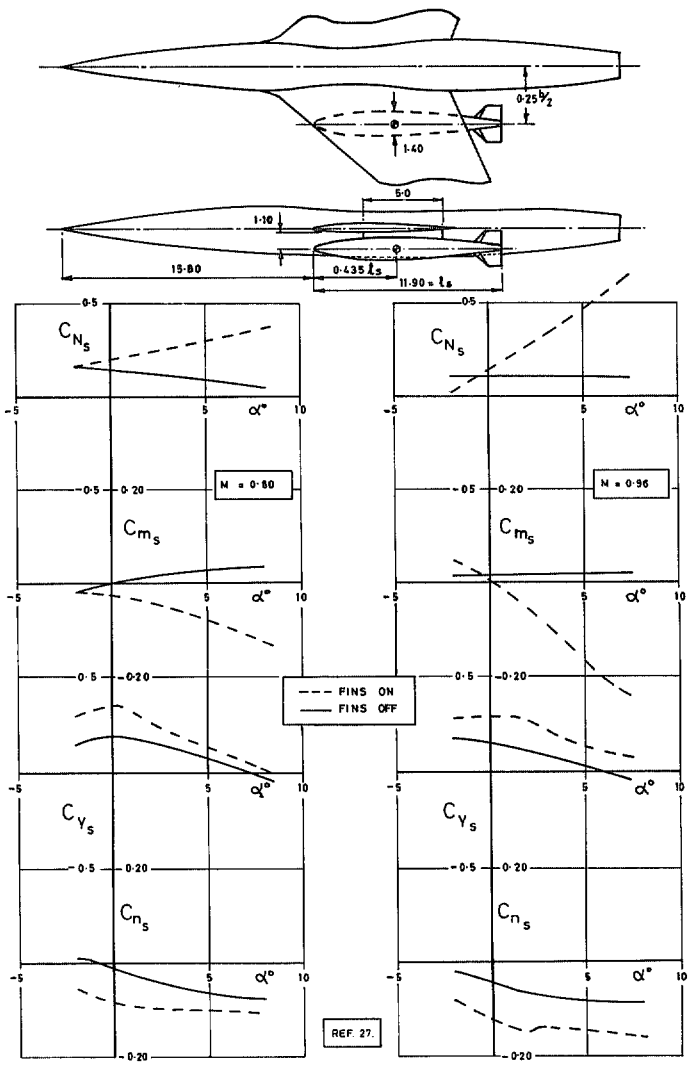

FIG. 20. Effect of fins on store loads beneath a 45 deg swept wing at high subsonic Mach number.

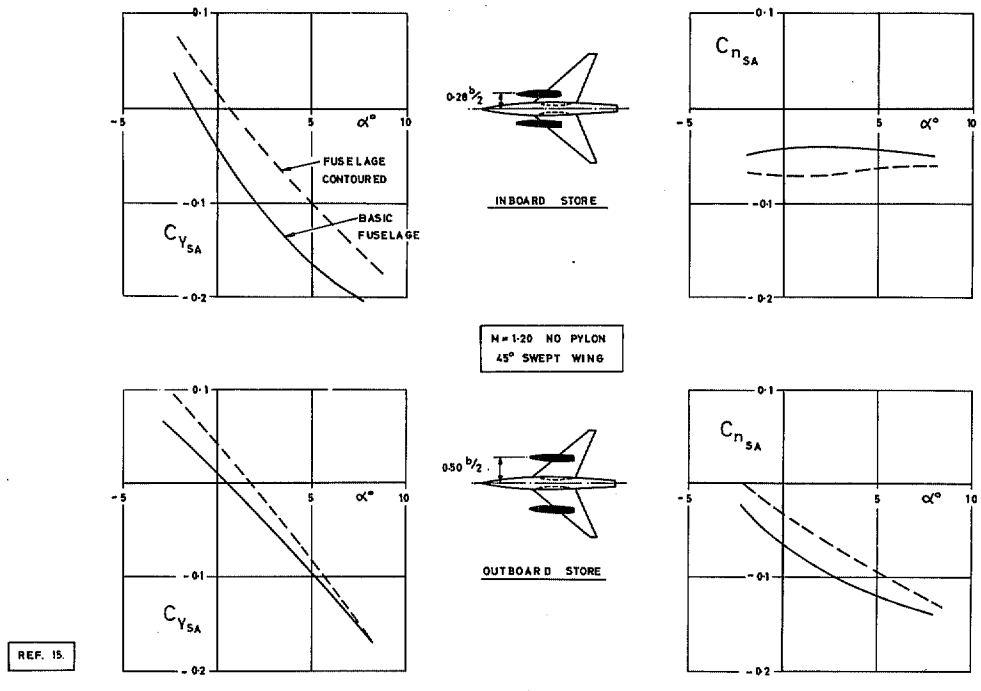

FIG. 21. Effect of fuselage contouring on store lateral characteristics for an inboard and outboard store.

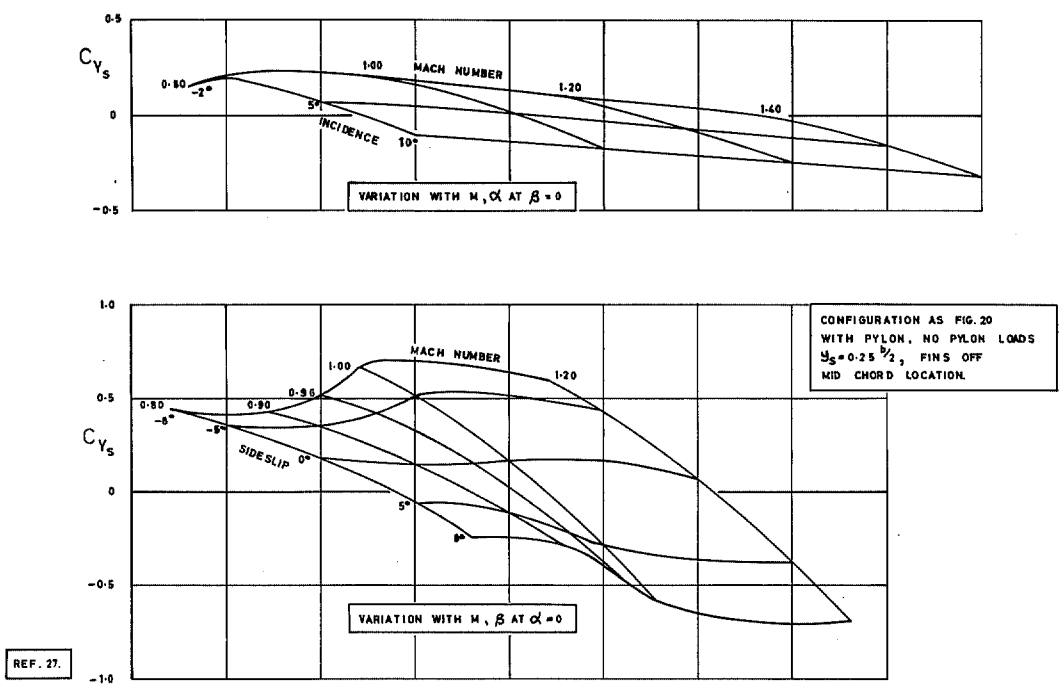

FIG. 22. Variation of store side force with incidence sideslip and Mach number.

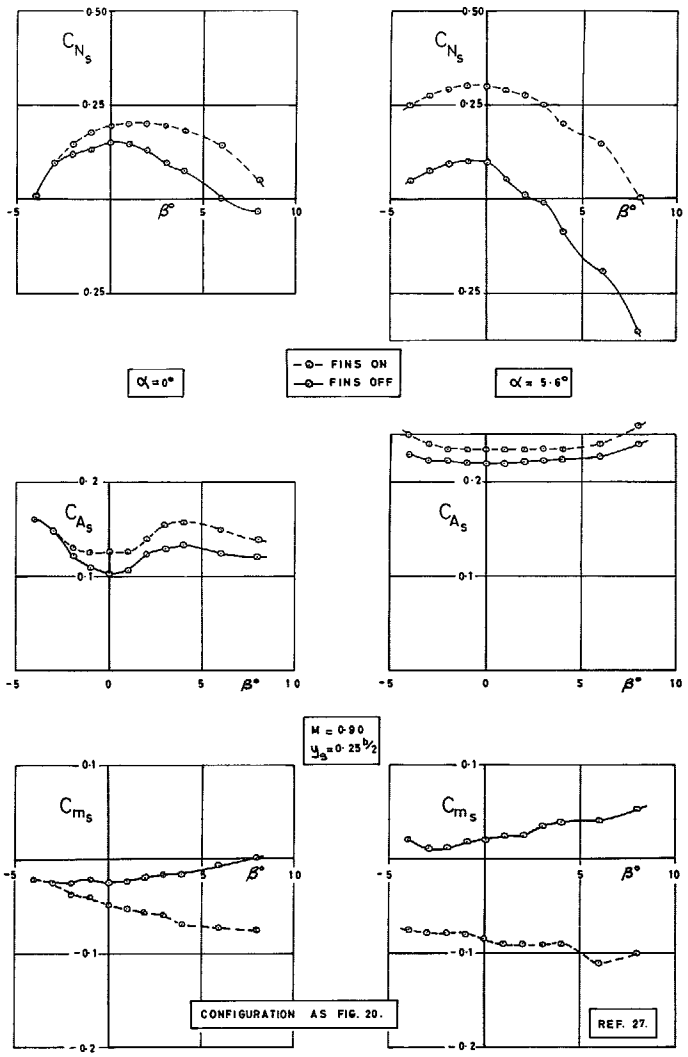

FIG. 23. Variation with sideslip of store longitudinal coefficients at high subsonic speed.

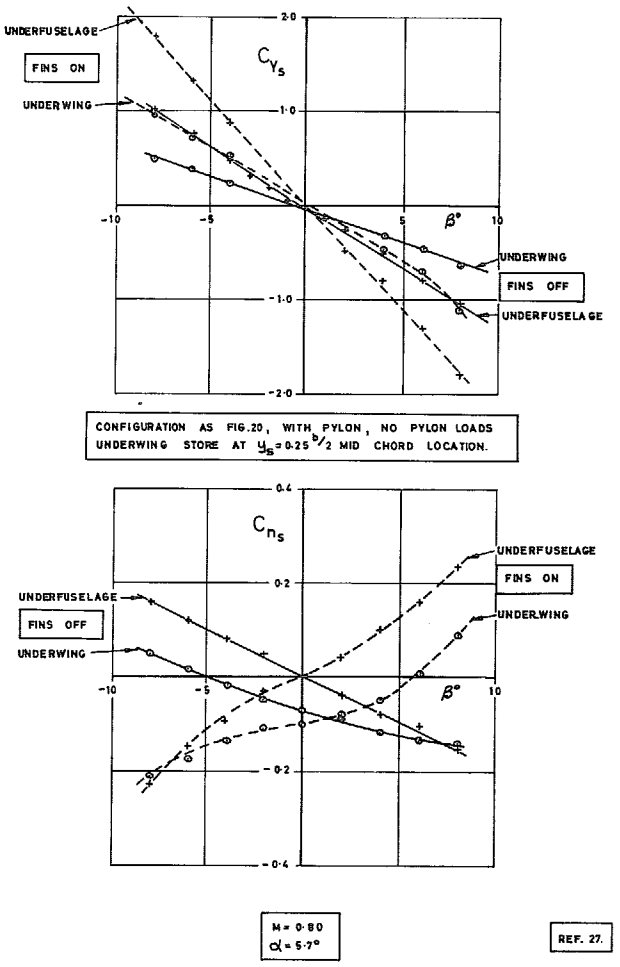

FIG. 24. Variation with sideslip of the lateral characteristics of underwing and underfuselage stores.

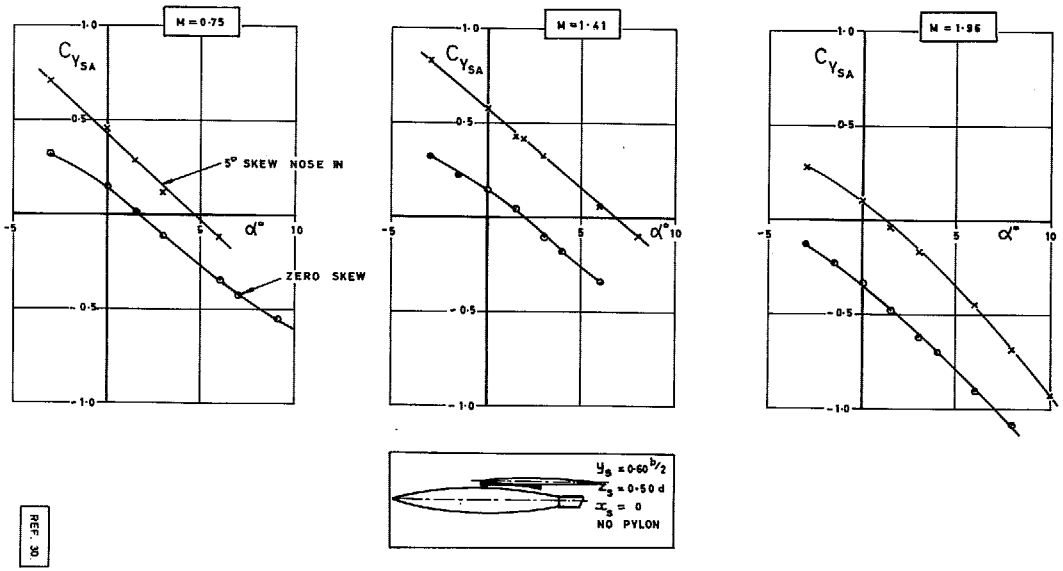

FIG. 25. Variation of store side force with incidence, with and without skew at subsonic and supersonic speeds.

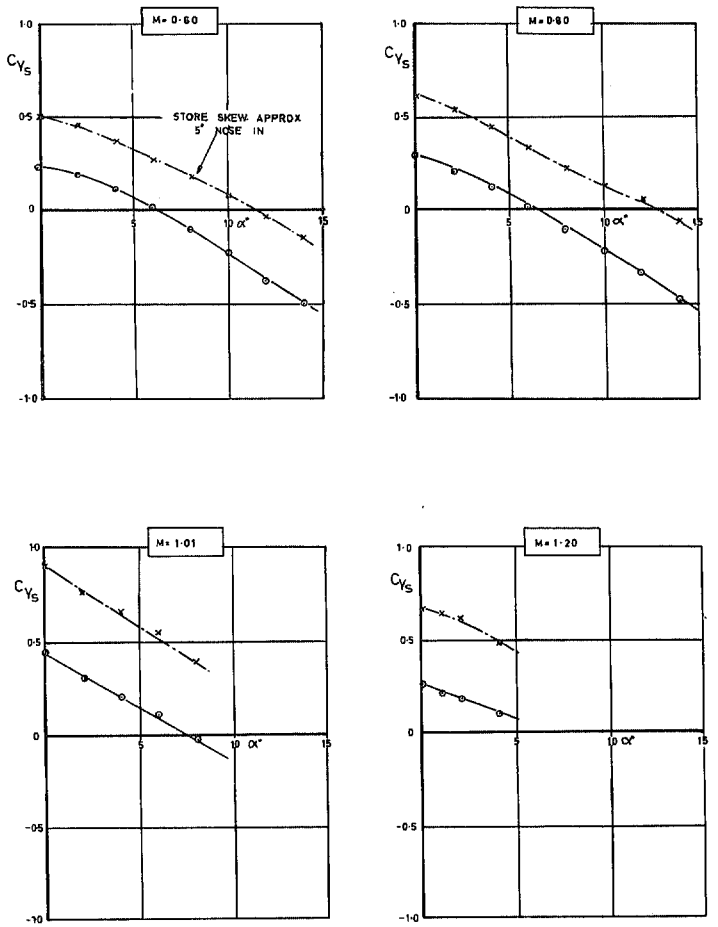

FIG. 26. Variation of store side force with incidence, with and without store skew at transonic speeds.

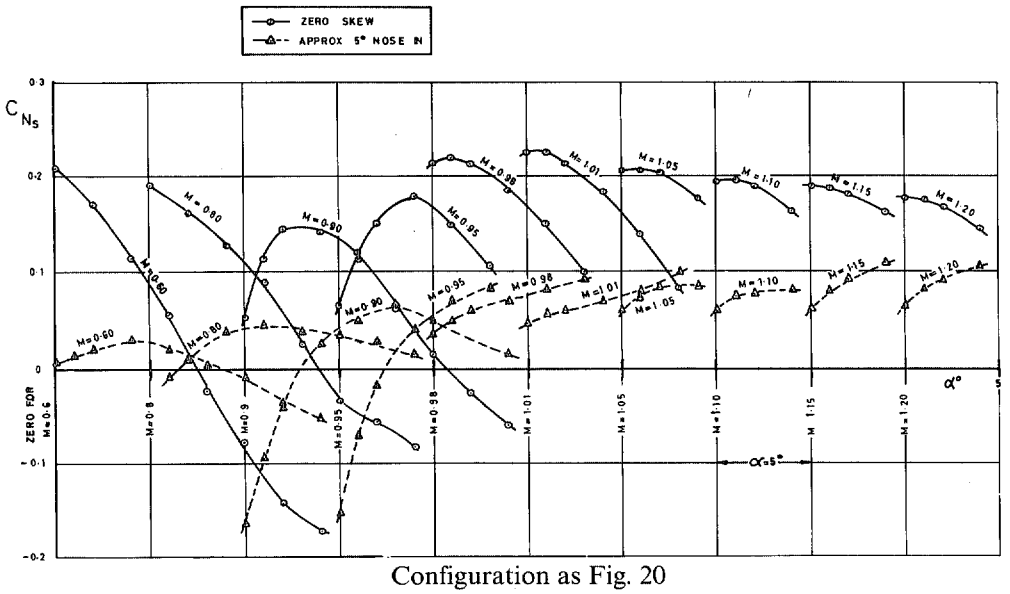

Configuration as Fig. 20

FIG. 27. Variation of store normal force with incidence and Mach number with and without store skew.

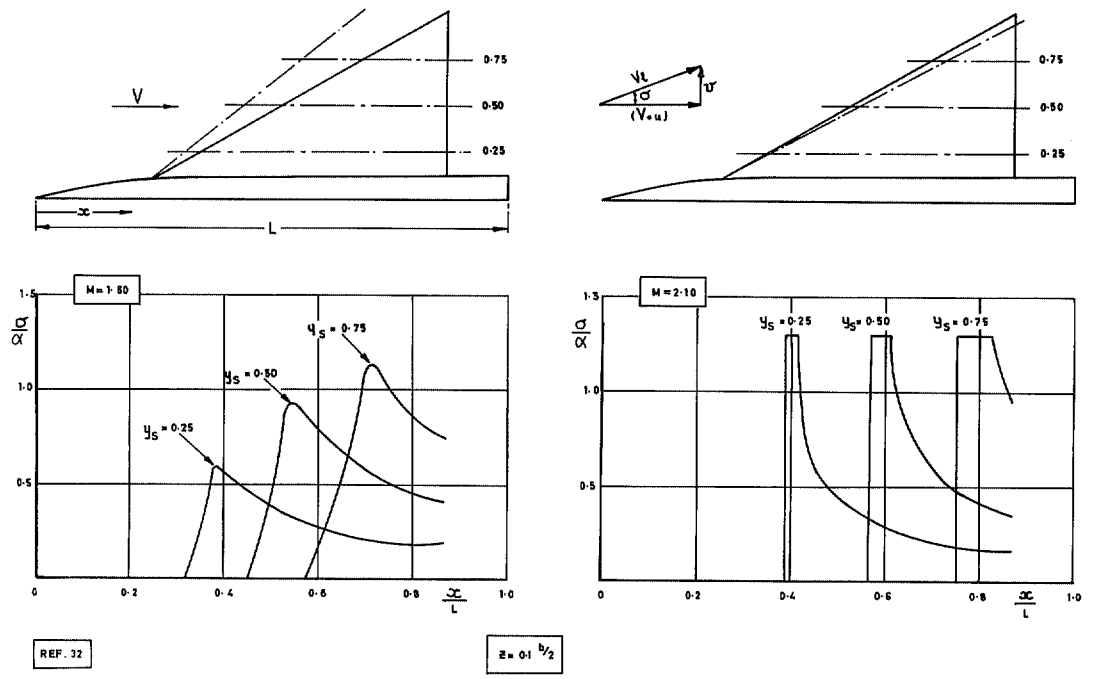

FIG. 28. Supersonic delta wing-body lateral flow angularity due to incidence.

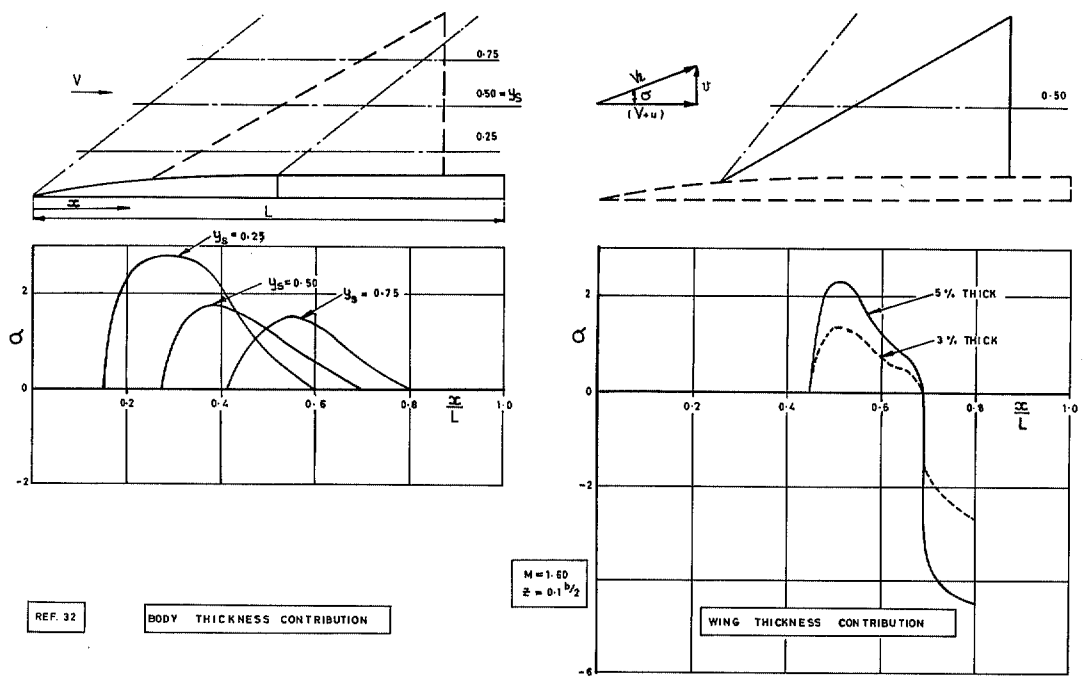

FIG. 29. Supersonic delta wing-body lateral flow angularity due to body and wing thickness.

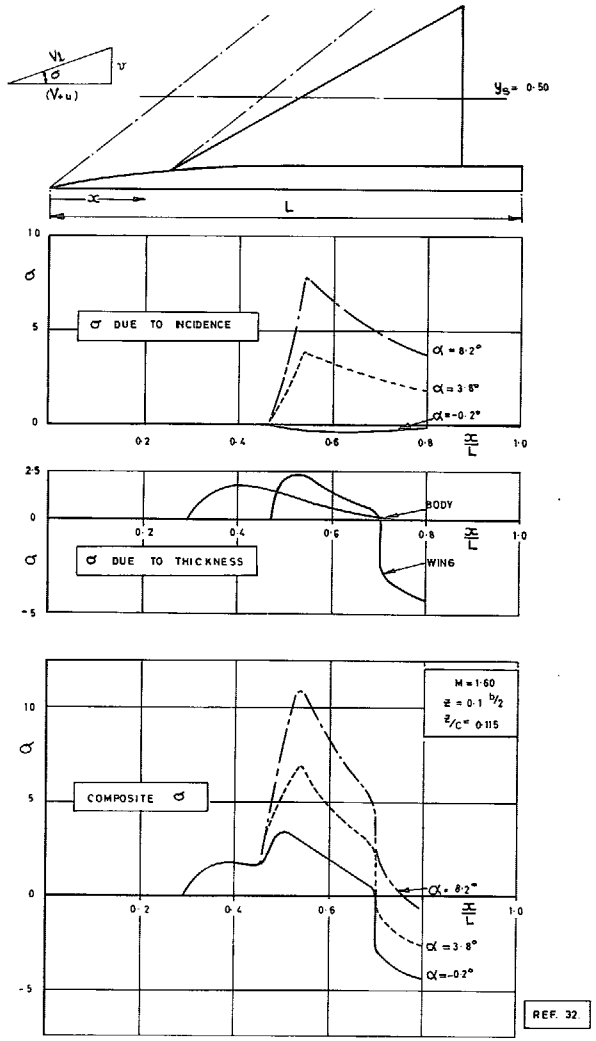

FIG. 30. Supersonic delta wing-body lateral flow angularity due to incidence and thickness at mid semispan.

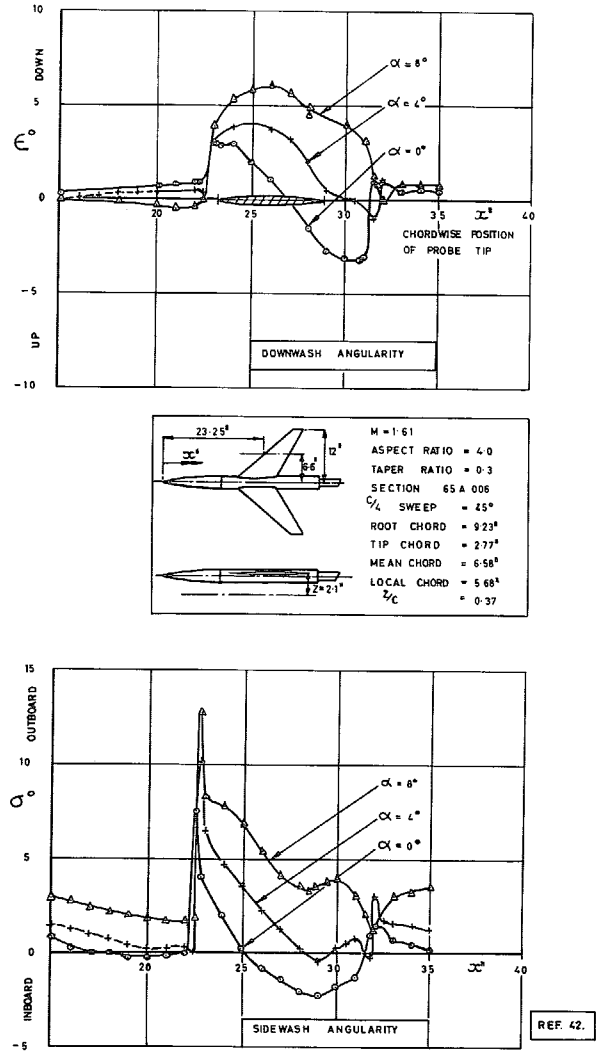

FIG. 31. Experimental downwash and sidewash angularity at supersonic Mach number.

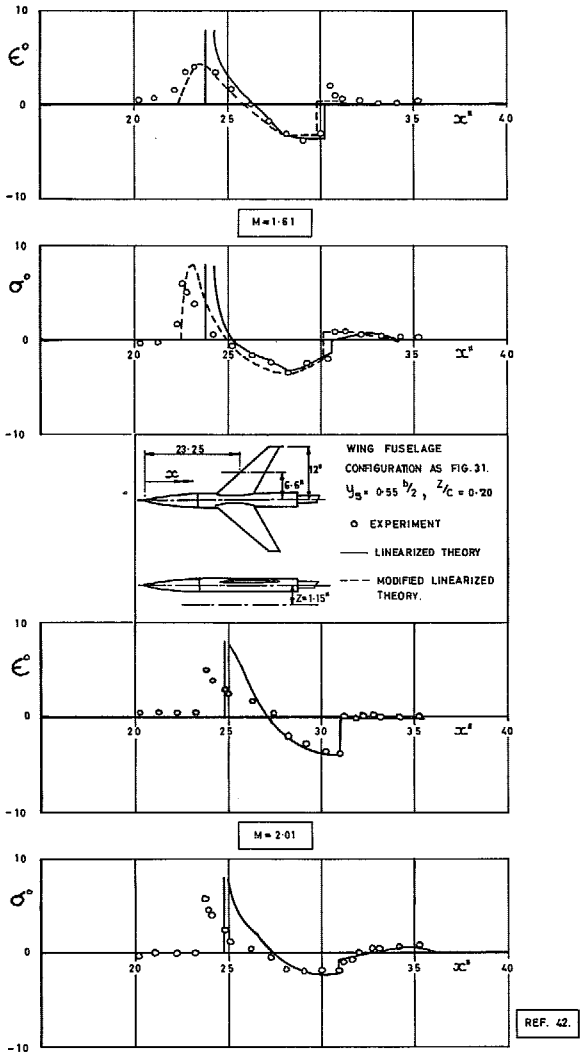

FIG. 32. Comparison of theoretical and experimental flow properties at zero incidence.

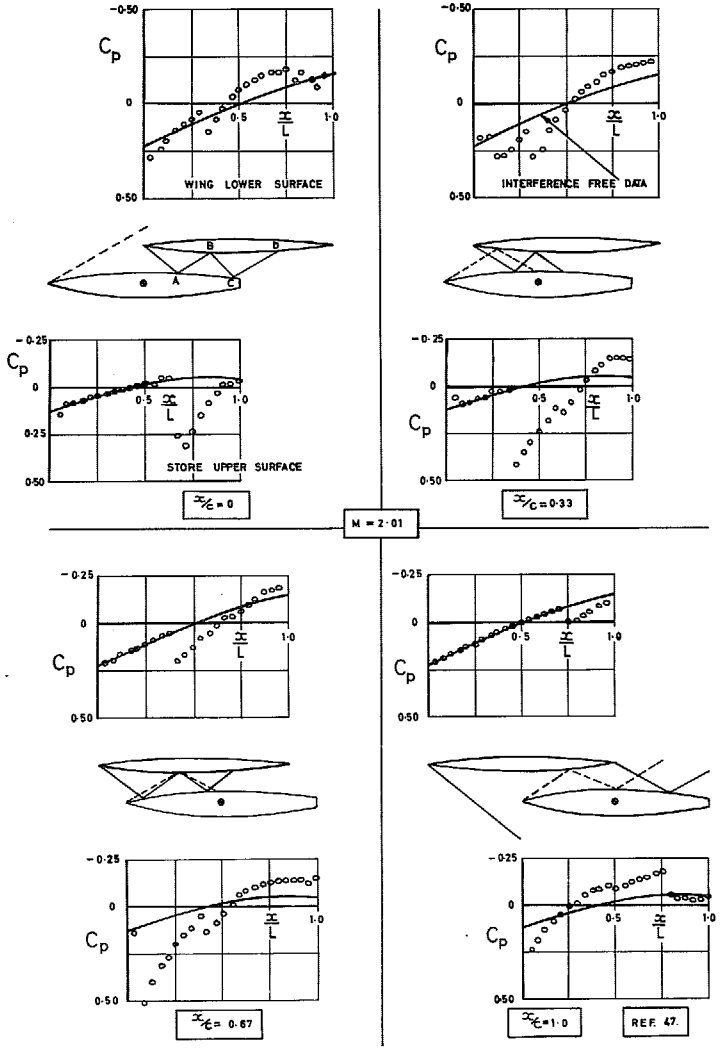

FIG. 33a. Illustrative example of the pressure-coefficient. Variation on a store and unswept circular arc wing.

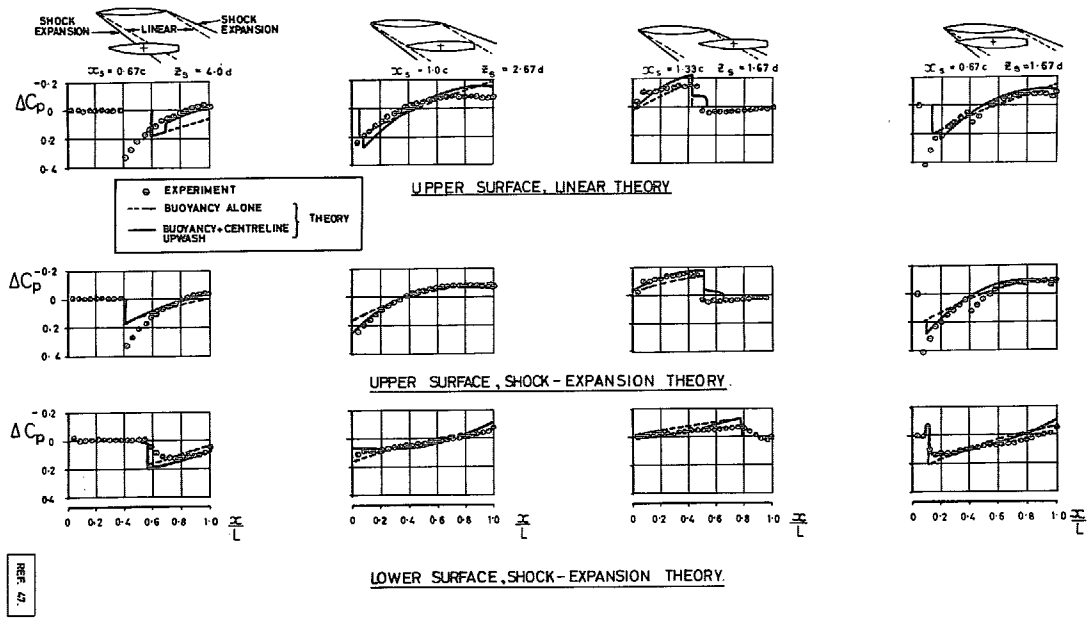

FIG. 33b. Comparison between experiment and theoretical store pressure distributions in presence of circular-arc wing.

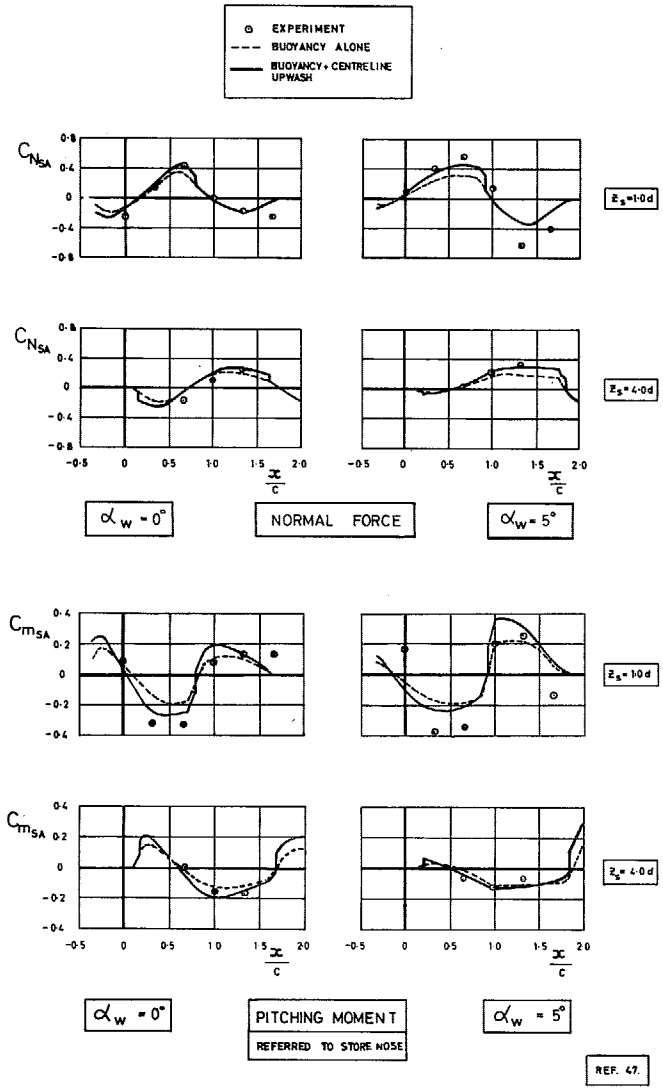

FIG. 33c. Effect of wing pressure and downwash fields on store C_N and C_m at $M = 2{\cdot}0$.

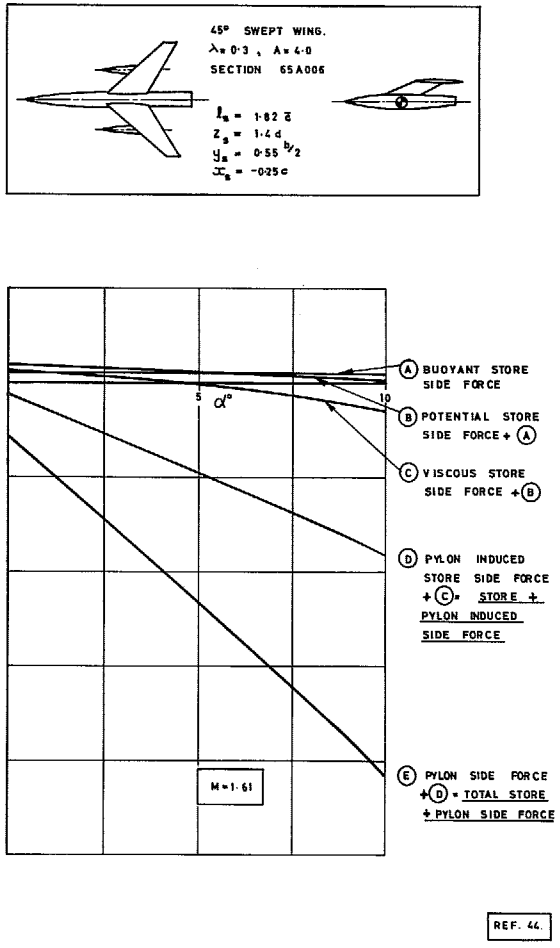

FIG. 34. Relative theoretical contributions to store/pylon side force at $M = 1{\cdot}61$.

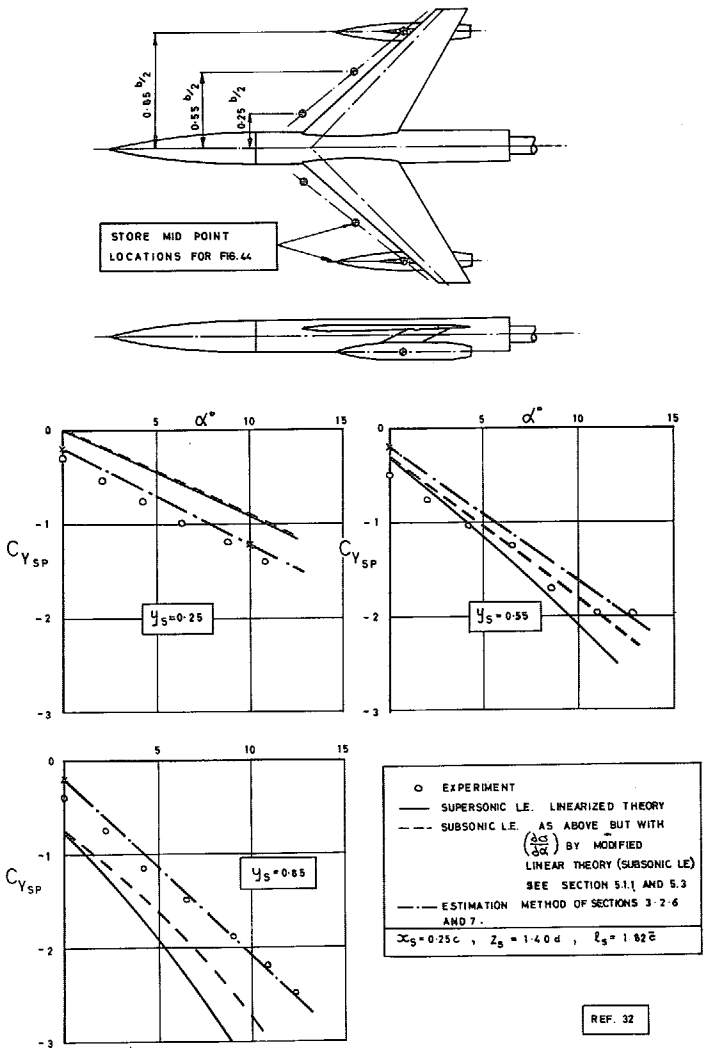

FIG. 35. Variation of total store plus pylon side-force coefficient with spanwise position at $M = 1{\cdot}61$.

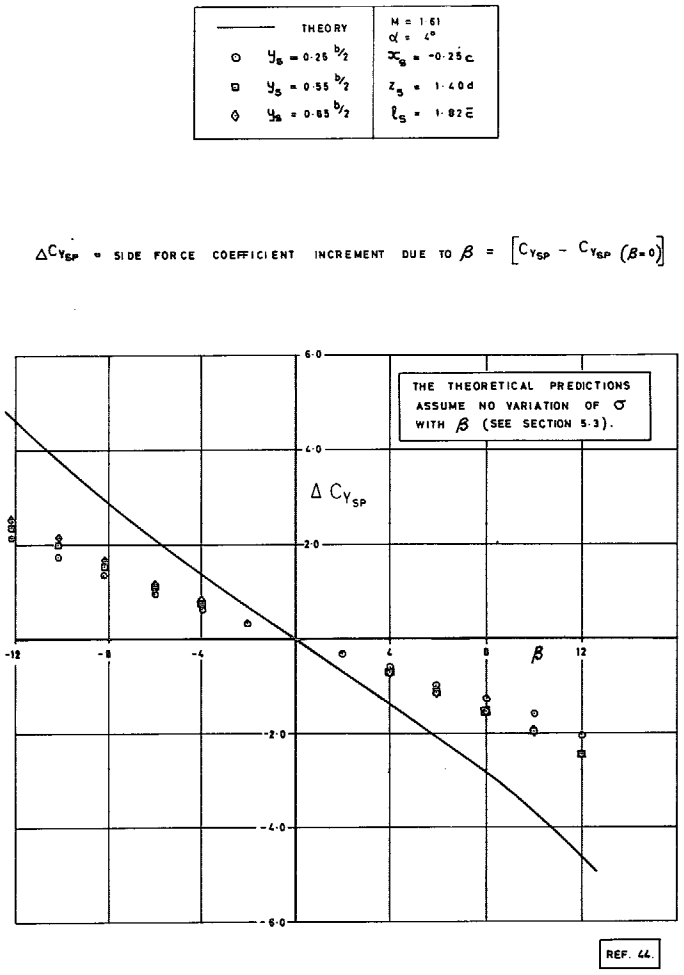

FIG. 36. Comparison of theoretical and measured variation of store/pylon side force with sideslip.

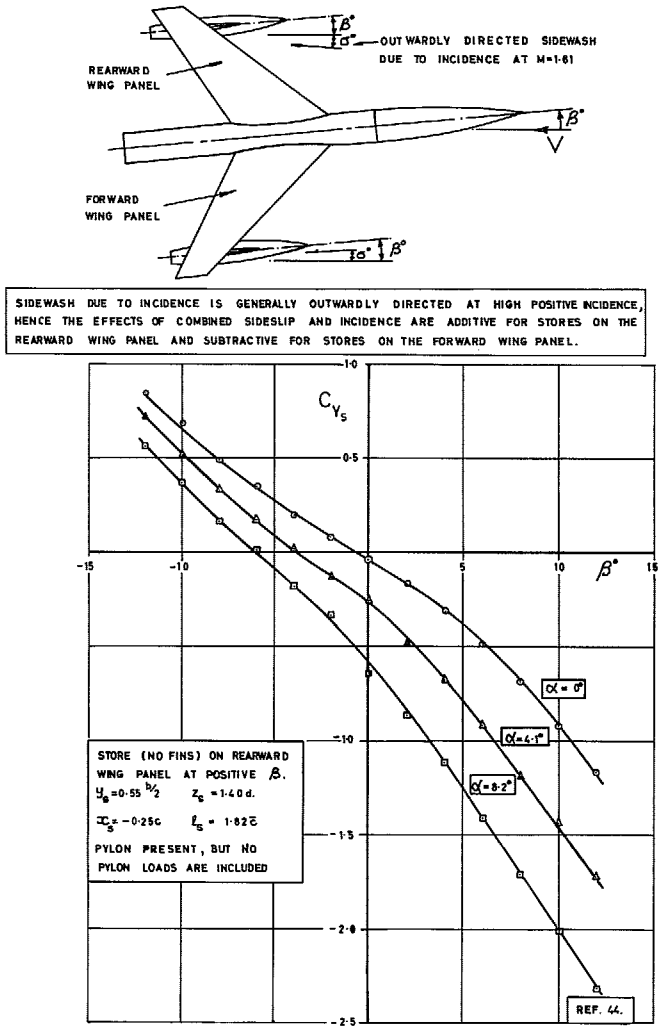

FIG. 37. Variation of store side force with combined sideslip and incidence beneath a 45 deg swept wing a $M = 1{\cdot}61$.

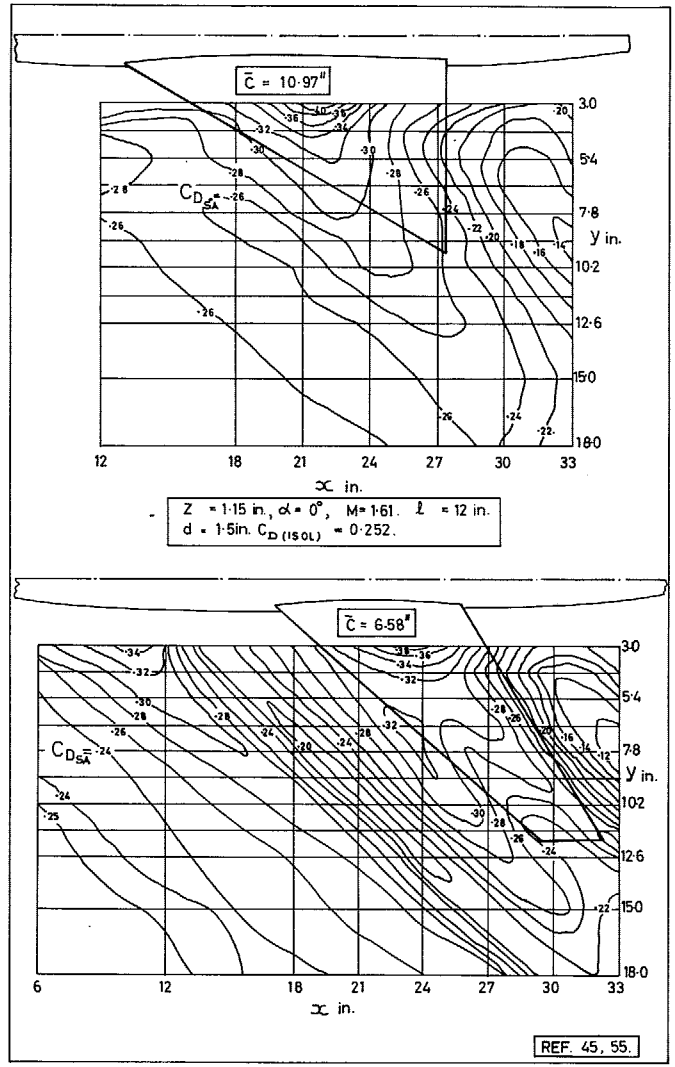

FIG. 38a. Contour plot of the drag of a store in the presence of wing-fuselage combinations.

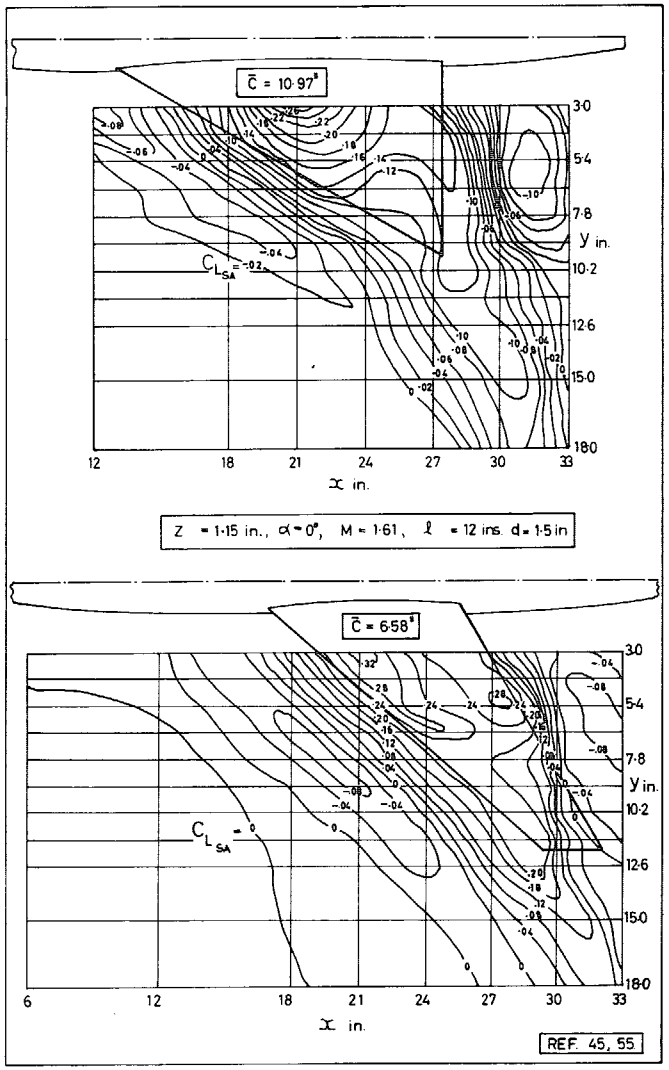

FIG. 38b. Contour plot of the lift of a store in the presence of wing-fuselage combinations.

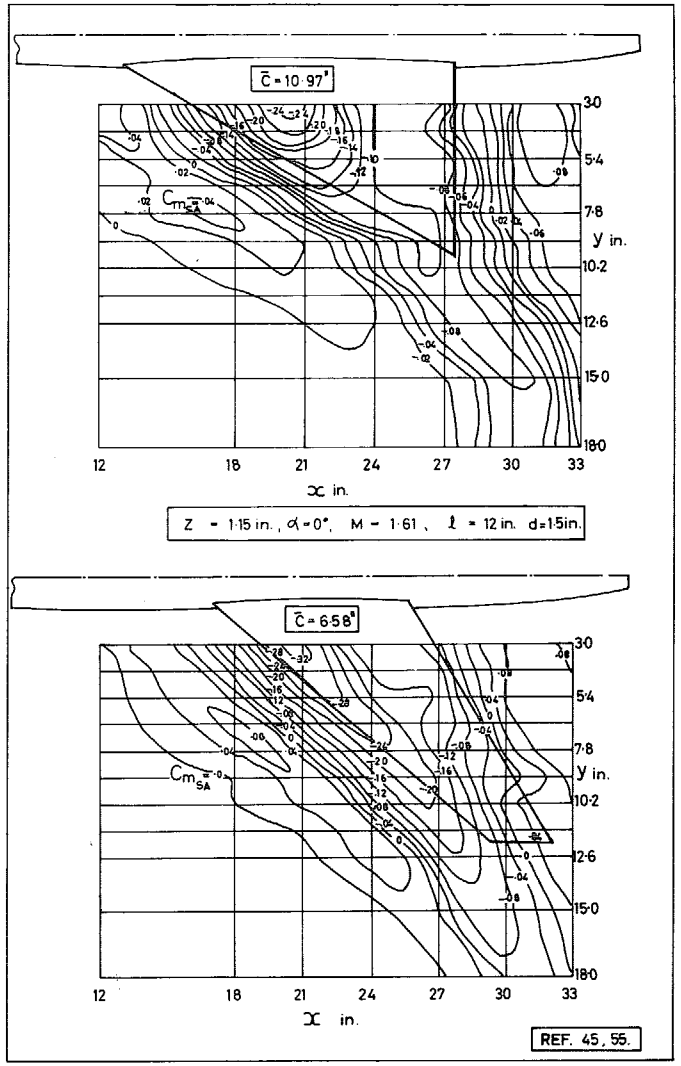

FIG. 38c. Contour plot of the pitching moment of a store in the presence of wing-fuselage combinations.

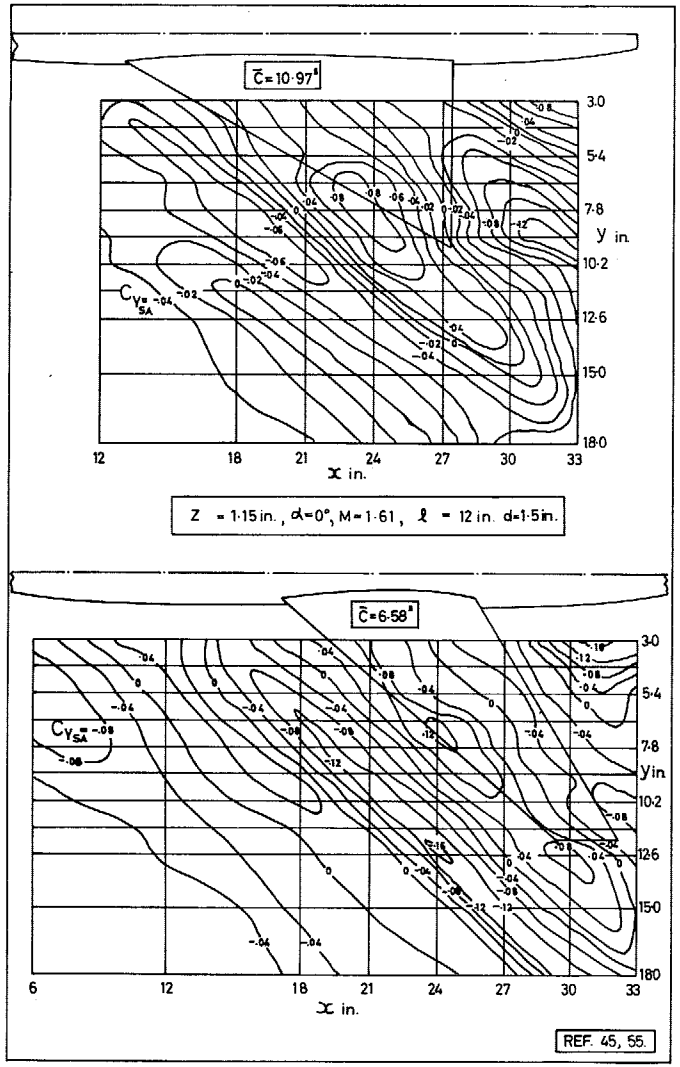

FIG. 38d. Contour plot of the side force of a store in the presence of wing-fuselage combinations.

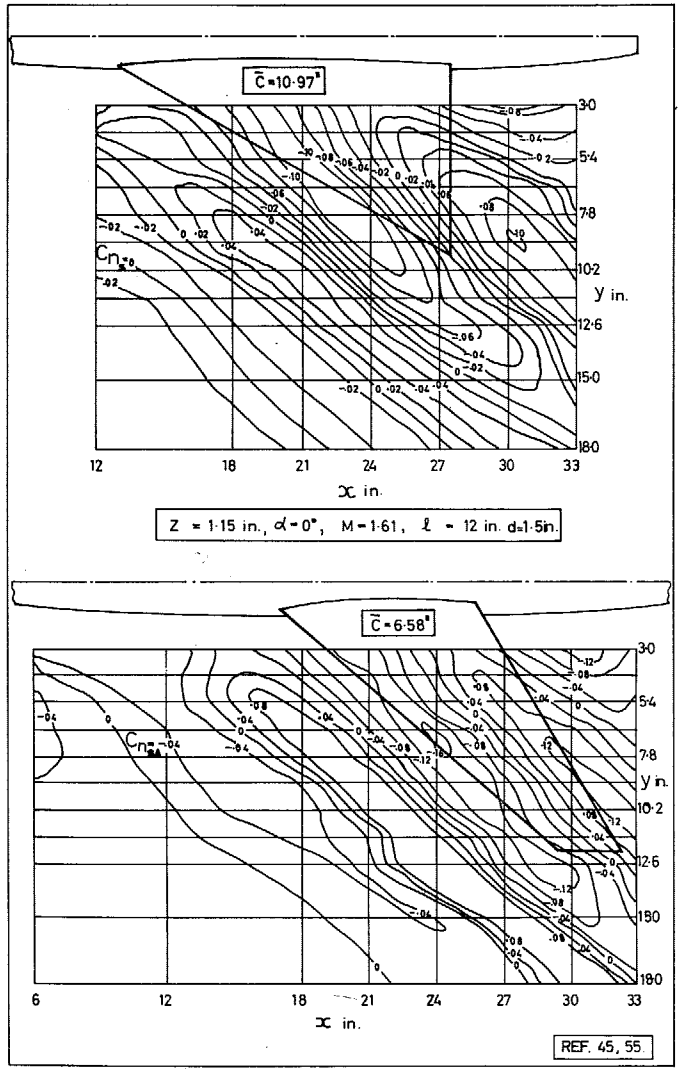

FIG. 38e. Contour of the yawing moment of a store in the presence of wing-fuselage combinations.

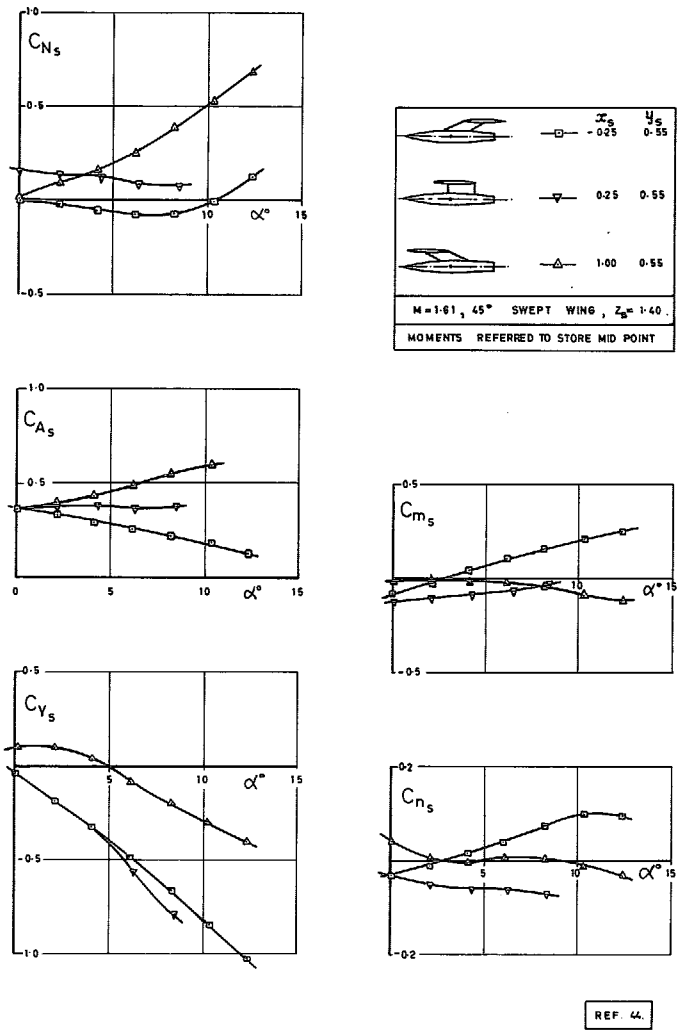

FIG. 39a. Effect of chordwise location on store aerodynamic characteristics.

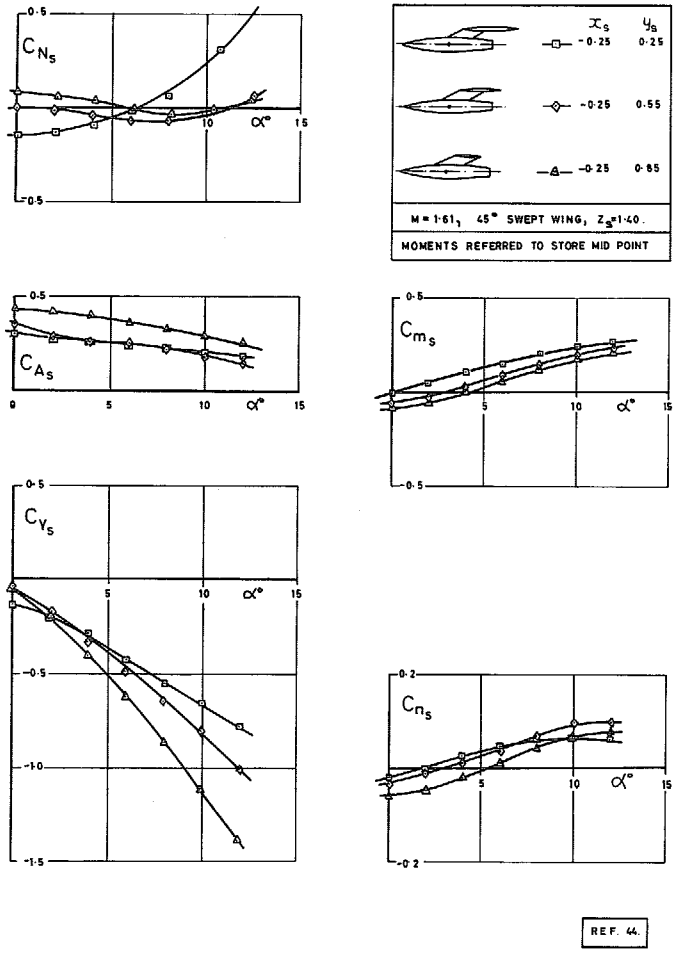

FIG. 39b. Effect of spanwise location on store aerodynamic characteristics.

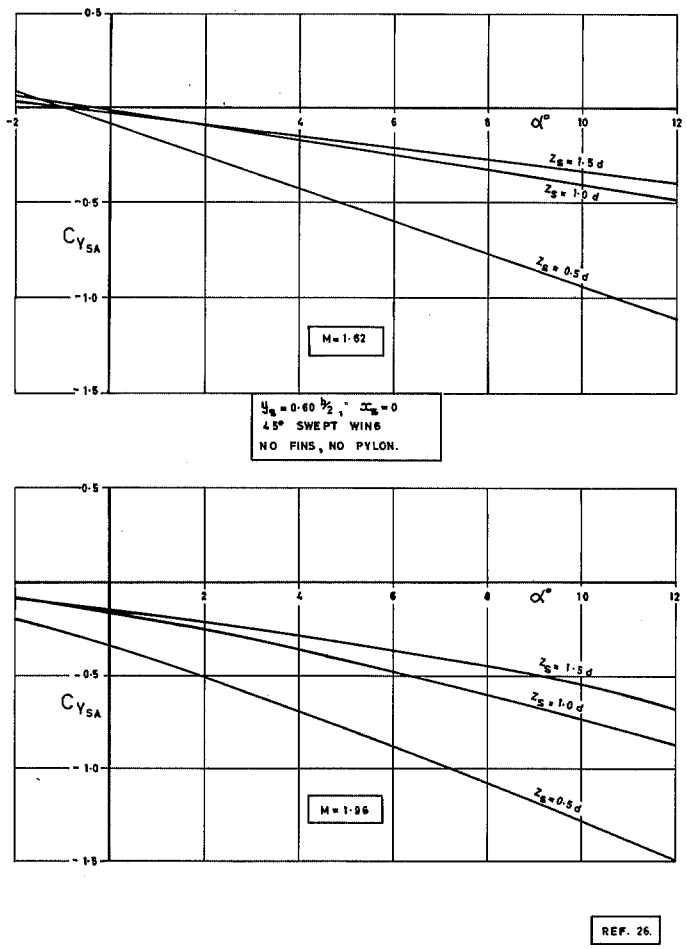

FIG. 40. Effect of store vertical location on the variation of side force with incidence.

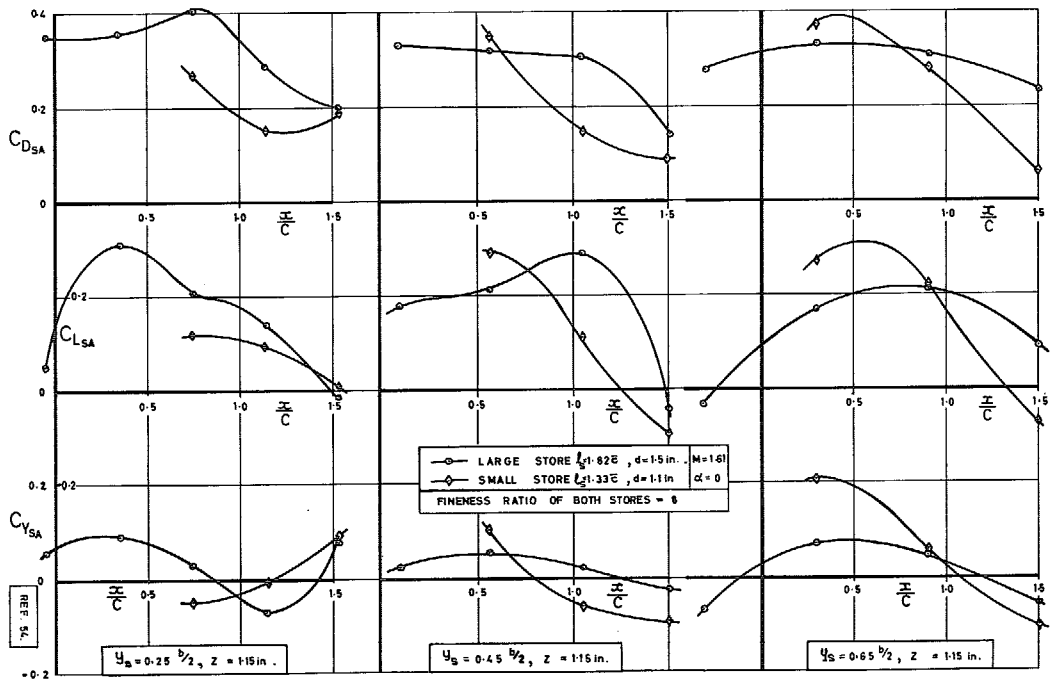

FIG. 41. Effect of store size on the variation of store alone forces beneath a 45 deg swept wing.

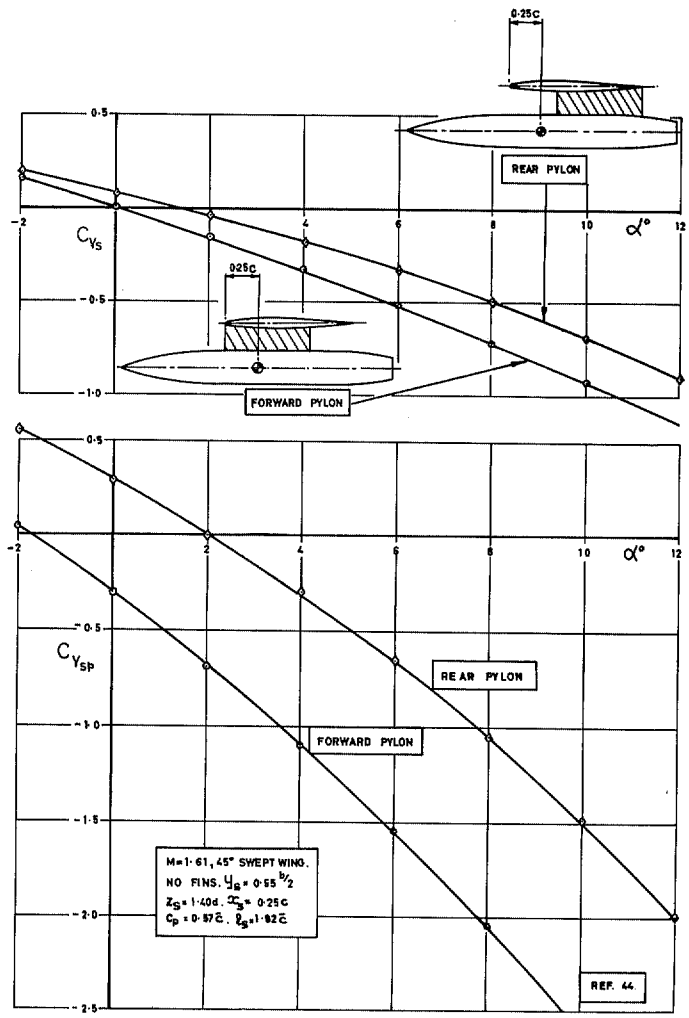

FIG. 42. Effect of pylon position on the variation of C_{Y_S} and $C_{Y_{SP}}$ with incidence.

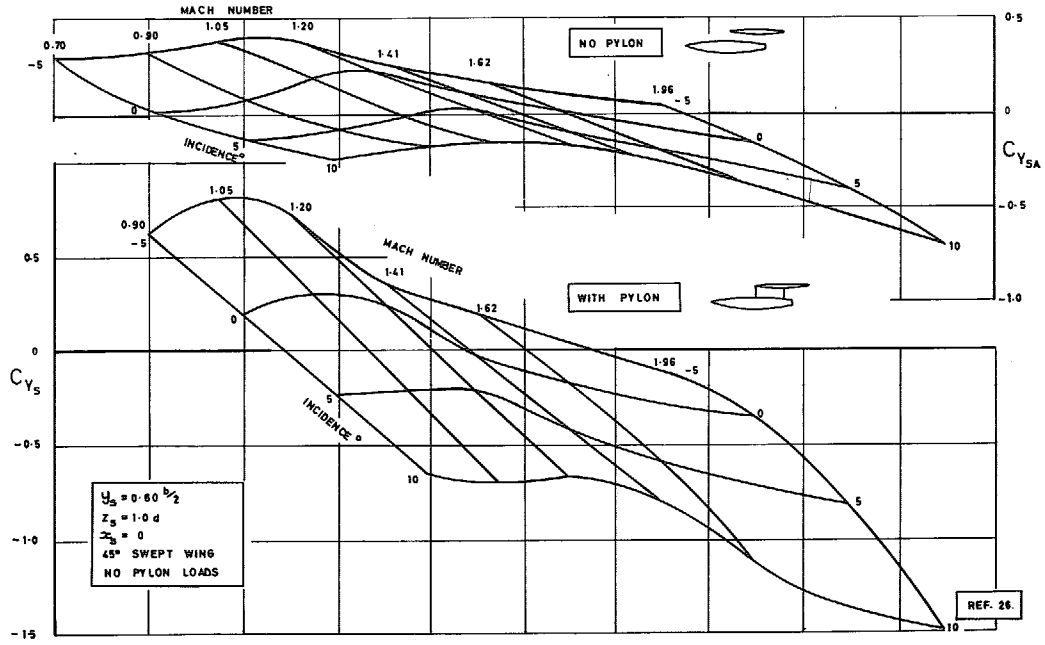

FIG. 43. Effect of Mach number on the variation of side force with incidence, with and without pylon.

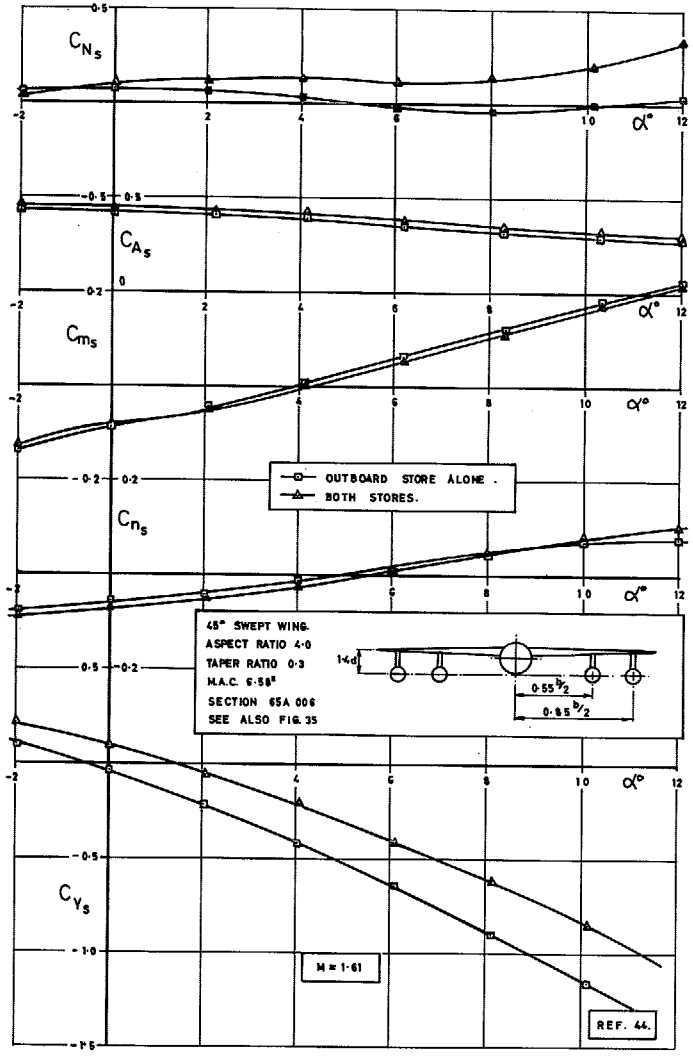

FIG. 44. Effect of an inboard store on the aerodynamic characteristics of an outboard store.

$$(C_Y)_\alpha = \left[(C_{Y_o}) \cdot K_{m_3} + K_{m_1} \cdot K_{m_2} \alpha \cdot \left(\frac{dC_Y}{d\alpha}\right)\right] K_{m_4}$$

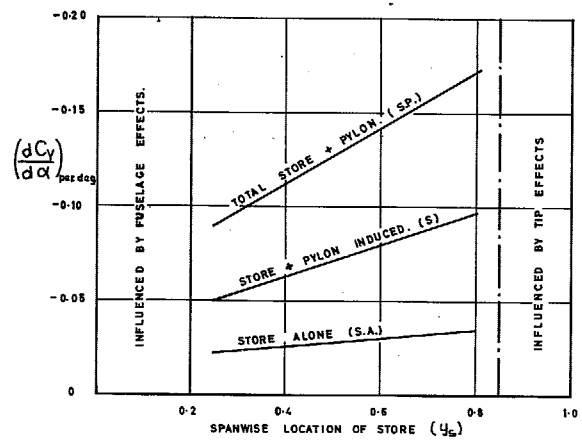

FIG. 45. VARIATION OF $\left(\frac{dC_Y}{d\alpha}\right)$ WITH SPANWISE LOCATION.

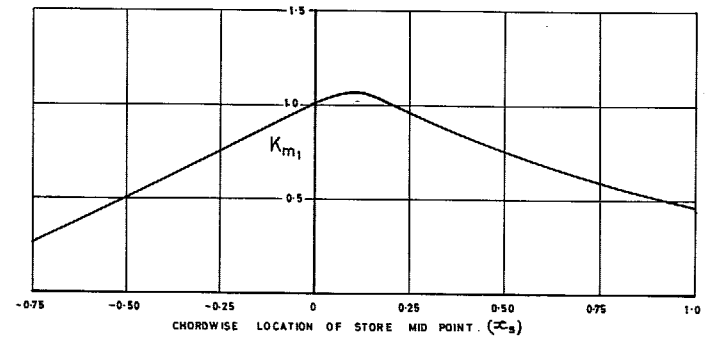

FIG. 46. Variation of K_{m_1} with chordwise location of store mid-point.

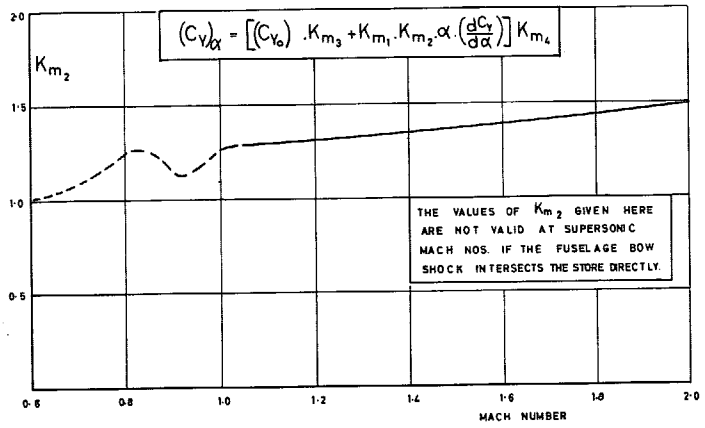

FIG. 47. Variation of K_{m_2} with Mach number.

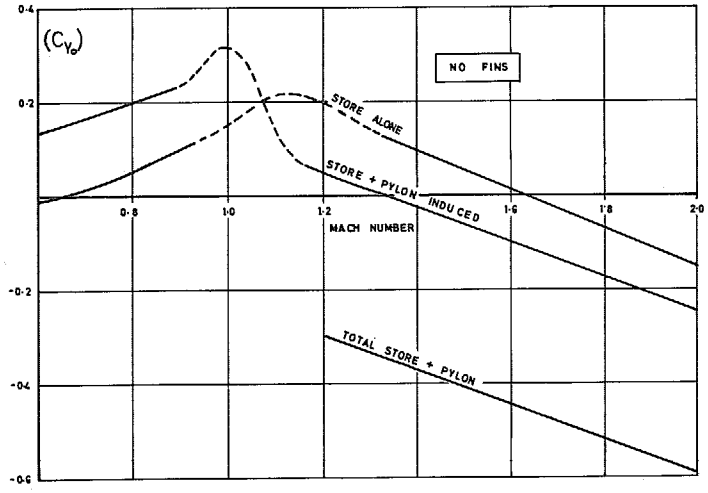

FIG. 48. Variation of side force at zero incidence (C_{Y_0}) with Mach number.

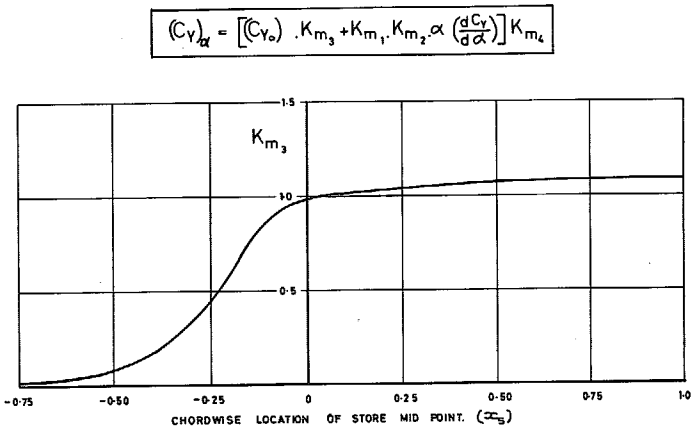

FIG. 49. Variation of K_{m_3} with chordwise location of store mid-point.

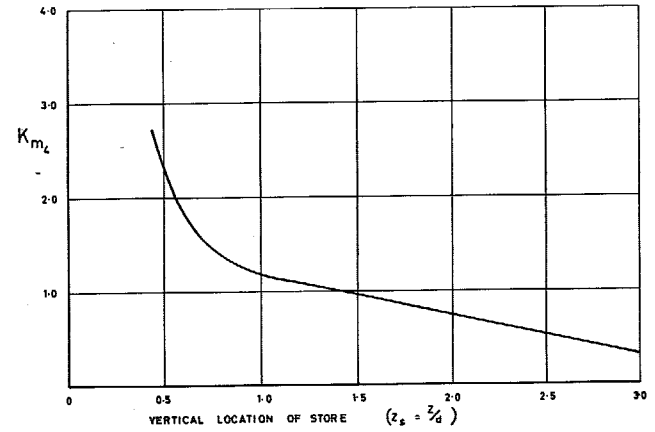

FIG. 50. Variation of K_{m_4} with store vertical location.

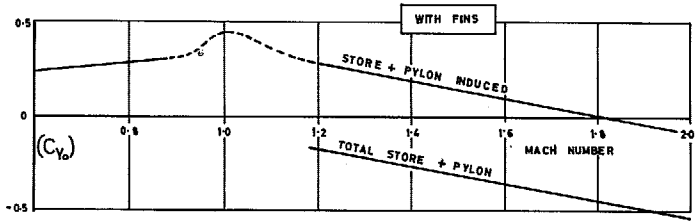

FIG. 51. Variation of (C_{Y_0}) with Mach number for store with fins.

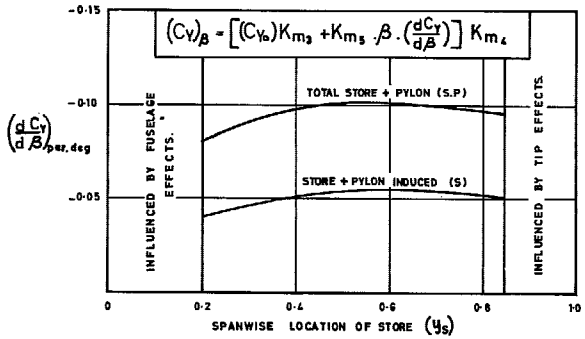

FIG. 52. Variation of $\frac{dC_Y}{d\beta}$ with spanwise location.

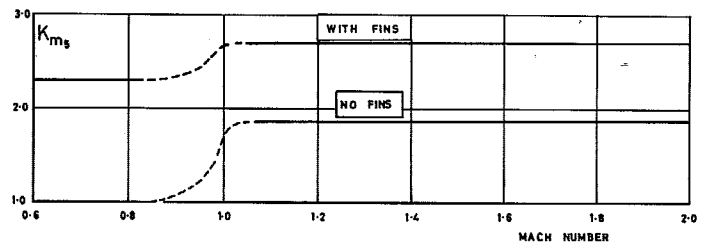

FIG. 53. Variation of K_{m_5} with Mach number, with and without fins.

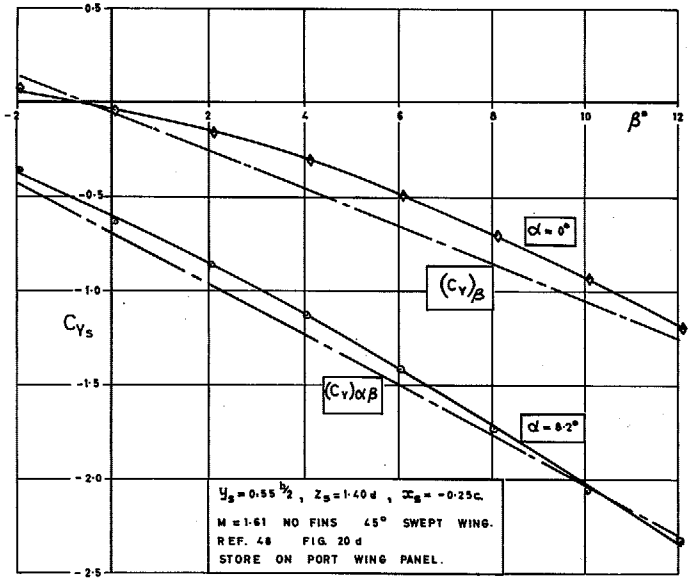

FIG. 54. Comparison of measured and estimated side force values at supersonic Mach number.

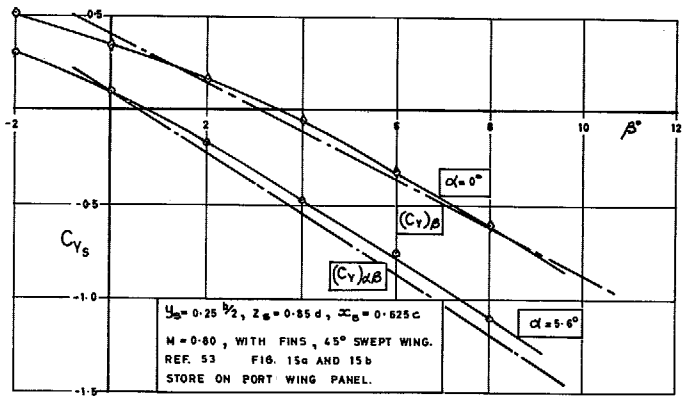

FIG. 55. Comparison of measured and estimated side-force values at high subsonic Mach number.

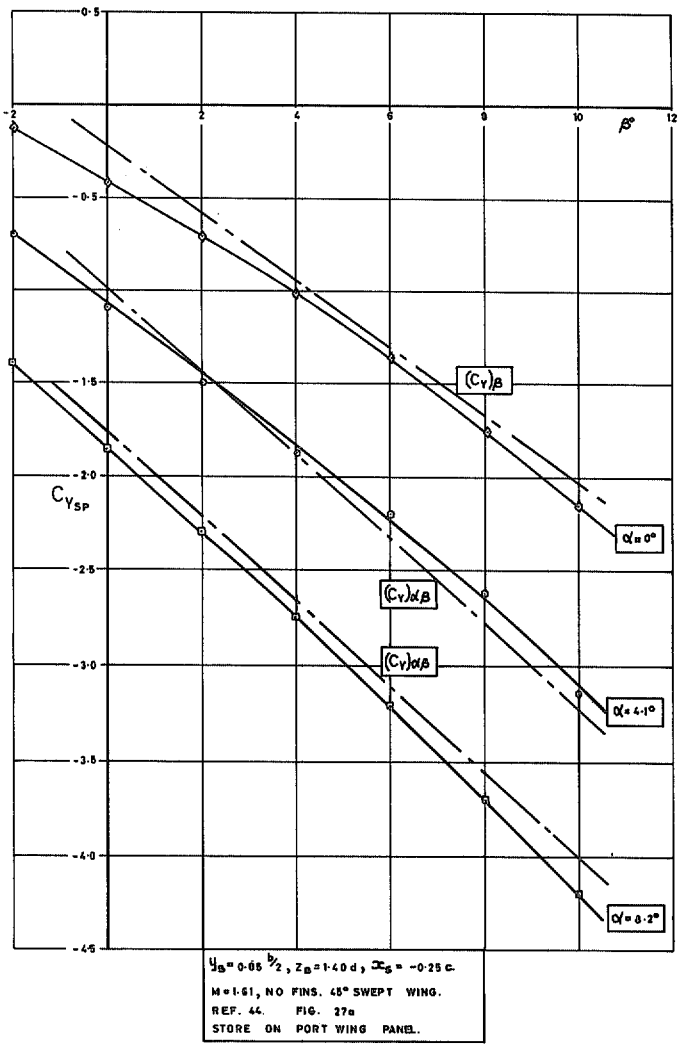

FIG. 56. Comparison of measured and estimated total store plus pylon side forces.

Printed in Wales for Her Majesty's Stationery Office by Allens Printers (Wales) Limited.

Dd.129527 K5

Published by
HER MAJESTY'S STATIONERY OFFICE

To be purchased from
49 High Holborn, London W.C.1
423 Oxford Street, London W.1
13A Castle Street, Edinburgh 2
109 St. Mary Street, Cardiff
Brazennose Street, Manchester 2
50 Fairfax Street, Bristol 1
35 Smallbrook, Ringway, Birmingham 5
7–11 Linenhall Street, Belfast 2
or through any bookseller

S.O. Code No. 23–3503